EVALUATING GROUNDWATER IN A PERMAFROST WATERSHED USING SEASONAL GEOCHEMICAL AND ISOTOPE DISCHARGE TRENDS, OGILVIE RIVER, YUKON

Natalia Baranova

Thesis submitted to the Faculty of Graduate and Postdoctoral Studies
in partial fulfillment of the requirements for the degree of
MASTER OF SCIENCE in Environmental and Earth Sciences

Ottawa-Carleton Geoscience Centre
and
University of Ottawa
Ottawa, Canada

Thesis Supervisor:

Dr. Ian Clark (University of Ottawa, Department of Environmental and Earth Sciences)

Abstract

This study focuses on a mid-sized watershed of upper Ogilvie River (~4,500 km^2 at the western extent of the 77,000 km^2 Peel River basin) located at the northern extent of the discontinuous permafrost in central Yukon. Annual hydrograph is analyzed by characterizing the river flow components using geochemical tracers (anions, cations, and dissolved organic and inorganic carbon), stable isotopes (δ^2H, $\delta^{18}O$, and $\delta^{13}C$) and radioactive isotopes (^{14}C and ^{3}H). The 2014 and 2015 flows are characterized by high weathering solute concentrations (Ca^{2+}, Mg^{2+}, SO_4^{2-}, and DIC) in the winter that spike just prior to freshet, diluted to the lowest concentrations at the peak of freshet, and slowly recover throughout the summer and fall responding to overall flow fluctuations. Biogenic solutes (K^+ and DOC) are lowest in the winter time and spike at the start of freshet.

Two groundwater components, shallow and deep, were identified with corresponding tritium-based residence times of less than a year and three years, respectively. The local meteoric water line, developed based on the local precipitation samples $\delta^2H=6.77\cdot\delta^{18}O-24.54$ ($R^2=0.98$), was used to determine the recharge mix of the groundwaters: 65% rain and 35% snowmelt.

The recharge waters interact greatly with soil (open system weathering) and carbonate bedrock (closed system weathering) as evident via the $\delta^{13}C$ and $F^{14}C$ signatures of the active layer waters, shallow groundwater and deep groundwater. Radiocarbon of DIC proved to be an important tool to differentiate the weathering conditions by demonstrating $F^{14}C$ carbonate dilution resulting in groundwater $F^{14}C$ as low as 0.57.

Based on the $\delta^{18}O$ based hydrograph separation, deep groundwater comprised almost half of the annual discharge. The groundwater discharge reached its maximum flow of 129 m^3/s during freshet when it contributed 44% to the flow. The potential groundwater recharge pathways include thermal contraction cracks in permafrost and bedrock fractures. The recharge is thought to occur over vegetated areas. In the summer, likely only large precipitation events result in recharge.

In comparison to discharge, the annual DIC exports from the study catchment (5.6 $gC/m^2/yr$) were disproportionally high in the winter time and the DOC exports (2.1 $gC/m^2/yr$) varied proportionally with discharge.

Acknowledgements

The first thank you goes to my supervisor Dr. Ian Clark for giving me a delightful opportunity to work in the Arctic and add Yukon to the list of places I love. This project would not have been possible without his vision, support, and funding. I was lucky to have great field crew that made sampling and camping both efficient and fun. Laurianne Bouchard, Anthony Lapp, Amber Dyck and Ian Clark were most excellent field companions. Thank you, Anthony, for showing me the ropes of sampling in the Arctic. The great search for the Elephant Rock, popping corn on a campfire, and tracking sgnomes will remain fond Yukon memories. Peter Nagano and Terry Taylor of the Engineer Creek Highway Maintenance Camp were of great help collecting samples between sampling trips and providing some logistical support. Thank you, Peter, for watching out for that grizzly bear the day we met.

Back in the labs, a supportive group of lab personnel ensured all my samples could be analyzed entirely within the Advanced Research Centre building on campus. Thank you to Paul Middlestead, Wendy Abdi, and Patricia Wickham at the G.G. Hatch Isotope Lab, Monika Wilk, Sarah Murseli, and Carley Crann at the A.E. Lalonde AMS Lab, Ping Zhang, Nimal DeSilva at the Geochemistry lab. It was a pleasure to work with every one of these knowledgeable and generous people.

I would also like to thank Matt Herod for always being happy to talk about Yukon rivers and taking the time to be supportive. A special thank you goes to Liz Ashby, Maeve Moriarty, and Magda Celejewski for essential graduate studies moral support. Justin Emberly, Jacob Nunn, and Laurianne Bouchard, you were great office mates.

Other instrumental people in my master's journey include my sister Yuliya, it was great to live in the same city again; my roommates Audrey and Mar, whose encouragement and faith in me helped a lot; and my parents, who truly supported my return to graduate school.

Table of Contents

List of Figures

List of Maps

List of Tables

List of Appendices

List of Abbreviations

d-excess	Deuterium Excess
DIC	Dissolved Inorganic Carbon
DOC	Dissolved Organic Carbon
EMMA	End-Member Mixing Analysis
GMWL	Global Meteoric Water Line
LCE	Line Conditioned Excess
lc-excess	LCE as deviation from LMWL
LC-excess	LCE as deviation from GMWL
LMWL	Local Meteoric Water Line
MAAT	Mean Annual Air Temperature
PCA	Principal Component Analysis
pCO_2	Partial pressure of CO_2
pMC	Percent Modern Carbon
TU	Tritium Unit
VPDB	Vienna Pee Dee Belemnite
VSMOW	Vienna Standard Mean Ocean Water

1 Introduction

The studies of the groundwater resources in the north have been sparse and our understanding of the hydrology and hydrogeology is far from comprehensive. The permafrost extent ranging from sporadic to continuous can affect the groundwater distribution and behaviour in various ways. Permafrost or ground that remains below 0°C for two or more years underlies between 22% and 26% of the world's land surface (Brown et al., 1998; Williams and Smith, 1989). The distribution of permafrost, in general, depends on the air temperature with significant contributions of more local features such as water bodies, vegetation cover, topographic conditions, and soil types (Williams and Smith, 1989).

Most of the relevant literature with publication dates ranging from the 1960s to the present, agree that our knowledge of the groundwater systems in the permafrost regions is limited, especially for the subpermafrost aquifers (Kane and Stein, 1983; Streletskiy et al., 2015; Williams, 1970). This is particularly true in Yukon where hydrologist Gilles Wendling acknowledged the need to delineate and characterize the groundwater aquifers (Cruickshank, 2014). One of the limitations of our knowledge of the groundwater in permafrost is the sparsity of available information and absence of integrated data (van der Ploeg et al., 2012). The lack of comprehensive information can be partially attributed to the low density of hydrometric and meteorological stations as well as short or discontinuous records. The groundwater watersheds are rarely defined in the northern regions with the implication that groundwater discharged in one surface water watershed may originate from a different area, even if it is, for example, on the other side of a continental divide (Kane et al., 2012). However, the studies are amassing and the information is compiled and synthesized to draw parallels between different regions (Carey and Pomeroy, 2009; Woo, 2012).

Subarctic or arctic climates and permafrost presence can control many aspects of the hydrological cycle. The climate controls precipitation amounts and their temporal distribution. Permafrost watersheds are usually characterized by short hydrologically active seasons. In central Yukon, the freshet occurs around mid- to late May and the rivers freeze up by early to mid-November (Fisheries and Environment Canada, 1978). Permafrost affects groundwater recharge and discharge with respect to timing and amount of water exchanged. Snow, glaciers,

and other permafrost features such as aufeis can act as long term water storage and may provide source of the stream flow later in the flowing season.

The permafrost, especially when continuous, is traditionally thought to present an impermeable barrier to groundwater recharge. However, there are many examples of groundwater recharge being an important component in the hydrological cycle in the permafrost regions. The numerous groundwater discharge features that are most widespread in the discontinuous permafrost areas but are also present in the continuous zones. They are some of the most obvious evidence of the groundwater recharge existence and magnitude.

The basic understanding of groundwater in permafrost region can be summarized with three main groundwater types as illustrated on Figure 1.

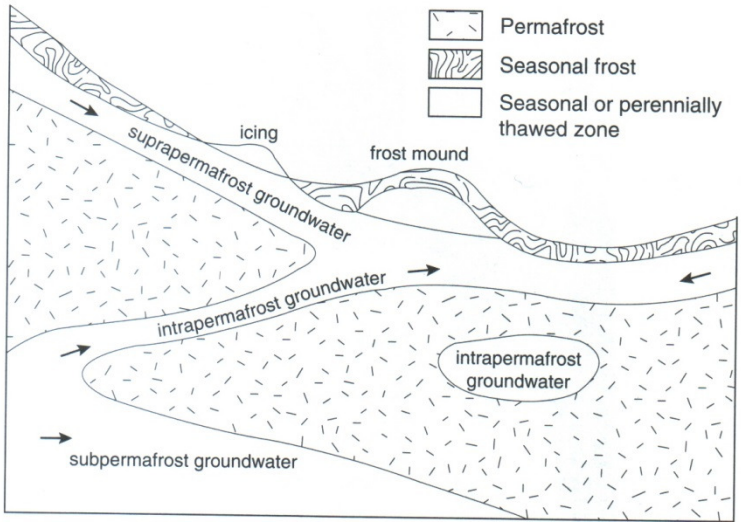

Figure 1 **Groundwater in Permafrost Regions** (Woo, 2012, reproduced with permission of Springer)

There are suprapermafrost, intrapermafrost and subpermafrost groundwaters. The suprapermafrost waters undergo full or partial seasonal freezing. The intrapermafrost waters can connect the shallow and deep waters or they may be enclosed. The subpermafrost waters flow below the permafrost formations and may have a really wide range of residence times (Woo, 2012).

Frequently, groundwater in permafrost regions is studied from the standpoint of the discharge as either baseflow into the arctic rivers or as surficial features such as springs, icings, frost blisters,

and pingos. Icings (aufeis) are the most obvious feature as they can cause flooding and damage infrastructure. Groundwater discharge may keep the rivers from completely freezing in the winter time or sustain year-round flow to some springs. Understanding of recharge locations, timing, and processes can provide useful insights into utilization of groundwater resources, effects on infrastructure development, and effects of climate change.

Some studies suggest changes to the groundwater contributions to the streamflow in the permafrost regions. For example the baseflow to the Yukon River subwatersheds in Yukon and Alaska showed an increase in groundwater baseflow contribution at a rate of approximately 0.9% per year over a 30 year period while the overall discharge remained unchanged (Walvoord and Striegl, 2007).

The potential groundwater recharge pathways are frequently attributed to areas with no permafrost (Kane et al., 2012). However, other recharge possibilities are through taliks, faults, fractures, and karst terrain (Brook and Ford, 1980; Kane et al., 2012; Woo, 2012), through the river channel bottoms (Sokolov, 1991), and through the base of glaciers (Haldorsen et al., 1996). The processes involved in the subglacial recharge discussed by Haldorsen et al. (1996) can also be applied to the groundwater recharge by the glacial meltwater. The perennial springs on Axel Heiberg Island in the High Canadian Arctic are thought to be fed by modern meteoric waters from a glacially dammed lake via a fault (Andersen et al., 2002; Pollard et al., 1999). There, the subsurface flow is through the evaporate unit where the groundwater is able to reach geothermal temperatures before upward migration towards the surface spring discharge locations.

2 Objectives

The main objectives of this research project on the upper Ogilvie River watershed are

- to characterize temporal variation of chemistry of the river and its inputs
- to understand the contribution of groundwater to the overall river flow
- to correlate groundwater recharge and discharge with geological, cryological, and meteorological controls
- to examine potential groundwater recharge pathways

The general approach is to characterize flow components using geochemical tracers (anions, cations, and dissolved organic and inorganic carbon), stable isotopes (δ^2H, $\delta^{18}O$, and $\delta^{13}C$) and radioactive isotopes (^{14}C and ^{3}H). The flow component signatures are then analyzed for trends and relationships to understand the hydrological processes in the watershed. Using mixing model approach to separate the hydrograph, the contribution of groundwater to the overall river flow is examined. Additionally, the riverine DIC and DOC exports are quantified for the watershed.

3 Literature Review

3.1 Hydrological Cycle in Permafrost Environments

The general hydrological cycle in permafrost regions is the same as in the temperate regions. The precipitation consisting of rain or snow provides the main input into the surficial hydrological unit (i.e. a watershed). Other inputs include surface runoff and groundwater flow into a watershed. The water leaves a watershed via surface discharge, evaporation and evapotranspiration. Active layer above the permafrost table provides temporary water storage. As active layer thaws throughout the summer, it releases previously stored water and provides additional subsurface flow pathways.

The cold-region specific features such as permafrost, snow, glaciers, and aufeis add significant influences to the hydrological cycle via redistribution of the precipitation inputs temporally and spatially and via redirecting groundwater and surface water flow (Woo, 2012).

3.1.1 Precipitation

In the arctic regions a large portion of annual precipitation falls as snow and is released during spring snowmelt in a large pulse. Frequently, the freshet stream flows are the largest of the year. In central Yukon average annual precipitation is 300 to 400 mm, and its associated snowfall portion is between 160 and 280 cm (Fisheries and Environment Canada, 1978).

The direct precipitation onto the water bodies is generally negligible unless large surface area lakes are present in the watershed (Mook et al., 2001).

The relationship between the stable isotopes δ^2H and $\delta^{18}O$ in precipitation defines a meteoric water line. Globally, the linear correlation is called the global meteoric water line (GMWL),

which is the relationship defined by Craig (1961) based on world-wide samples of precipitation, rivers and lakes ($\delta^2H=8\cdot\delta^{18}O+10$). Local meteoric water lines (LMWL) can be defined for a distinct geographical region using precipitation isotopic values that reflect regions specific origin of water vapour and rainout patterns (Clark, 2015). For example, the LMWL for Whitehorse, Yukon, is $\delta^2H=6.4\cdot\delta^{18}O-31$ (Clark, 2015), for Dawson City, Yukon, is $\delta^2H=6.3\cdot\delta^{18}O-36$ (Lapp, 2015), for Mayo, Yukon, is $\delta^2H=6.3\cdot\delta^{18}O-37$ (Lacelle, 2011), and for Inuvik, NWT, is $\delta^2H=7.3\cdot\delta^{18}O-3.5$ (Lauriol et al., 2010).

The LMWL provides a starting point in evaluating the components of the hydrological cycle with respect to the precipitation (Gat, 2010). Other than the visual comparison with the LMWL, deuterium excess (d-excess or d) and line conditioned excess (LCE) are parameters that allow to evaluated the relative deviation from the LMWL (Benjamin et al., 2004; Gat, 2010). The d-excess is calculated as $d=\delta^2H-8\cdot\delta^{18}O$ and is caused by the kinetic evaporation processes (Clark, 2015). Landwehr and Coplen (2006) defined line conditioned excess as deviation from either the GMWL (LC) or the LWML (lc) as LC (lc)-excess = $\delta^2H-a\cdot\delta^{18}O-b$, where a is the slope and b is the intercept of the GMWL (LC) or the LMWL (lc). Thus, line conditioned excess is a measure of offset from the MWL. If the value is greater 0, the sample in question plots above the MWL and if the value is less than 0, the sample plots below the MWL.

Precipitation isotopic signature varies with latitude and altitude (Clark, 2015). The latitudinal changes are expressed as the LMWL deviation in its slope and deuterium intercept from the GMWL. The precipitation becomes depleted by 0.15 to 0.5‰ $\delta^{18}O$ and by 1 to 4‰ δ^2H per 100 m in elevation gain (Clark, 2015). The elevation gradients may also differ between summer and winter. For example, steeper winter gradients (-0.56 to -0.60‰ per 100 m) were observed in the Swiss Alps compared to the summer gradients (-0.15 to 0.22‰ per 100 m) (Kern et al., 2014). Large local variations in the precipitation isotopic values can make it difficult to distinguish the presence and magnitude of altitude effects (Dietermann and Weiler, 2013) and other effects such as amount effect that may account for observed variations (Kang et al., 2002). The amount effect describes the pattern where larger precipitation events have more depleted isotopic signatures (Mazor, 2004). Despite possible local variations, Poage and Chamberlain

(2001) state the $\delta^{18}O$ elevation gradient is fairly constant around the world at -0.28‰ per 100 m based on a compilation of 68 studies.

The isotopic signature of the snowpack is subject to alteration via sublimation. The snow pack metamorphism is a complex and dynamic process that does not follow straightforward sublimation (Ekaykin et al., 2009; Sokratov and Golubev, 2009). The laboratory studies show that the remaining snowpack during snowmelt becomes enriched in $\delta^{2}H$ and $\delta^{18}O$ similarly to the evaporation effect (Sokratov and Golubev, 2009). The sublimation effects can be dependent on the altitude resulting in reduction of the $\delta^{18}O$ elevation gradients especially in low-humidity environments (Lechler and Niemi, 2012). Other smaller scale factors may affect the enrichment of the snow pack. For example, south facing slopes in the Swiss Alps experienced greater isotopic enrichment compared to the north facing slopes (Dietermann and Weiler, 2013).

Precipitation information in Yukon is collected via a network of seven meteorological and 58 snow survey stations. A number of private stations and stations that collect only partial meteorological information also exist.

3.1.2 Runoff Generation

Slope aspect plays an important role in runoff generation in the permafrost environments. North facing slopes get less sunlight and, therefore, are colder, have a higher percent of permafrost, and build up more organic matter. The south facing slopes drain faster and, therefore, are dryer. As such, south facing slopes are usually responsible for generation of downward runoff that feeds rivers at the valley bottoms, while the north facing slopes result in lateral flow (Woo, 2012). The rain or snowmelt waters interact with the soil. The depth of interaction depends on the thickness of the fully drained organic matter in the spring and on the thickness of the active layer that increases throughout the summer season. The extent of the interaction depends on the duration of the soil-water contact. In the flat areas and during small rain events the ground becomes saturated but little runoff is generated. During the snowmelt and large rain events the new water partially runs off the surface and partially displaces the pre-existing water (Woo, 2012).

3.1.3 Water-Soil Interactions at Recharge

The sub-surface flow during runoff events and groundwater flow provide opportunities for the water to interact with the soil. The interactions may include dissolution of organic matter into the

water as well as soil weathering. The amount of CO_2 in the soil drives the weathering process. The atmospheric CO_2, currently around 400 ppmv globally ($pCO_2 = 10^{-3.4}$), is increased in shallow soils via decomposition of organic matter and microbial respiration by an order of magnitude to the levels as high as 3,000-10,000 ppmv (Clark, 2015). Therefore, carbon, including its concentration, $\delta^{13}C$ and $F^{14}C$, is an important indicator in assessing the soil-water interactions. The CO_2 concentrations are expressed as partial pressure, pCO_2. Table 1 summarizes the expected $\delta^{13}C$ signatures for several carbon reservoirs.

Table 1 Typical $\delta^{13}C$ signatures (Clark, 2015)

Carbon Reservoir	$\delta^{13}C$ Signature (‰ VPDB)
Atmospheric CO_2	-8.3‰
C3 plants	-27‰
Soil CO_2	-23‰ to -20‰
Groundwater DIC	-19‰ to -7‰
Groundwater DOC	-30‰ to -20‰
Marine Carbonates	0±1‰

3.1.4 Weathering

Chemical weathering can generally be defined as carbonate or silicate based on the substrate being weathered and open or closed system weathering depending on the CO_2 supply conditions.

During weathering, acidity induced by $CO_{2(aq)}$ in equilibrium with H_2CO_3, results in the reaction of CO_2 with the rock producing bicarbonate ion HCO_3^-. In case of silicate weathering, bicarbonate is derived from $CO_{2(aq)}$ in its entirety and during carbonate weathering bicarbonate is formed both from the aqueous CO_2 and carbonate in the rock as shown in Equation 1.

Equation 1 Example reactions of silicate weathering using olivine (1a) and carbonate weathering using calcite (1b), (Tank et al. 2012)

$$Mg_2SiO_4 + 4CO_2 + 4H_2O \rightarrow 2Mg^{2+} + 4HCO_3^- + H_4SiO_4 \quad (1a)$$

$$CaCO_3 + CO_2 + H_2O \rightarrow Ca^{2+} + 2HCO_3^- \quad (1b)$$

The $\delta^{13}C$ can be helpful in understanding the weathering processes in a watershed. Similarly to concentrations $\delta^{13}C$ signature in carbonate weathering will be a mixture between that of the CO_2

and of the carbonate material, while in case of the silicate weathering the $\delta^{13}C$ signature will retain values of the CO_2.

The open system will continually provide CO_2 from the atmosphere or biogenic soil gases. In the closed system the CO_2 amount is not replenished from external source and, thus, the weathering only proceeds for as long as there is available CO_2. In an open system carbonate weathering, the soil CO_2 remains in equilibrium with the generated inorganic carbon and the $\delta^{13}C$ CO_2 signature will be enriched by a fractionation factor $\varepsilon^{13}C_{DIC\text{-}CO2}$ = ~10‰ (this factor is temperature dependent $\varepsilon^{13}C_{DIC\text{-}CO2} = 0.00032 \cdot T^2 - 0.124 \cdot T + 10.87$, where T is in °C) to result in the $\delta^{13}C$ of DIC of approximately -10 to -13‰ (Clark, 2015). In case of closed system carbonate weathering, the CO_2 responsible for weathering does not exchange with the soil CO_2 resulting in the $\delta^{13}C$ of CO_2 to be diluted by the ~0‰ carbonate (Table 1) resulting in $\delta^{13}C$ DIC of -10 to -12‰ (Clark, 2015).

As such, the $\delta^{13}C$ signatures cannot always be used to distinguish between open and closed weathering systems. Radiocarbon analysis is a useful additional tool to differentiate between these systems. In closed system weathering up to half of the original carbon can be substituted for carbon from the carbonate bedrock minerals. When carbonate substrate is 'dead' ($F^{14}C=0$) , modern waters may have radiocarbon signatures as low as $F^{14}C$~50 pMC or percent modern carbon (Clark, 2015).

3.1.5 Groundwater Recharge Investigation Tools

The common approach to evaluating groundwater recharge in permafrost areas is to study in detail the groundwater discharge and then try to match it with precipitation (Clark and Lauriol, 1997; Haldorsen et al., 1996; Kane et al., 2012). The typical discharge occurrences are groundwater springs, aufeis, and winter stream flow that are assumed to be fully fed by groundwater. The discharge features such as aufeis redistribute the time of the runoff of the groundwater. The winter groundwater discharge partially forms runoff and partially forms icings which delays release of the groundwater resources into the active hydrological cycle (Woo, 2012).

While it is mostly thought that recharge occurs through non-frozen soils such as permafrost free areas and taliks, the frozen soils cannot be ruled out as recharge medium. The frozen soils can

have hydraulic conductivities high enough to provide a reduced recharge potential (Kane and Stein, 1983). The moisture content is the primary control on the hydraulic conductivity of the frozen soils. The dry soils at temperatures below 0°C can have conductivities on the order of 10^{-5} to 10^{-6} m/s; however, with increased moisture content and decreased temperature the conductivity values can drop to 10^{-12} m/s or lower (Kane and Stein, 1983; Williams and Smith, 1989).

Many tools are used to study the groundwater recharge. Field investigations, aerial reconnaissance, aerial photography and satellite imagery can all be used to identify discharge features. In the study area, the Ogilvie River continues to flow throughout the winter fully sustained by the groundwater (Schreier, 1979).

Geochemical and isotopic tracers are frequently used to trace the groundwater from discharge to recharge. Kane et al., 2012, provides a great example of using field and laboratory geochemical data to track the recharge are of the springs discharged on the north side of Brooks Range in Alaska. Another investigation by Clark and Lauriol (1997) used similar techniques to trace the origins of the water in the aufeis of the upper Firth River in northern Yukon.

On the ground, important field data collected is usually pH, conductivity, and temperature. The geothermal heat added to the sub-permafrost groundwater in its deeper flow paths can provide indication of the groundwater residence times. The warmer groundwater is assumed to have travelled through deeper formations in order to absorb the geothermal heat and, therefore, warmer waters are likely to have longer travel paths. Such conclusions were drawn based on the springs temperatures on the north side of Brooks Range in Alaska (Kane et al., 2012).

Conductivity and pH measurements can help identify different sources of groundwater especially if mixing is present. These parameters can also reflect the geochemical conditions at recharge and along the flow paths.

Geochemical parameters such as cations and anions (including bicarbonate) provide helpful clues as to the rock-groundwater chemistry in aquifers. The type of weathering (silicate or carbonate) can be inferred from the saturation indices of the groundwater with respect to various minerals (Clark, 2015). Kane et al (2012) and Haldorsen and Heim (1996) analyzed saturation indices of carbonate minerals in the discharge to understand residence times in carbonate units.

In the case of discharge springs at Ester mine in Svalbard, the silicate weathering indicators identified porous sandstone as the main aquifer units (Haldorsen et al., 1996). Stable carbon isotope analysis ($\delta^{13}C$) can aid in the investigation of the weathering regime (Clark and Lauriol, 1997). If distinct, this information can be used along with geological understanding of the area in order to identify the groundwater recharge regions and aquifer locations, as for example was done in the investigation of the Firth River aufeis (Clark and Lauriol, 1997).

Another important groundwater investigation tool, both in temperate and in permafrost regions, is the stable isotopes $\delta^{18}O$ and $\delta^{2}H$. These stable isotopes are useful tracers of the origins of meteorological waters (Clark and Lauriol, 1997; Kane et al., 2012). By comparing the signature of the groundwater discharge to the precipitation signatures in the area, the general recharge location may be identified, especially if large topographical features such as mountains result in significant change in the isotopic signature of the precipitation. In the Brooks Range, the isotopically heavier precipitation on the south side of the range matched the discharge on the north side (Kane et al., 2012). Additionally, the timing of recharge may be inferred from the groundwater signature as compared to the range of meteoric water line values.

Radioactive isotopes such as radiocarbon and tritium may provide an idea of the groundwater residence times. Radiocarbon values cannot be directly used for groundwater dating as the atmospheric signature can be vastly altered by carbonate weathering of the groundwater by adding dead carbon ($F^{14}C=0$) to the atmospheric signature. Various correction methods and models exist, but they all require extensive additional data and other factors can introduce uncertainties (Clark, 2015; Kane et al., 2012). Nonetheless, the results can provide useful constraints on the age of the groundwater in order to back track the recharge location. Radiocarbon can also be used as a direct tracer. Tritium concentrations are useful to track modern meteoric waters and can be applied to waters younger than 50 years (Clark, 2015). When tritium is present, the groundwater flow paths are likely shallower, but depending on the permafrost distribution, may still be indicative of sub-permafrost flow. The really old groundwater systems may be dated using ^{36}Cl dating techniques.

As the watershed size increases the discharge integrates larger spatial and temporal inputs. It is more difficult to identify responses to single storm or snowmelt events resulting in reduced contrast of seasonal patterns and masking of true low flow events (Woo, 2012)

Streamflow duration curves correlate magnitude and frequency of precipitation and are used in temperate watersheds to evaluate the flow variability (Healy, 2010). While separate studies are required to directly correlate flow probability to the groundwater-fed baseflow, the curve can provide insight into the role of the groundwater contribution to the stream. The shallow slope of the curve is usually an indication of significant groundwater discharge into the stream.

3.1.5.1 Radiocarbon

Radiocarbon, $F^{14}C$, is a heavy and radioactive isotope of carbon. Radiocarbon sources in the atmosphere include natural cosmogenic production from ^{14}N and historical thermonuclear bomb testing. The atmospheric ^{14}C generally follows the fate of CO_2 (Beta Analytic Limited, 1990). The half-life of radiocarbon was determined by Libby in 1949 to be 5,570 years; this value was later refined to 5,730 years (Geyh, 2000). The 100 percent modern (pMC) concentration (equivalent to $F^{14}C=1$) of radiocarbon was set at atmospheric radiocarbon levels in 1950 (Hua, 2009). The bomb tests of the 1950s and 60s increased the radiocarbon levels to almost 200 pMC. If not used for direct dating of the groundwaters, radiocarbon can be used as a natural tracer of flow system components.

3.1.5.2 Tritium

Tritium, ^{3}H or T, is a heavy and radioactive isotope of hydrogen. Tritium sources in the atmosphere include cosmogenic production, historical thermonuclear bomb testing and historical or current anthropogenic tritium releases (Clark and Fritz, 1997). Tritium occurs in the atmosphere in three major forms: as tritiated molecular hydrogen (HT), tritiated water (HTO) vapour and tritiated methane (CH_3T) (Boyer et al., 2009). In general, the fate of tritium in the environment follows hydrogen (Boyer et al., 2009). Atmospheric tritium in the form of HT and HTO undergo wet or dry deposition directly onto soil or plants. Of interest in this study is the wet deposition of tritium in precipitation and migration of tritium via runoff, infiltration, and evaporation process. Tritium can be used as a natural radioactive tracer of meteoric waters (Clark, 2015).

The half-life of tritium is 12.32 years (Clark, 2015). Approximately 7 half-lives are required to radioactively decay material to approximately 1% of its original mass. Tritium concentrations are usually expressed in tritium units (TU) equal to activity of $1x10^{-18}$ Bq/L. Cosmogenic production of tritium in the atmosphere results in precipitation concentrations of 5-20 TU around the globe. Concentrations elevated above that are affected by anthropogenic sources. The concentrations of tritium in the precipitation has been steadily decreasing after its anthropogenic peak cuased by the bomb tests of the 1960s.

3.1.6 Hydrograph Separation

Hydrograph separation is an approach to calculate contributions of various flow components (such as groundwater and runoff) to the streamflow (Healy, 2010). The separation can be performed either on the precipitation event or seasonal basis (Gat, 2010): the latter is of interest in this study. Some of the limitations on the effective hydrograph separation include watershed size, and presence of flow control structure or reservoirs. Gat (2010) states that maximum drainage area of approximately 1,300 km^2 should be subjected to separation techniques that are only based on the discharge data. Another approach is to use chemical and isotopic tracers end-member mixing analysis (EMMA) to establish the mass balance of the tracers. The tracers have to be well characterized and be conservative (i.e. not react along the flow paths in the system). In the two-member mixing analysis, components are groundwater and surface runoff. The surface runoff needs to be characterized carefully to represent assumed homogeneous input across the watershed. The runoff frequently does not only flow across the surface, but also permeates surface soils thus interacting with soil and displacing waters from previous events (Gat, 2010). Due to extensive data collection required for the EMMA, the technique is frequently applied to small watersheds of less than 10 km^2 (Healy, 2010). However, this technique has been applied to watershed of varying sizes from <1 km^2 to 2,050 km^2 (Klaus and McDonnell, 2013).

Some of the assumptions as summarized include (Healy, 2010; Leibundgut et al., 2009)

- thorough mixing of all inflow components by the time the streamflow reaches the sampling point
- conservative nature of selected tracers
- concentrations of tracers in equilibrium with the environment

- linearly independent tracers (for example, only δ^2H or $\delta^{18}O$ can be used as they are dependent on each other)
- sufficiently different initial tracer concentrations in different flow components
- homogeneous concentrations of groundwater across the watershed
- homogeneous concentrations of surface runoff across the watershed

Examples of natural tracers include δ^2H or $\delta^{18}O$, chloride, silica, and tritium.

3.2 Riverine Carbon Exports

Riverine exports of dissolved organic and inorganic carbon are an important component of the Arctic Ocean's carbon budget. Figure 2 shows major stocks and fluxes of carbon through the northern polar region. Some of the estimates of total dissolved carbon transferred to the ocean via rivers range from 54 Tg C (Anderson et al., 1998) to 80 Tg C per year (McGuire et al., 2010). Based on the carbon mass estimates provided by Anderson et al. (1998) the dissolved inorganic carbon (DIC) exported to the Arctic Ocean via rivers constitutes approximately 1% of the total oceanic DIC inputs and exported riverine DOC constitutes up to 15% of the total oceanic DOC inputs on an annual basis. The residence time of carbon in the Arctic Ocean varies greatly from four to five years in the coastal seas to over 400 years in the deepest sections of the Canadian and Eurasian oceanic basins (Anderson et al., 1998).

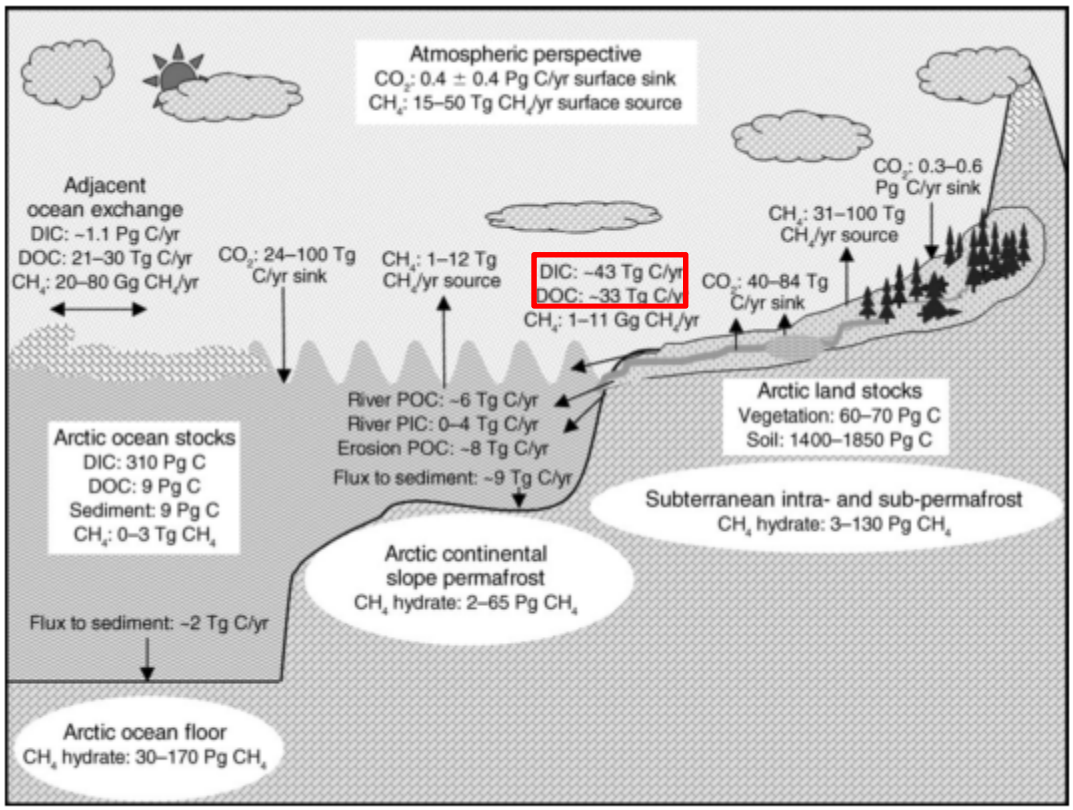

FIG. 3. The current state of the Arctic carbon cycle based on a synthesis of the information presented in this review. Values shown are the ranges of uncertainty.

Figure 2 **Carbon Budget of the Northern Cryosphere (McGuire et al., 2009, reproduced with permission). Riverine DIC and DOC exports to the Arctic Ocean are outlined in the red box.**

Carbon locked in terrestrial permafrost areas is considered to be a large pool of 1,400 to 1,850 Pg C (McGuire et al., 2010). Organic carbon stores in the permafrost soils make up approximately half of the global soil carbon (Holmes et al., 2013). A variety of potential disturbances such as permafrost degradation and hydrological cycle changes may lead to larger portion of the carbon stocks becoming mobile and available for uptake and export.

Dissolved Inorganic Carbon or DIC in the rivers consists of carbonate species H_2CO_3, HCO_3^-, CO_3^{2-} and dissolved CO_2 in its aqueous phase. At the near neutral pH levels that characterize the majority of large Arctic rivers, the principal component of DIC is bicarbonate, however CO_3^{2-} and CO_2 may play an important role in the biogeochemical interactions. The rivers are the main sources of bicarbonate to the oceans. The equilibrium of carbonate species in the Arctic Ocean is an important balance as carbonate controlled pH may affect saturation state of calcium

carbonate. Low water temperatures of the Arctic Ocean and its seas result in particular susceptibility to acidification. Decreasing saturation index of $CaCO_3$ minerals calcite and aragonite below 1 may lead to dissolution of calcifying layers of shells and skeletons of marine organisms (Tank et al., 2012).

The main sources of bicarbonate and carbonate DIC species in river waters are chemical weathering of silicate or carbonate bedrock in the watershed, glacial weathering and weathering of particulate inorganic carbon in-stream during downriver transport (Tank et al., 2012). The weathering process is an important terrestrial CO_2 sink (Holmes et al., 2013); however, the partial pressures of CO_2 in the rivers are usually greater than atmospheric resulting in overall CO_2 flux from the water to the atmosphere (Striegl et al., 2007). The decomposition of organic material constitutes the second major source of DIC in the form of CO_2 mineralized from the organic matter (Hernes et al., 2014).

Dissolved Organic Carbon or DOC, also known as terrigenous DOC (Hernes et al., 2014), in the rivers originates from the soluble phases of organic matter derived from plant, animal and microorganism activities and consist of humic and non-humic fractions (British Columbia Ministry of the Environment, n.d.). Flushing of DOC from soil to water represents a net source of CO_2 to the atmosphere (Holmes et al., 2013). The main sources of DOC in river waters are influx of DOC rich waters that have come into contact with terrestrial material in its flow path and biological activity occurring directly in the river and its tributaries.

4 Ogilvie River

4.1 Site Location

This thesis is focused on the watershed of the Ogilvie River, Yukon. Drainage area above the crossing of Ogilvie River and the Dempster Highway, excluding the contributions of Engineer Creek, was included in this study, further referred to as upper Ogilvie River (Map A) or the study watershed. Ogilvie River, located in central Yukon, flows west to east and is a tributary of Peel River (77,000 km^2 watershed) which in turn flows further east to join north-flowing Mackenzie River that discharges to the Arctic Ocean. The main sampling point on the Ogilvie River was located at 65°21′30.6″N, 138°18′19.8″W.

The upper Ogilvie River watershed drains undeveloped area of approximately 4,475 km^2 (Map B). The area is dominated by stream water features with few lakes. Main orientation of the slopes are north and south facing with only a small portion of flat areas mostly along the bottom of the river valleys. The elevations range from 567 to 2,134 m amsl with the average elevation of 1,030 m amsl.

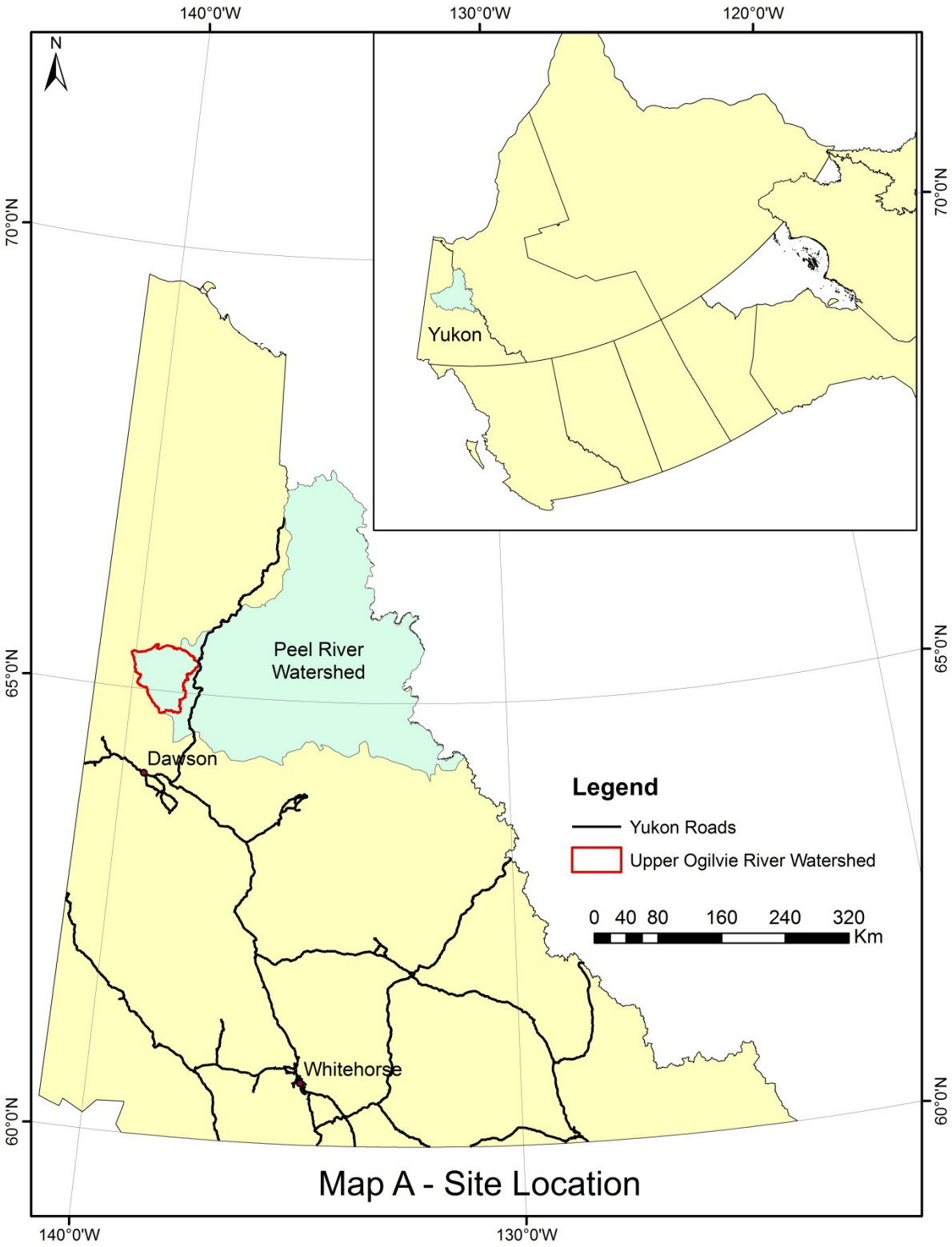

Map A - Site Location

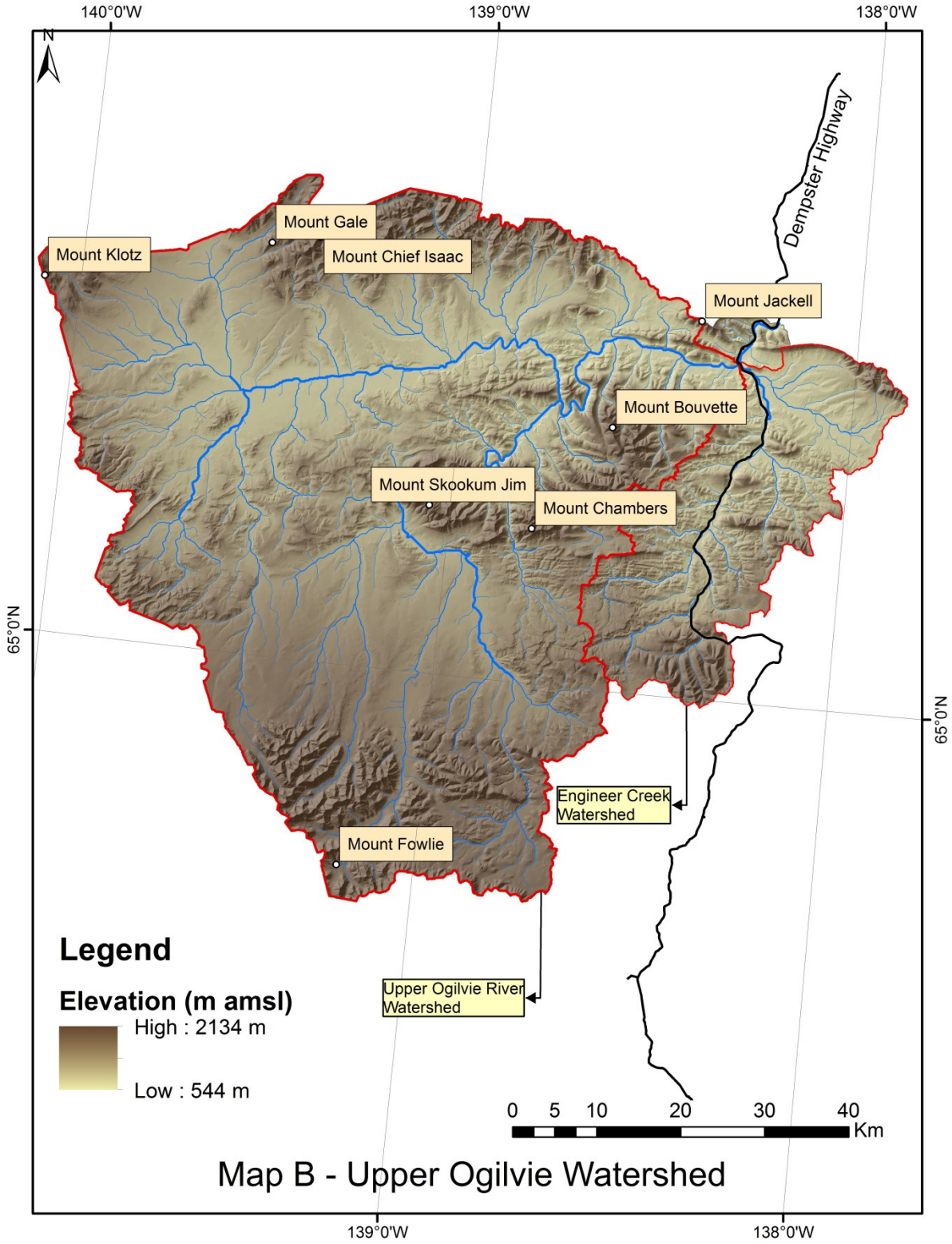
140°0'W
139°0'W
138°0'W
N
Dempster Highway
Mount Gale
Mount Klotz
Mount Chief Isaac
Mount Jackell
Mount Bouvette
Mount Skookum Jim
Mount Chambers
65°0'N
Engineer Creek Watershed
Mount Fowlie
Upper Ogilvie River Watershed
Legend
Elevation (m amsl)
High : 2134 m
Low : 544 m
0 5 10 20 30 40
Km
Map B - Upper Ogilvie Watershed
139°0'W
138°0'W

4.2 Permafrost

The study site is entirely located in a permafrost region. Various literature sources identify the type of permafrost differently: either continuous (Heginbottom et al., 1995; Smith and Lesk-Winfield, 2012), widespread discontinuous (Fisheries and Environment Canada, 1978; Heginbottom and Radburn, 1992), or as a mix of both (Brown et al., 1998). See Table 1 in Appendix A for a more detailed summary. For the purposes of hydrological analysis of this thesis, the watershed is considered to be underlain by widespread discontinuous permafrost with low to medium ice content. According to the permafrost index map developed by Gruber (2012) for the equilibrium conditions, the permafrost in the upper Ogilvie watershed is present in all conditions at the higher elevations of the watershed and in medium-favourable conditions along the stream channels. Such distribution, in general, corresponds to the discontinuous permafrost zone on the International Permafrost Association (IPA) map (Brown et al., 1998).

The information on the permafrost thickness is scarce and variable. The available values are 2.1 - 27.4 m (Smith and Lesk-Winfield, 2012), 79 to 89 m (Taylor et al., 1998), and as deep as 244 m (Smith and Burgess, 2002). Mean annual ground temperature is less than or equal to -4.3°C (Smith and Burgess, 2000). Available information on permafrost thickness and temperatures are summarized in Table 2 of Appendix A.

The available information on the active layer depth in the area around sampling locations ranges from 35 to 80 cm (Idrees et al., 2015; Lacelle et al., 2009).

4.3 Geology

The upper Ogilvie watershed is located in the Mackenzie Platform of the Foreland belt (Mougeot and Walton, 1996). Many folds of the Taiga-Nahoni Fold Belt bring the older (Proterozoic and lower Paleozoic) rock units to the surface. Generally, sedimentary formations older than 130 Ma, such as black calcareous shale and limestone; Ogilvie Formation limestone; Michelle Formation black shale, limestone, and dolomite; Unnamed Shale unit; and Road River Formation black shale and limestone, are of marine origin. These rocks are overlain by younger non-marine sedimentary and unconsolidated clastic strata (Mougeot and Walton, 1996).

The description of the bedrock of the watershed is based on the digital data set by the Yukon Government (Yukon Geological Survery, 2001) which compiled information from the 1982

geological map of Ogilvie River by D.K. Norris and the 1995 geological compilation of the geology of Dawson area by R. Thompson (Norris, 1982; Thompson, 1995).

The majority of the geologic units are of Paleozoic and Cenozoic eras, with some areas formed as early as late Proterozoic era. Unconsolidated quaternary deposits of silts, sands and gravels are located along the main Ogilvie River channel and in the Taiga Valley south of Mount Skookum Jim and Mount Chambers. The bedrock surfaces of pediments are mostly covered with colluvium and/or organic deposits.

Lower Proterozoic shale deposits, thrust upwards by faults, surround the Ordovician Bouvette Formation dolostone in the areas of Mount Skookum Jim, Mount Chambers and Mount Bouvette south of the Ogilvie River. Carboniferous and Permian shale, chert and limestone lie between the main river valley and the above mentioned mountains (Pyle et al., 2007).

The southern part of the watershed is underlain by middle Proterozoic to lower Devonian shales, siltstones and mudstones with multiple small intrusions of diorite and gabbro sills and dykes.

Mount Klotz area in the northwestern part of the basin is composed of Carboniferous/Permian sedimentary rocks such as siltstone, sandstone, limestone, mudstone and shale. Similar formations can be found in the folds along the north edge of the watershed from Mount Gale and Mount Chief Isaac in the mid-east to Mount Jackell in the west.

Two distinct upper Cambrian to lower Devonian outcrops of marine limestone and dolostone formations are located in the west and south of the watershed.

All areas outside of the unconsolidated deposits are characterized by multiple faults as well as fold trains and associated syncline-anticline systems. North of the main river valley, in the Nahoni range, the folds are oriented approximately north-south. South and west of the river valley, in Taiga ranges, the orientation is primarily east-west.

Overall, the surficial geology consists of sedimentary bedrock (63%), much of which is carbonate, and unconsolidated deposits (36%) as shown on Map C.

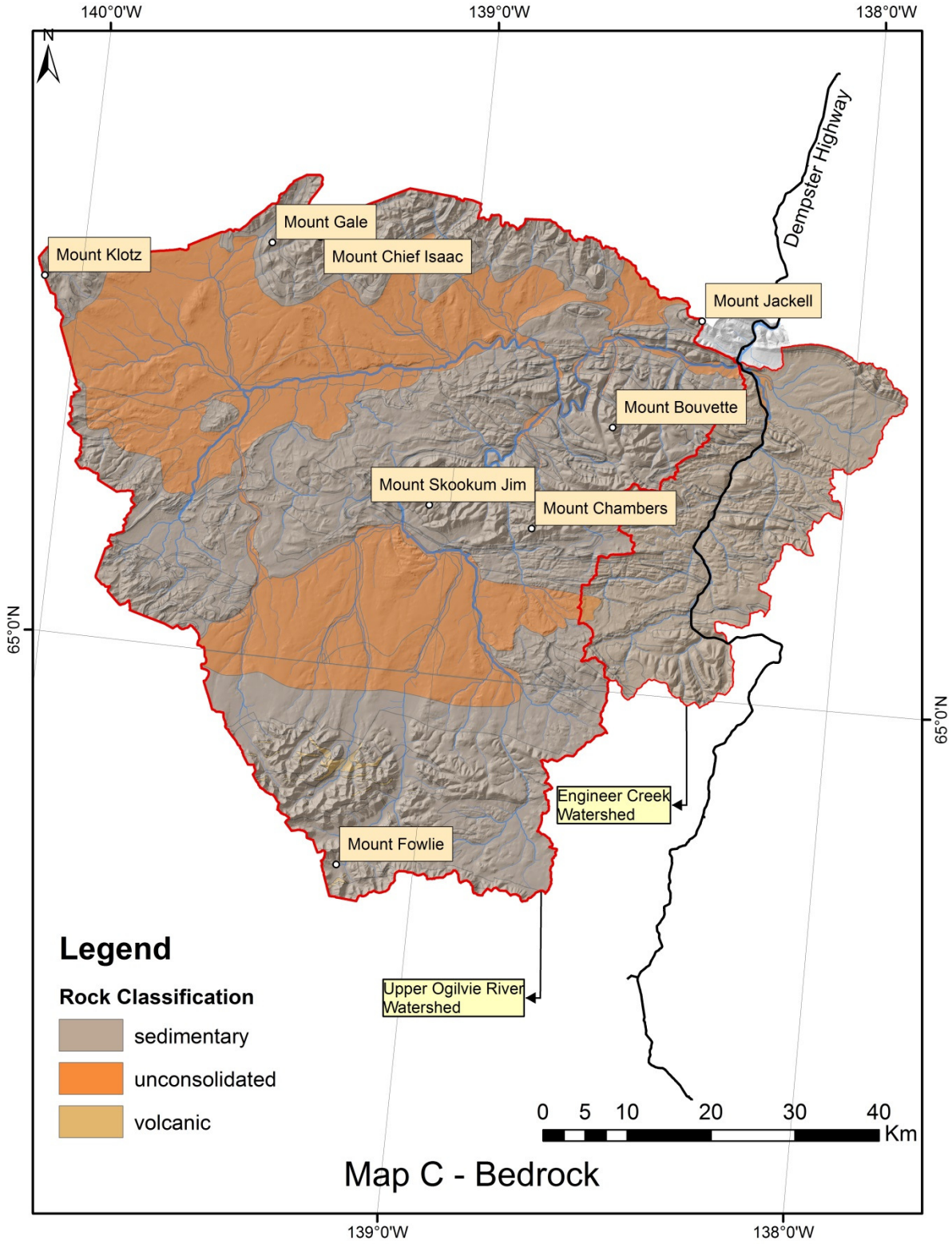
140°0'W
139°0'W
138°0'W
N
Dempster Highway
Mount Gale
Mount Klotz
Mount Chief Isaac
Mount Jackell
Mount Bouvette
Mount Skookum Jim
Mount Chambers
65°0'N
Engineer Creek Watershed
Mount Fowlie
Upper Ogilvie River Watershed
Legend
Rock Classification
sedimentary
unconsolidated
volcanic
0 5 10 20 30 40
Km
Map C - Bedrock
139°0'W
138°0'W

4.4 Ecozone: Physiography, Soils, and Vegetation

Ogilvie watershed is located in the North Ogilvie Mountains Ecoregion of the Taiga Cordillera Ecozone (Yukon Ecoregions Working Group, 2004) which was mostly unglaciated during the last glaciation period. Part of the North Ogilvie physiographic region, the area is characterized by many streams, deep cut valleys, flat topped hills, and castellations. There are infrequent forest fires ignited by a lightning strike usually affecting small areas (Yukon Placer Secretariat, n.d.).

The upper Ogilvie River watershed is mainly undeveloped; however, some exploration activities took place in the 1960s and 1970s. Seismic exploration lines were located in two areas in the west most end of the watershed and in one area at the northeast extent (Canadian Parks and Wilderness Society, 2004). The watershed is home to major waterfowl migration route and is also used by the Porcupine Caribou Herd (Canadian Parks and Wilderness Society, 2004).

The watershed is mostly covered with turbel-type gelisol order soils where the ground is not bare (Tamocai et al., 2002). Many bare limestone mountain tops are succeeded by coarse-gravelled covered upper slopes, well-drained middle slopes that are capable of supporting aspen and white spruce vegetation, and valley bottoms with abundant moisture content and permafrost. Near-surface permafrost may be absent along the gravelly river valleys. (Yukon Ecoregions Working Group, 2004).

Located in the Taiga Cordillera Ecozone, the land cover consists mainly of herb-type vegetation (grasses, forbs, sedges, etc.) and low shrubs. Occurrences of shrub and herb wetlands, sparse and open coniferous forests, lichens and mosses occupy approximately 10% of the land and another 10% is not vegetated (Natural Resources Canada, 2000; Yukon Ecoregions Working Group, 2004). The main vegetation types encountered in the watershed are herbs and low shrubs (Natural Resources Canada, 2000). Aspen, white and black spruce, and tamarack grow in the river valleys (Pyle et al., 2007).

4.5 Glaciation History

Many of the defining physiographical features in the Ogilvie watershed were established at the time of the Pliocene to early Pleistocene Pre-Reid glaciation event (Duk-Rodkin, 1999; Yukon Ecoregions Working Group, 2004). This was the most extensive glaciation event in Yukon and in the study watershed (Bond, 2004). The pediment features such as outwash plains, terraces and

colluvial moraines were the result of a mixture of glaciated and unglaciated corridors at the time. The piedmont glaciers spilled into the western Ogilvie watershed east of Mount Klotz. Glacier drainage is evident in the vicinity of Mount Skookum Jim in the southern tributaries region. Outwash plains and terraces were formed along Ogilvie River and its southern tributaries at the location of the glacier terminus (Duk-Rodkin, 1999; Yukon Ecoregions Working Group, 2004).

Middle Pleistocene Reid glaciation event affected the northwest headwaters of the Ogilvie watershed rerouting the flow of the river north into Miner River, which is now in the Yukon River basin (Duk-Rodkin, 1999; Yukon Ecoregions Working Group, 2004).

Most recent McConnel glaciation of the Late Pleistocene only affected several individual valleys in the Mount Klotz area at the western boundary of the watershed (Duk-Rodkin, 1999; Yukon Ecoregions Working Group, 2004).

4.6 Climate

According to the Köppen climate classification, the central Yukon area is within the Dfc zone characterized by cold climate without a dry season and with cold summers (Peel et al., 2006).

The long term climatic data for the region including the Ogilvie-Mackenzie Mountains climatic zone relies on sparse network of active and inactive weather stations. The weather station closest to the study area is located at the outflow of the Upper Ogilvie watershed at the intersection of Ogilvie River and Dempster Highway. Other weather stations in relative proximity are at Klondike River at Dempster Highway, in Dawson City, and Parkin station southwest of Eagle Plains (Smith et al., 2004).

The North Ogilvie Mountain ecoregion has mean annual air temperatures (MAAT) ranging from -7 to -10°C, with the temperature of approximately -8°C near the Ogilvie River weather station and throughout the watershed (Yukon Ecoregions Working Group, 2004). Temperature inversions in the valleys are not uncommon and due to cold-air drainage, Ogilvie valley is the coldest location along the Dempster Highway, where mean annual air temperatures (-9.2°C) are similar to those of Inuvik (-8.2°C) (Burn et al., 2015; Idrees et al., 2015).

4.7 Precipitation

Available weather records for the study area are from the Ogilvie highway Maintenance camp weather station that was recording temperature and precipitation year-round between 1971 and 2007. Since then, the daily temperatures and summer precipitation are recorded. Not all records are complete with gaps up to several months long not unusual. Only 17 years provide full records (Appendix B). Based on those records, the average annual precipitation is 343 mm comprised of 63% of rain and 37% of snow. These values are comparable to the climate normals for the weather station in Dawson (Table 2).

Table 2 Annual Precipitation Summary

Station	Annual Rain (mm)	Annual Snow (cm)	Total Annual Precipitation (mm)	Notes
Ogilvie River @ Dempster Highway	216.8	126.2	343	Based on 17 years of full-year data between 1971 and 2007. 1 cm snow = 1 mm rain
Dawson A	201.3	166.5	324.4	Climate Normal 1981-2010 1 cm snow = 0.74 mm rain
Notes: Data from Environment Canada, Climate				

A snowpack monitoring station 10MA-SC02 located just south of the flow gauging station has been operational since 1976. Snow depth and snow water equivalency are measured three times a year, around March 1, April 1 and May 1. The values for 2014-2016 are summarized in Table 3 below.

Table 3 Snowpack Measurements at 10MA-SC02 (2014-2016)

Date	Snow Depth (cm)	Water content (mm)	Average Water Content in Snowpack as of 2015 (mm)
26-Feb-2014	62	108	90
27-Feb-2015	66.2	137	
1-Mar-2016	57.5	97	
26-Mar-2014	60	129	106
1-Apr-2015	67	139	
1-Apr-2016	66.25	71	
30-Apr-2014	0	0	72
1-May-2015	53	139	
1-May-2016	45	72	

Note:
Data from Yukon Snow Survey Bulletin & Water Supply Forecast (March, April, May 2014; March, April, May 2015; March, April, May 2016).

4.8 Hydrology

The Ogilvie watershed is located in the Interior hydrologic region which is in the drainage reservoir of Beaufort Sea via Mackenzie River (Yukon Ecoregions Working Group, 2004). Streamflow characteristics of the hydrological region match those of the subarctic nival flow regime. The North Ogilvie Mountains ecoregion has mean annual runoff of 324 mm and mean annual flow of $10.28 \cdot 10^{-3}$ $m^3/s/km^2$ (Yukon Ecoregions Working Group, 2004). Groundwater discharges to the surface year round sustaining winter flow in the Ogilvie River. Spring and river icings (aufeis) are also present in the general area indicating active groundwater systems (Burn et al., 2015; Schreier, 1979; Williams and Smith, 1989).

Hydrologic Atlas of Canada (Fisheries and Environment Canada, 1978) places the study watershed in the Northern Hydrological Regime where the rivers freeze up between November 1 and 15 and become ice-free between May 15 and June 1. The snow cover forms between October 7 and 27 and is lost between April 30 and May 20.

The interior of the Cordillera hydrogeological region is characterized by groundwater of generally good quality that is recharged with snowmelt in late spring and early summer (GIN, 2014).

The groundwater bedrock flow is largely through factures and fault zones (Fisheries and Environment Canada, 1978).

The Upper Ogilvie watershed was gauged historically between 1974 and 1996. The station 10MA002 was located downstream of the sampling point and included flow from the study watershed as well as from Engineer Creek draining a total area of 5,410 km^2 (Maps B and D, marked as Ogilvie River Gauge). Operated by Water Survey of Canada, the station collected flow data manually and seasonally in 1974 and continuously by a recorder starting in 1975. The discharge curves are shown in Appendix C. Based on the hydrographs (Figure 3), the hydrological regime can be characterized as subarctic nival (Woo, 2012), characterized by low winter flows, high discharge spring freshet and late summer flow peaks generated in response to rain events.

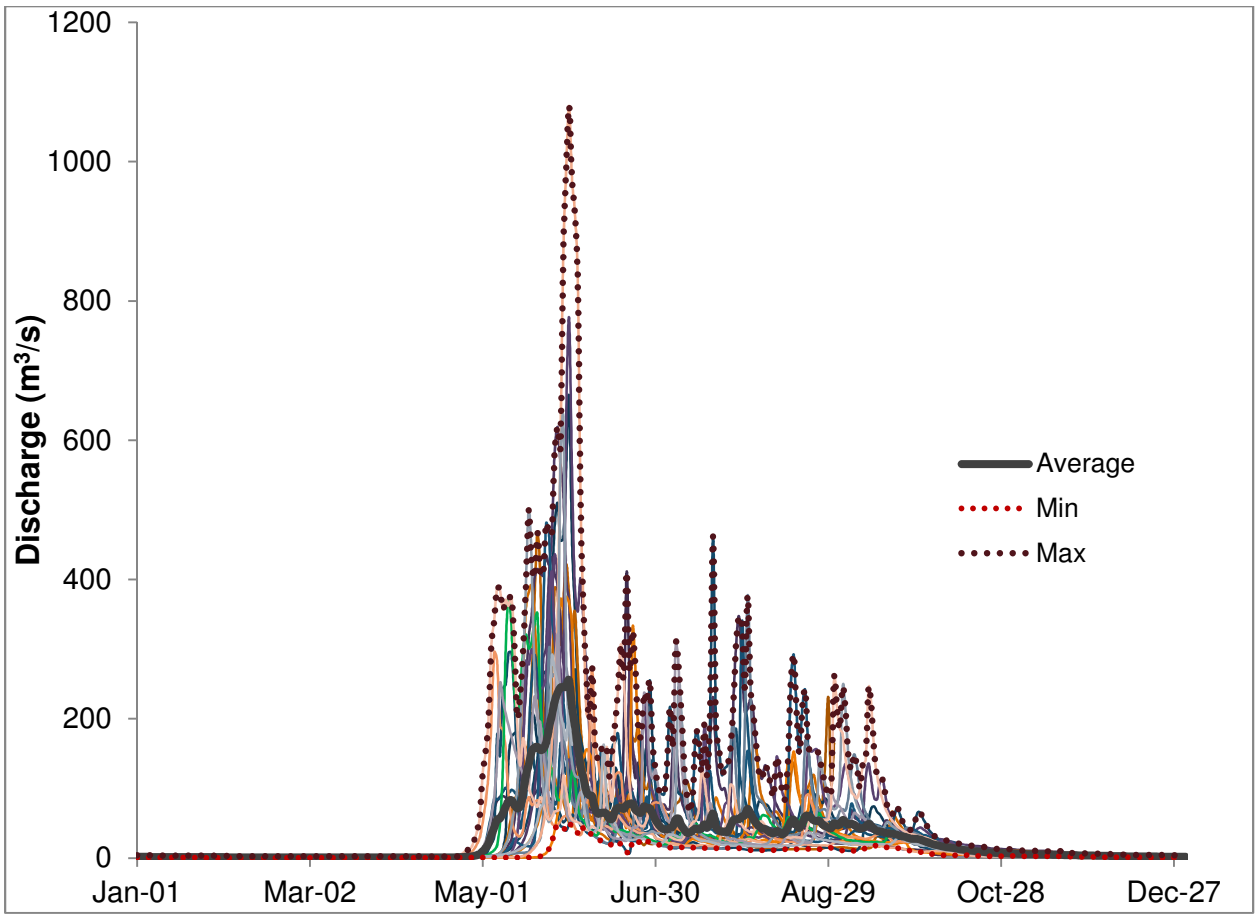

Figure 3 Historical Hydrographs for Ogilvie River at 10MA002 (1974-1996)

4.9 Basin Flow and Precipitation

There are a total of 13 hydrological years (October 1 – September 30) of historical data that have complete or close to complete records of discharge and precipitation measurements (Table 4).

Table 4 Summary of Annual Precipitation and Runoff for the Ogilvie River Watershed including Engineer Creek sub-watershed

Year	Total Annual Discharge (m^3)	Total Annual Precipitation (mm)	Total Annual Precipitation (m^3)	Evapo-transpiration (m^3)	Low Flow (December – March) (m^3)	Runoff Coefficient
1979-1980	9.13E+08	368.5	2.0E+09	1.1E+09	2.02E+07	0.46
1981-1982	1.02E+09	252	1.4E+09	3.4E+08	1.26E+07	0.75
1983-1984	1.02E+09	384.9	2.1E+09	1.1E+09	1.20E+07	0.49
1985-1986	6.36E+08	251.4	1.4E+09	7.2E+08	1.13E+07	0.47
1986-1987	9.99E+08	396.5	2.1E+09	1.1E+09	1.56E+07	0.47
1987-1988	1.15E+09	421.8	2.3E+09	1.1E+09	1.91E+07	0.51
1988-1989	8.38E+08	356.6	1.9E+09	1.1E+09	2.18E+07	0.43
1990-1991	9.27E+08	338.8	1.8E+09	9.1E+08	2.55E+07	0.51
1991-1992	1.06E+09	335.5	1.8E+09	7.5E+08	1.46E+07	0.59
1992-1993	1.04E+09	328.1	1.8E+09	7.3E+08	1.19E+07	0.59
1993-1994	1.02E+09	388.9	2.1E+09	1.1E+09	2.50E+07	0.48
1994-1995	1.31E+09	343.2	1.9E+09	5.4E+08	1.32E+07	0.71
1995-1996	5.74E+08	339	1.8E+09	1.3E+09	7.29E+06	0.31

Notes:
(a) The data is presented for a hydrological year from October 1 to September 30
(b) Watershed area is 5,410 km^2

The average total annual discharge was $9.6 \cdot 10^8$ m^3. Runoff coefficient ranged from 0.31 to 0.75 with an average of .52. The average value is in line with the 0.4 to 0.6 range typical of low Arctic and above the world average of 0.38 (Woo, 2012). The low flows during the winter period of December to March did not show any trend over the available data period.

4.10 Historical studies

4.10.1 Water Quality

The area of the Ogilvie River has been studied in two main contexts. In the late 1970s, the route of the proposed Alcan pipeline passed through the watershed. The water quality and microbiological activity of Ogilvie River was studied in the field in 1978/79 by L.J. Albright and H. Schreier resulting in several publications (Albright, 1980; Albright et al., 1980; Ennis and

Albright, 1982; Schreier, 1979; Schreier et al., 1980). More recently, the Dempster Highway conditions have been examined in light of permafrost degradation along the highway corridor (Burn et al., 2015; Idrees et al., 2015).

Schreier (Schreier, 1979; Schreier et al., 1980) studied a section of Ogilvie River from the air strip, approximately six kilometers upstream of the Dempster Highway bridge, down to where Ogilvie River departs from the highway. They described the watershed to have sedimentary bedrock geology and continuous permafrost with springs and groundwater discharge along the channel. Sampling points 10, 11, and 12 are the within the upper Ogilvie watershed. The water quality sampling included assessment of temporal and spatial variation of parameters such as dissolved oxygen (DO) cations (Ca^{2+}, Mg^{2+}, K+, Na^{+}), anions (Cl^{-}, SO_4^{2-}, HCO_3^{-}), nitrogen, organic components, pH and specific conductance. At the time, the watershed was gauged and flow records were available. The six sampling events assessed conditions in peak flow, late summer flow, freeze-up, mid-winter, late winter, and during or after ice break-up. The general trends for their study area were as follows: DO, Fe, N-compounds, P and trace metals decreased their concentration through the winter and then spiked during the freshet; alkalinity, Ca^{2+}, Mg^{2+}, Na^{+}, Si and SO_4^{2-} concentrations exhibited a reverse trend of reaching highest concentrations in late winter. The groundwater discharge was thought to be controlled by a series of limestone and shale syncline-anticline features orthogonal to the river channel. The authors concluded that several groundwater sources were present each feeding a different section of the stream and the winter flow was partially discontinuous. The water in the river and below the riverbed was thought to be forced up along the upstream side of a fold resulting in open water sections on top of the anticlines. Then the water was forced downwards towards the syncline resulting in river aufeis caused by overflow.

The microbiological investigations, reported by Albright (Albright, 1980; Albright et al., 1980), included examination of microbiological activity and its vulnerability to potential suspended sediment loads due to construction. The water quality parameters of interest were dissolved organic carbon (DOC), particular organic carbon (POC), total inorganic carbon (TIC). TIC, DO and DOC concentrations peaked in later spring-summer and dropped to their minimum in fall-winter. DOC reached the lowest concentration of ~1.2 mgC/L in December and then spiked to its maximum concentration of ~10.2 mgC/L in May during spring melt. POC concentrations

followed the same pattern as DOC but remained at lower levels than DOC by 50% or more. TIC exhibited a reverse trend to DOC, staying high (35-50 mgC/L) throughout the winter and decreasing to its minimum of 9 mgC/L at spring melt. Light and DOC were considered to be limiting factors for the microbial activity that was highest in spring and summer. In the late fall and winter, the phytoplankton and bacteriaplankton came under physiochemical stress.

The DO saturations levels were closest to full saturation during spring break-up and at fall freeze-up (up to 15 mg/L). The DO concentrations were slightly below peak in the summer and they reached lowest concentrations in the winter (as low as 5 mg/L). Respiration rates range from 0.048 mg O_2/L/d in late winter to 0.15 mg O_2/L/d during freshet.

The biological activity of the river is most sensitive to particulate loadings, such as organic-containing streambank and sediment materials, in the winter time. At this time of year of reduced light availability, the limited availability of DO would be further reduced via respiration. Microbial attempts to re-establish themselves would be hampered by layers of silt on the streambed.

4.10.2 Permafrost Conditions

The baseline data collection and assessment of the permafrost conditions along the Dempster Highway began in 2013-14 with the establishment of four long-term monitoring sites (Burn et al., 2015; Idrees et al., 2015). Based on the 2004 climatic data from the Ogilvie Highway maintenance camp, annual mean air temperatures (AMAT) of -9.2°C, winter mean air temperatures (WMAT) of -29.7°C, summer mean annual temperatures (SMAT) of 13.2°C, rainfall of 104.4 mm and snowfall of 176.5 cm. Mean annual ground temperature (MAGT) at a 2009 borehole drilled by A. G. Lewkowicz (Lacelle et al., 2009) was -2.5°C. Site 1, located 15 km east of the upper Ogilvie watershed, was found to have thin permafrost of approximately 7 metres. The thin permafrost was attributed to shallow groundwater circulation transferring additional heat into the system. Developed groundwater system presence was also supported by extensive icing in the adjacent Blackstone River. The main geohazards in the Engineer Creek and Ogilvie valleys are rock slides off the bare road-side slopes, landslides, and flooding during spring melt and heavy rain events.

5 Field Methodology

The upper Ogilvie River watershed was selected as a continuation of the hydrological research at the Wolfe Creek basin near Whitehorse (Li, 2013) in the sporadic discontinuous permafrost area and at the North Klondike basin in the Tombstone Territorial Park (Lapp, 2015) in the discontinuous permafrost zone. The study site located sequentially further north is representative of the widespread discontinuous permafrost conditions.

Samples of the Ogilvie River water, surface runoff, rain precipitation, snowpack, groundwater, active layer water, and soil samples were collected in order to distinguish the geochemical and isotopic signatures of the hydrological system constituents. All sampling locations are shown on Map D.

Main sampling location of upper Ogilvie River was selected based on several factors such as the ease of access via the Dempster highway and availability of the support by the Dempster highway maintenance personnel. This watershed has minimal local anthropogenic effects and as such presents a good medium-sized watershed to study natural hydrological conditions. Ogilvie River above confluence with Engineer Creek was selected to remove any influences of the acid rock drainage historically observed in this tributary (Kwong et al., 2009).

Because of the difficulty of access further upstream on the Ogilvie River, several surface run-off tributaries were selected slightly downstream. These tributaries (C1, C2, and C3 on Map D) flow through similar terrain as those within the study watershed and were, therefore, considered to be adequate analogue sampling points.

Some opportunistic samples were collected including drinking water samples at the Ogilvie Highway Maintenance Camp which originated in a shallow well and soil samples (grab and soil cores).

Samples were collected over two active flow seasons in 2014 and 2015. The timing of the sample collection targeted the following flow conditions: pre-spring freshet (late April), during spring freshet (early to mid-May), and late summer flow conditions (mid- to late August). Additional samples in the summer time and in early fall were collected by the highway maintenance camp personnel.

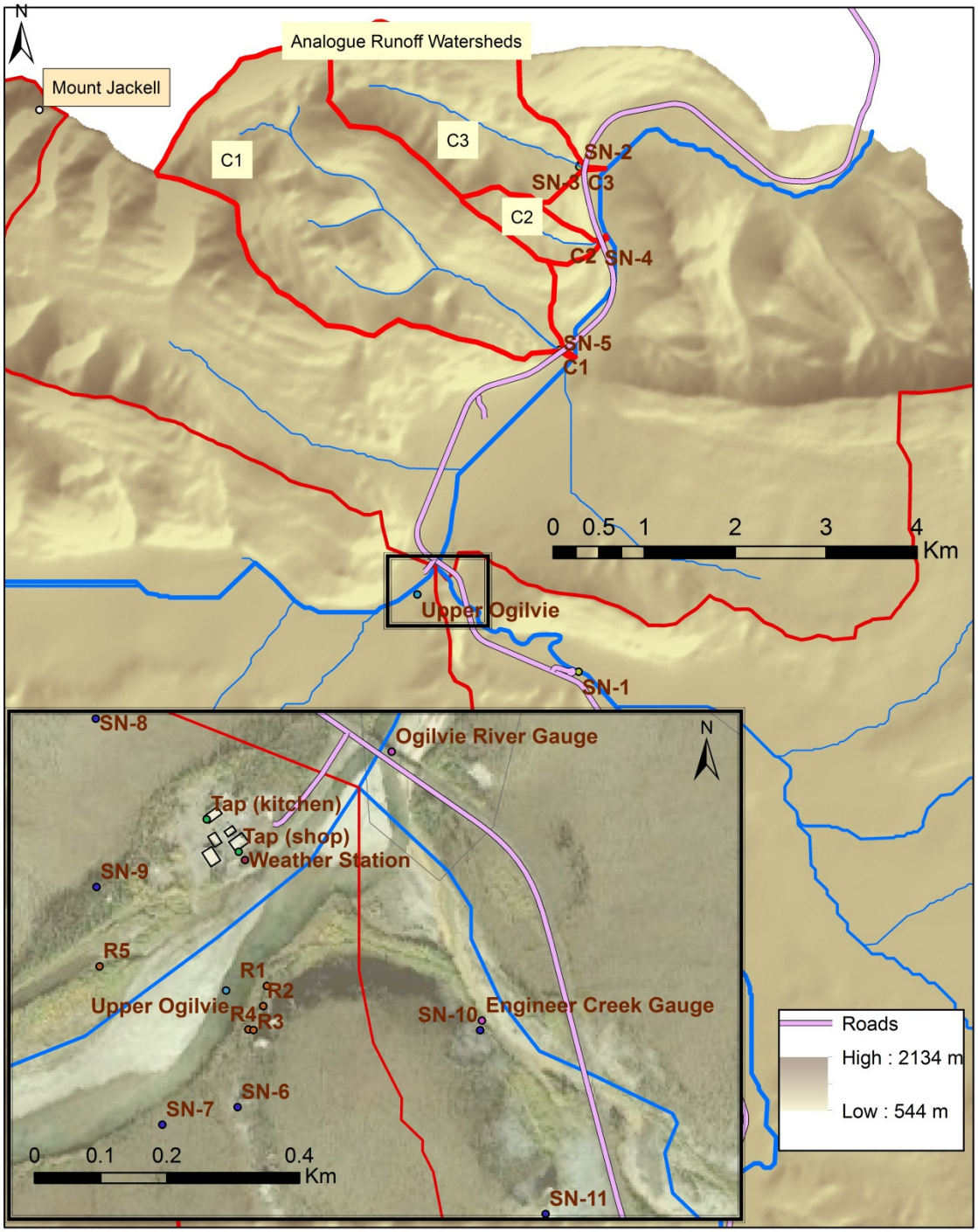

Map D - Sampling Locations

5.1 Flow Gauging

To quantify the discharge of the upper Ogilvie River a pressure transducer (Solinst LTC Levelogger Junior, Model 3001) was installed to monitor the stage. The location of the transducer installation was selected to coincide with the historical rating curve location on the downstream side of the Dempster Highway bridge (Hydrometric Station 10MA002). This point is downstream of the confluence with Engineer Creek. A second pressure transducer of the same model was installed to monitor Engineer Creek and a rating curve was developed to correlate stage and flow. The data obtained by the pressure transducers was corrected for the barometric pressure recorded by a separate logger (Solinst Barologger, Model 3001) deployed in the area. The Engineer Creek discharge was subtracted from the Ogilvie River discharge at the bridge to obtain the discharge at the sampling point. Locations of the probes are shown on Map D.

The transducer probe installation in the Ogilvie River was attempted in the spring of 2014. By the late summer it became clear that the probe was lost due to insufficiently strong anchoring technique required for maximum freshet flows. New probes were deployed in Engineer Creek and Ogilvie River in April 2015 before the start of the spring runoff event. The Ogilvie River probe was removed for the period between May 10 and 14, 2015, when large volumes of ice in the river posed danger to the probe. Manual water level measurements were taken several times a day during this period. All probes recorded data until permanently removed on April 24, 2016.

Appendix C includes the historical rating curve for Ogilvie River, the newly developed rating curve for Engineer Creek and the hydrographs for the 2015 flow season.

5.2 Surface Water Sample Collection

Surface water from the Ogilvie River, analogue tributaries C1, C1, and C3, and from surface seeps was collected as grab samples directly from the streams. In-stream temperature, pH, and conductivity were collected using YSI Professional Plus multi-parameter probe. The samples were processed within 24 hours of sample collection as outlined in Table 5.

Table 5 Field Water Sample Processing Summary

Analyte	Bottle Type	Processing
Dissolved Organic Carbon (concentration and $\delta^{13}C$)	40 mL EPA amber vial	Filtered with 0.45 µm nitrocellulose filter (note a). Added PTFE-rubber septa to the EPA vial (note b).
Dissolved Inorganic Carbon (concentration and $\delta^{13}C$)		
Dissolved Organic Carbon ($F^{14}C$)	Spring 2014: LDPE plastic (1L) Summer 2014: HDPE plastic bottle (1 L); Spring and Summer 2015: 500 mL glass amber bottles, some HDPE plastic (1L)	2014: None 2015: Field filtered with 0.45 µm nitrocellulose filter (a)
Dissolved Inorganic Carbon ($F^{14}C$)		
$\delta^{2}H$ and $\delta^{18}O$	15 mL or 50 mL plastic tube	Filtered with 0.45 µm nitrocellulose filter
Anions/Cations	50 mL plastic tube	Filtered with 0.45 µm nitrocellulose filter
Tritium	250-1000 mL LDPE or HDPE plastic	None

Notes:

(a) The filters were leached with at least 100 mL of the sample or the DI water (Khan and Subramania-Pillai, 2006)

(b) PTFE-rubber septum was added to prevent CO_2 diffusion through the septa.

Samples collected by the maintenance camp staff were stored unrefrigerated in plastic LDPE (2014) and HDPE (2015) bottles until pick up.

5.3 Field Alkalinity

Alkalinity titrations were performed in the field within 24 hours of the sample collection. The water was filtered using 0.45-µm nitrocellulose filter and titrated using HACH digital titrator with 1.6N or 0.16N sulphuric acid cartridges. A 100-mL filtered sample was titrated to an end point of pH=4.2 and pH was further lowered to below 4. Measurements of pH were made using YSI Professional Plus probe.

The field alkalinity was determined using Gran Function method (USGS, 2012). The F_1 Gran function (Equation (2) was calculated and plotted against volume of acid added.

$$F_1 = (V_0 + V_t) \cdot (10^{-pH})/\gamma \qquad \textbf{(2)}$$

where:

F_1 is the Gran Function
V_o is the volume of the sample (mL)
V_t is the volume of titrant (acid) added (mL)
γ is the activity coefficient for H^+ (set to 1)

The x-axis (volume of acid added) intercept of the straight line fitted to the linear portion of the F1 plot beyond the bicarbonate equivalence was considered to be the end point of the titration.

The hydrogen ion activity corresponding to the end-point volume of added titrant was used to calculate the alkalinity (Equation (3)

$$Alk\left(\frac{meq}{L}\right) = \frac{B(mL) \cdot C_a\left(\frac{eq}{L}\right) \cdot CF}{V_o(mL)} \cdot 1000 \qquad \textbf{(3)}$$

where:

B	is the volume of titrant (acid) added to reach bicarbonate equivalence point (mL)
C_a	is the concentration of the titrant (eq/L)
CF	is the correction factor (1.01 when using HACH digital titrator)
V_o	is the volume of sample (mL)

The calculated values of field alkalinities were then converted to ppm C and ppm HCO^{3-}.

5.4 Precipitation Sampling

Basic weather observations are carried out at the Ogilvie highway maintenance camp. Temperature and rain amounts are recorded. Precipitation in the winter is not monitored. Precipitation amount data for January 2014 to April 2016 was provided by the Government of Yukon (2016). There are many gaps in this record. Camp staff assisted with the collection of the rain samples throughout the 2014 and 2015 summers. The samples were collected from the rain gauge at the time of daily weather observations and stored at ambient conditions in 50 mL plastic tubes.

Snowpack samples were collected on April 23 and 24, 2015. Some ripening of the snowpack has begun at the time of sampling, however, samples are considered to be representative of the isotopic signature of the snowpack. A total of eleven locations were sampled with the depth of snowpack separated into three intervals (see Map D for sampling locations). A more detailed profile consisting of five samples was collected at the SN-3 location. Snow was allowed to melt in individual Ziploc bags and then transferred to 15 mL plastic tubes or 500 mL LDPE bottles.

Snow and rain samples were analyzed for δ^2H and $\delta^{18}O$ and several composite samples were analyzed for tritium activity.

5.5 Well Sampling

A shallow drinking water well in the Living Complex of the Ogilvie Highway maintenance camp provides drinking water to the maintenance camp year-round (Map D). The well is

approximately 5.6 m deep advanced through river gravel, cobbles and boulders mixed with sand and silt. The static water level was at approximately 3.6 m below grade at the time of installation. No permafrost was encountered during well installation (Fraser, 2016). The well was locked with a lid on it and, therefore, no visual inspection of the water level at the time of site visits was possible.

An old drinking well located in the Maintenance Garage (shop) appears to be of similar shallow construction. The water level was approximately 2 meters below ground upon visual inspection in August 2014.

According to the staff personnel the water from the wells does not undergo any physical or chemical treatment prior to consumption. The tap water was sampled. In 2014, when the Maintenance Garage well was thought to be the active one, the tap in the garage washroom was sampled (shop). In 2015, when the active well was correctly identified, the kitchen tap in the Living Complex was sampled. No significant difference was identified between the two waters. Samples were processed in similar manner to the surface water samples. Samples collected by camp staff were stored unrefrigerated in plastic bottles until pick-up.

Well samples were analyzed for all or some of DIC, DOC, $\delta^{13}C$, $\delta^{2}H$, $\delta^{18}O$, anions, cations, tritium, and radiocarbon.

5.6 Soil Sampling

Frozen active layer and permafrost samples were collected using a CRREL-style 2-inch diameter auger driven by a hand-held gas-powered STIHL BT-45 drill head. Drilling took place in April and August 2015 in the locations around the highway maintenance camp (Map D). In late summer, grab samples of the thawed active layer were also taken. Samples were collected into Ziploc bags or Iso-Jars for frozen and unfrozen storage and transport.

Soil samples were analyzed for moisture content, organic content, and carbonate content. The pore waters extracted from the samples were analyzed for DIC, DOC, $\delta^{13}C$, $\delta^{2}H$, $\delta^{18}O$, anions, and cations. Soil samples were processed by Patrick Lajoie as part of his undergraduate honours thesis. Only $\delta^{2}H$, $\delta^{18}O$, and $^{13}CO_2$ are discussed in this thesis.

5.7 Transportation and Storage

Water and soil samples were shipped back to the University of Ottawa and stored in the refrigerator prior to analysis. Some soil samples were shipped and stored frozen.

6 Laboratory Methodology

6.1 DIC/DOC and $\delta^{13}C$

Filtered water samples were analyzed for $\delta^{13}C$ on the TIC-TOC analyzer Aurora Model 1030 in order to obtain concentrations of dissolved inorganic and organic carbon (DIC and DOC). Each sample was further passed on to the Finnigan Mat DeltaPlus XP isotope ratio mass spectrometer (IRMS) for the analysis of $\delta^{13}C$ isotopes. The TIC-TOC analyzer uses acidification to extract DIC and subsequent wet oxidation method to extract DOC components of the sample. The analytical precision is 2% for the concentrations and 0.2‰ for the isotopes. The isotope ratio $^{13}C/^{12}C$ results are expressed as $\delta^{13}C$ values with respect to the Vienna Pee Dee Belemnite (VPDB) standard. The analysis was conducted by the G. G. Hatch Stable Isotopes Laboratory at the University of Ottawa.

6.2 $\delta^{2}H$ and $\delta^{18}O$

Water samples were analyzed for $\delta^{2}H$ and $\delta^{18}O$ by laser absorption spectroscopy using the Los Gatos Research (LGR) patented off-axis integrated Cavity Output Spectroscopy (ICOS) on Water Isotope Analyzer. Some samples were re-analyzed using isotope ratio mass spectrometry (IRMS) on the Gasbench coupled with Finnigan MAT Delta plus XP IRMS. The precision for $\delta^{2}H$ and $\delta^{18}O$ is 0.5‰ and 0.1‰ respectively. The isotope ratios $^{18}O/^{16}O$ and $^{2}H/^{1}H$ results are expressed as $\delta^{2}H$ and $\delta^{18}O$ values with respect to the Vienna Standard Mean Ocean Water (VSMOW). The analysis was conducted by the G. G. Hatch Stable Isotopes Laboratory at the University of Ottawa.

6.3 Anions/cations

Cation samples were acidified in their field collection containers with the metal trace grade nitric acid. The samples were then diluted for analysis using DI water for anion analysis and 1% nitric acid for cation analysis. The cations were analyzed by ICP-AES or ICP-MS. The anions were

analyzed by ion chromatography. The analysis was conducted by the Geochemistry Laboratory at the University of Ottawa.

6.4 Radiocarbon

The radiocarbon analysis was performed on the DIC and DOC fraction of the carbon in the water samples. The carbon was extracted as CO_2 using off-line wet oxidation method. The DIC was oxidized under vacuum with 85% ortho-phosphoric acid at ~60°C, extracted, cryogenically purified on a vacuum line and sealed in a Pyrex breakseal. After the DIC extraction, the remaining DOC fraction was oxidized using sodium persulfate or potassium permanganate, in some cases, with addition of silver nitrate as a catalyst. The samples were heated to induce the oxidation reaction. The resulting CO_2 was extracted and captured in a breakseal in the same manner as the DIC CO_2. Carbon amounts between 0.5 and 4 mg C were extracted. The extractions were performed in the G.G. Hatch Stable Isotopes Laboratory at the University of Ottawa.

The CO_2 samples were then converted to graphite via Bosch hydrogen-reduction reaction and analyzed on the 3MV Accelerated Mass Spectrometer by High Voltage Engineering at the A.E. Lalonde AMS Laboratory at the University of Ottawa. Oxalic acid with the $F^{14}C$ of 1.34 was used as a reference material to normalize radiocarbon measurements. Individual measurement errors are calculated to represent 1σ confidence limits.

6.5 Tritium

The expected low tritium activities necessitated tritium enrichment. The enrichment process requires samples to have conductivities below 100 µS/cm. This was achieved either by distillation if the sample was coloured due to organics or by addition of the mixed bed ion exchange resin for clear-coloured samples. The samples then underwent an electrolytic enrichment, a method where lighter isotopes of hydrogen are preferentially electrolyzed thereby concentrating tritium in the remaining water sample. A 250 mL volume of deionized sample was mixed with sodium peroxide and enriched over the period of five days, after which a volume of 13-14 mL was left. The enriched samples were then vacuum-distilled to remove sodium peroxide and 10 mL of the sample was mixed with the scintillation liquid (Ultima Gold LLT). The tritium analysis was performed by liquid scintillation counting on Quantulus 1220 ultra-low level liquid

scintillation counter in the Radiohalides Laboratories at the University of Ottawa. Standards and blanks were enriched and analyzed in the same manner as the samples in order to determine exact enrichment factors and to ensure process quality.

6.6 Soil Gas

The soil gas was analyzed from the headspace of the soil samples collected and stored refrigerated or frozen in Iso-Jars. The analysis was completed on the Delta V Plus Isotope Ratio MS equipped with Agilent Technologies 7890A GC System and GC Isolink furnace. The frozen soil samples were allowed to thaw prior to analysis. Continued or resumed biological activity in samples was minimized by either storing samples refrigerated or by limiting the thawed time of the frozen samples to several days. The gas sample was withdrawn with a syringe through the rubber septa in the lid of the Iso-Jar. The isotopic concentration of ^{13}C in the CO_2 was measured. The ^{13}C signature was not considered to be significantly affected by the storage of the samples as the limited activity of the samples would be representative of the in-situ processes that generate the signature. The analysis was conducted by the G. G. Hatch Stable Isotopes Laboratory at the University of Ottawa.

7 Results

Full results are presented in Appendix C (Discharge Measurements) and Appendix D (Analytical Results). The Ogilvie River discharge data used for historical comparison was obtained downstream of the confluence with Engineer Creek (referred to as discharge at the historical gauging station). The geochemical and isotopic investigation is representative of the Ogilvie River above Engineer Creek. Therefore, the Engineer Creek flow contributions were subtracted from the Ogilvie River flow in order to correlate discharge with water chemistry at that point. The results presented in this section refer to the information collected above Engineer Creek unless otherwise stated.

The main flow components contributing to the Ogilvie River flow were identified based on physical understanding of the system and geochemical/isotopic signatures identified and are summarized in Table 6

Table 6 Summary of Sampled Hydrological Cycle Components

Hydrological Cycle Component	Samples	Notes
Ogilvie River overall discharge	Ogilvie River	
Surface Runoff	Analogue tributaries C1, C2, C3	
Shallow Groundwater	Camp Tap Water collected at Ogilvie Highway Maintenance Camp	Supra- and/or intra-permafrost groundwater
Deep Groundwater	Ogilvie River winter samples	Sub-permafrost groundwater
Active Layer	Surface Seeps (R- and AL- samples)	Aggregate geochemical signature for active layer
Soil Water	Water extracted from soil cores	Active layer water at various depths
Rain	Sampled at precipitation gauge at Ogilvie Highway Maintenance Camp	
Snowpack	SN- samples	
Soil gas	Soil core samples stored in Iso-Jars	

7.1 Ogilvie River

7.1.1 Discharge

The discharge hydrograph for the upper Ogilvie River above Engineer Creek for the period of April 24, 2015, to April 24, 2016, is shown in Figure 4. Also shown is are the precipitation record with its data gaps and daily average temperatures obtained from the barometric logger. The freshet began on May 9, 2015, when the discharge increased rapidly. The peak recorded flow of 526 m^3/s was reached on May 16. However, it is likely that the rough freshet conditions including in-stream ice, due to dynamic ice cover break-up, and high flows shifted the location of the pressure transducer in Ogilvie River. Therefore, many stage values had to be discarded in this period. The peak value was estimated based on the largest available stage value.

It is possible that larger flows than the recorded peak value were reached. For comparison, Engineer Creek flow remained high between May 12 and May 20 with the peak reached on May 17. By June 5, Ogilvie River (at sampling site upstream of Engineer Creek) returned to its baseflow conditions. The summer conditions indicate several local peak flows. Some of the larger events had flows of 31 m^3/s on July 3, 114 m^3/s on July 30, 159 m^3/s on August 29, 61 m^3/s on September 17, 64 m^3/s on October 1, and a late season peak of 110 m^3/s on November 2. The low flows continued to steadily decrease throughout the late fall and early

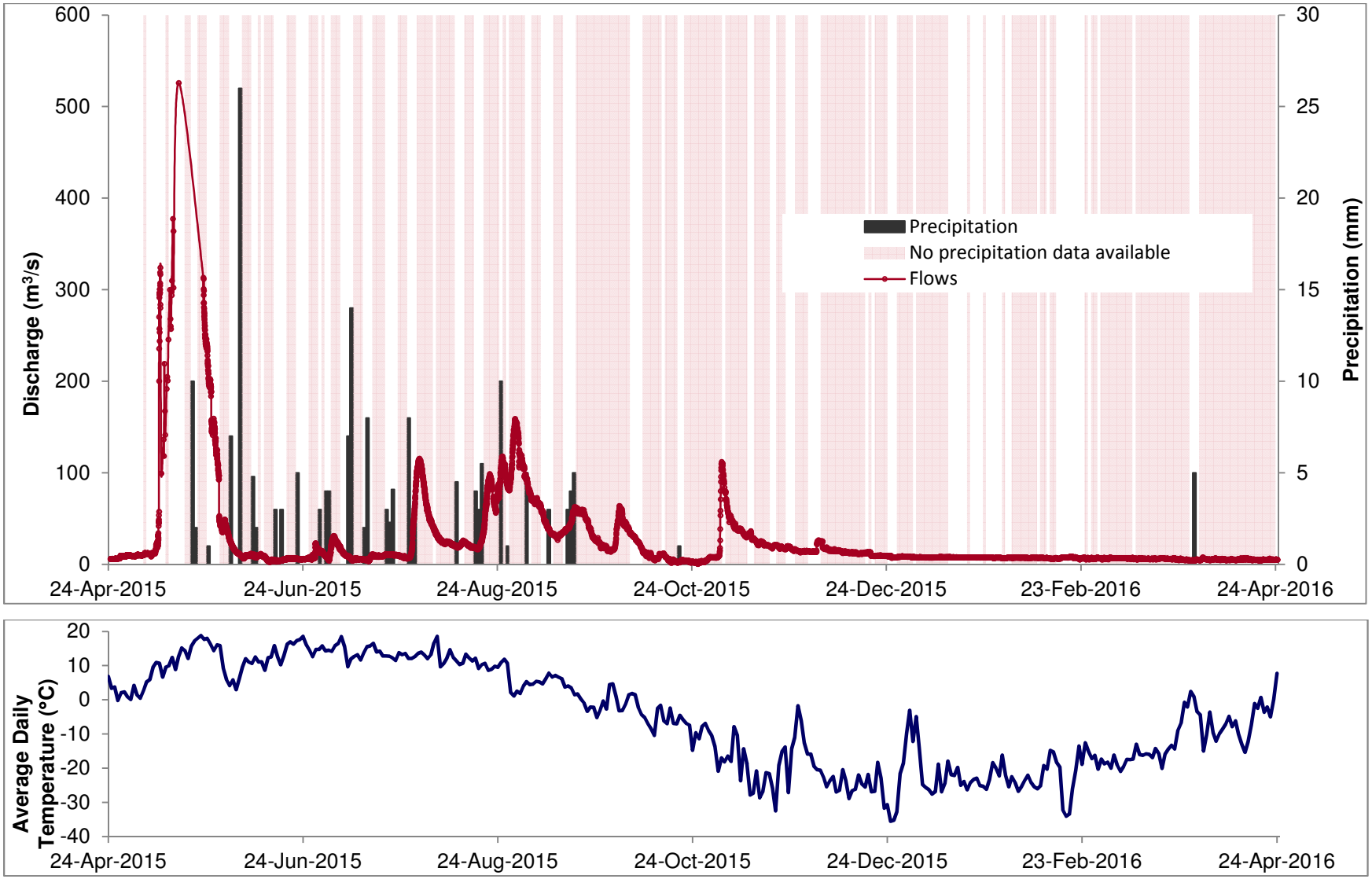

Figure 4 **Discharge hydrograph at the sampling site, upper Ogilvie River, with precipitation data collected at the maintenance camp and air temperature collected by the barometric logger.**

winter reaching flows of less than 10 m^3/s by mid-December and continued to decrease to a minimum of ~5 m^3/s.

As can be seen from Figure 4 the precipitation events did not correspond well to the local flow maxima. For example, a large 26 mm rain event on June 4 did not produce an increase in discharge. Similarly, two consecutive rain days on July 8 and 9 (combined 21 mm) also were not reflected in the hydrograph. On the other hand, rain events on July 27-29 (total of 14 mm), between August 17 and 25 (total of 22.5 mm) and on September 15-17 (total of 12 mm) corresponded to a slightly delayed flow increase. Of particular interest is the rapid flow increase event that started in the evening of November 1 and peaked in the morning of November 2 at 112 m^3/s, on par with the large summer flow peaks. The air temperatures at the barometric logger were fluctuating between -20°C and -8°C during this event. It is possible that a temperature inversion occurred in the valley prone to such events trapping the cold air at the valley bottom (Idrees et al., 2015). If it rained during this time at higher elevations, it would explain the sharp runoff peak in the stream. There are large gaps in the precipitation records, so it is not possible to complete the analysis. It is evident, that the data collected at weather station at the maintenance camp is not always representative of the conditions across the study watershed.

The air temperatures were above 0°C from the start of the monitoring period on April 24 to September 20. The maximum temperatures of 18-19°C were reached several times in the period between May 23 and August 5. Winter temperatures persisted after September 20 reaching the lows of below -30°C three times between November and February. The temperature clearly controls seasonal flow, however, individual precipitation events or local flow maxima are not directly correlated to the air temperature at the weather station.

7.1.2 DIC/DOC and $\delta^{13}C$

The DIC and DOC concentrations and their respective $\delta^{13}C$ signatures in the upper Ogilvie River undergo seasonal changes that are in general consistent between 2014 and 2015. The DIC concentrations as shown in Figure 5 were at their highest in the winter (> 50 ppm C). The concentrations dropped to their lowest at the peak of freshet to around 10 ppm C. The DIC levels increased throughout the summer and, presumably, the fall/winter period. The $\delta^{13}C$ follows a similar general pattern with the lower DIC concentrations corresponding to the more depleted $\delta^{13}C$ signature. The $\delta^{13}C$ values ranged from -11.4‰ to -6.7‰.

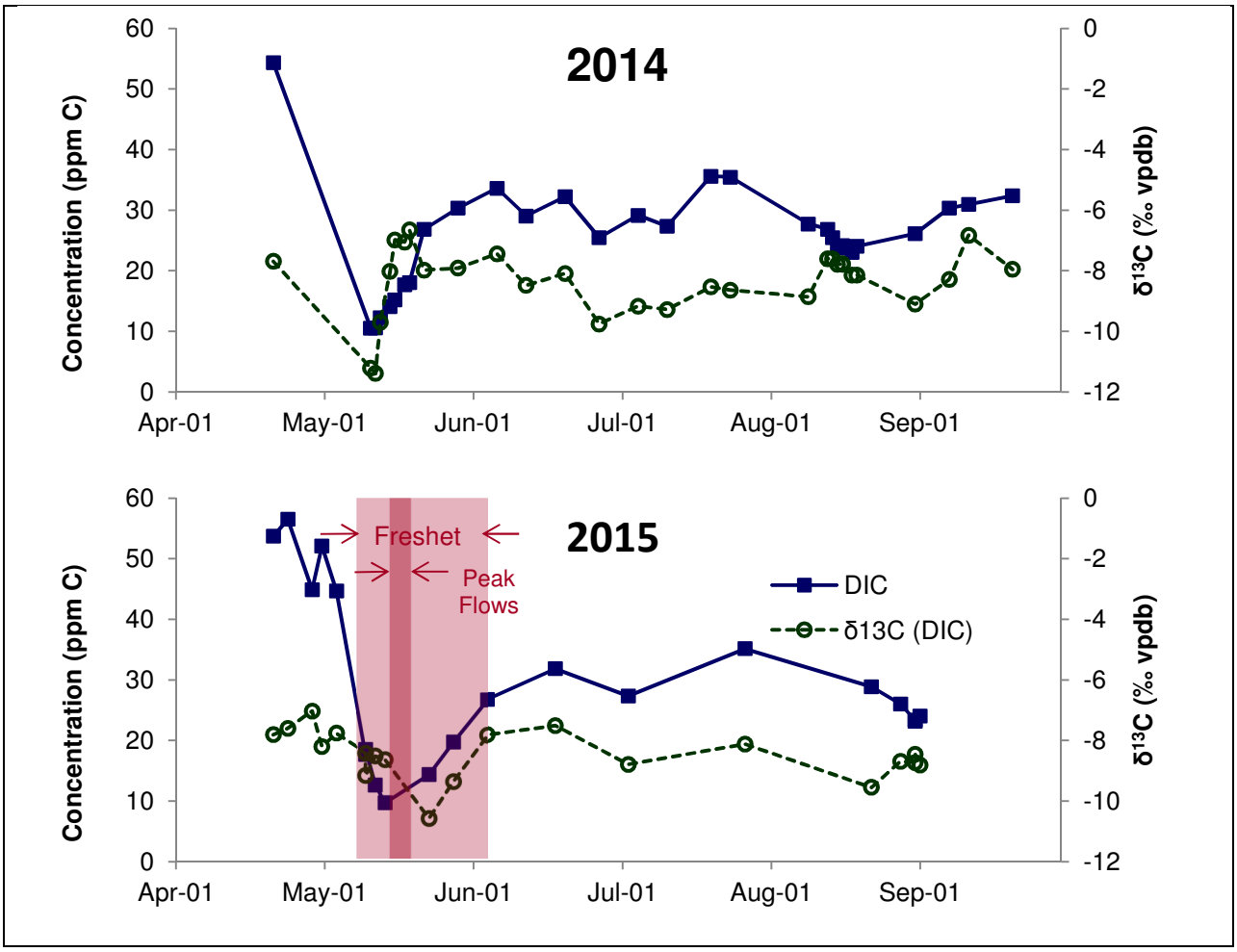

Figure 5 DIC and $\delta^{13}C$ in Ogilvie River at sampling site (2014, 2015)

The DOC concentrations follow a generally opposing trend to the DIC as can be seen from Figure 6. Low winter concentrations of 1-5 ppm C rapidly increased to the freshet peak concentrations of 13-14 ppm C. The summer concentrations fluctuated between 4 and 8 ppm C. It should be noted that the middle of the summer samples were collected by the maintenance camp staff and were stored unfiltered and unrefrigerated until pick up in August and are less reliable.

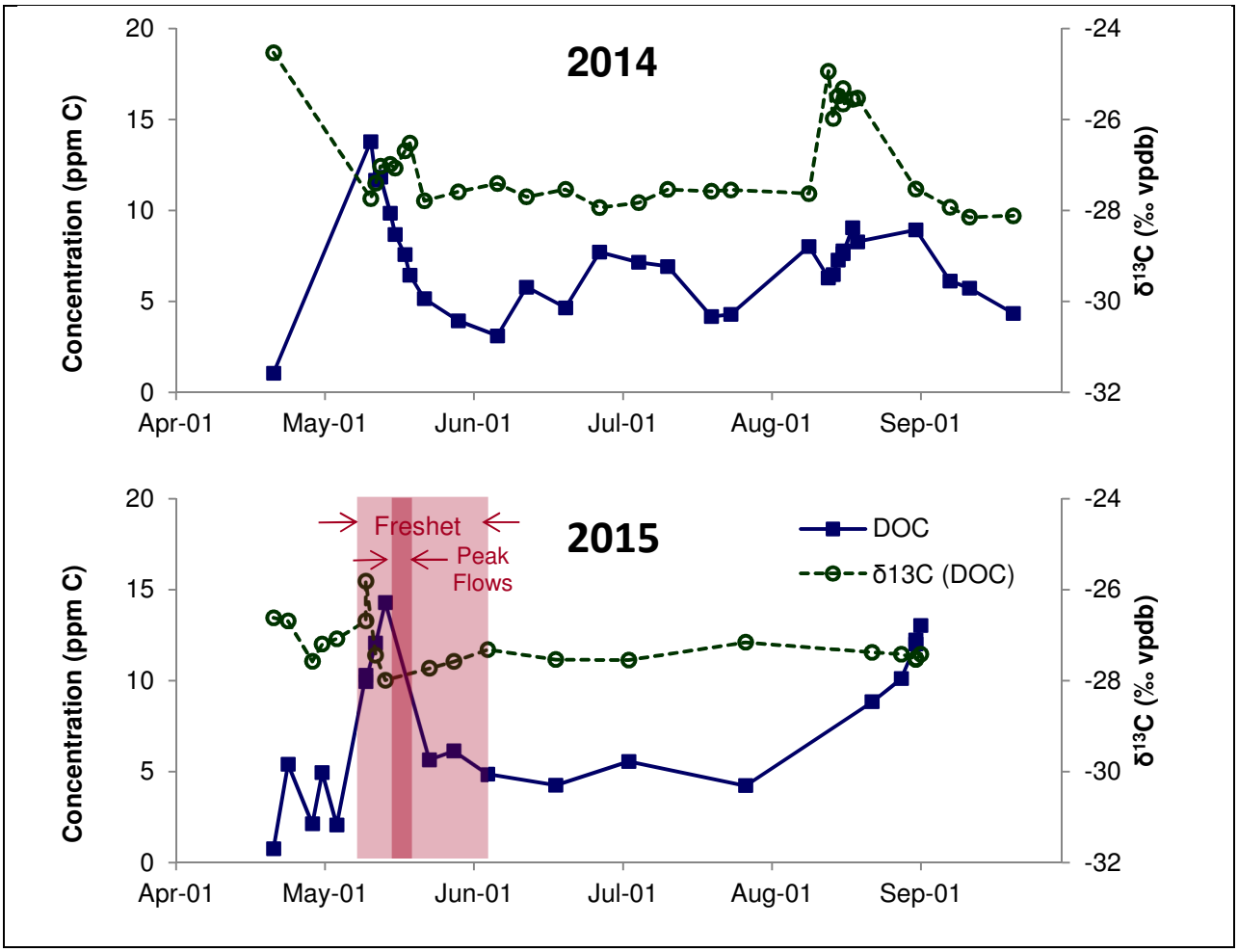

Figure 6 DOC and $\delta^{13}C$ in Ogilvie River at sampling site (2014, 2015)

The $\delta^{13}C$ of DOC values became more depleted at high concentrations, a trend opposite to that of DIC. In 2014, the winter $\delta^{13}C$ of -24.5‰ decreased to -27.7‰ at the peak of freshet and began to recover as the flows decreased afterwards. By the end of the summer the isotope signature recovered to ~ -25 to -26‰ range. The 2015 pattern does not fully match the 2014. Similarly, the $\delta^{13}C$ peaks just before freshet on May 10, 2015, at -25.8‰. The most depleted value -28.0‰ occurred on May 14, the sampling date closest to the freshet peak. The isotope signature then recovered slowly to a steady -27.2 to -27.6‰. Unlike in 2014, no late summer peaks were detected in 2015.

7.1.3 δ^2H and $\delta^{18}O$

The isotopic signature of the Ogilvie River at the sampling site varied seasonally and the trends were consistent between 2014 and 2015 (Figure 7). As both oxygen and hydrogen isotopes behave similarly as part of the water molecule the trends are the same for both isotopes.

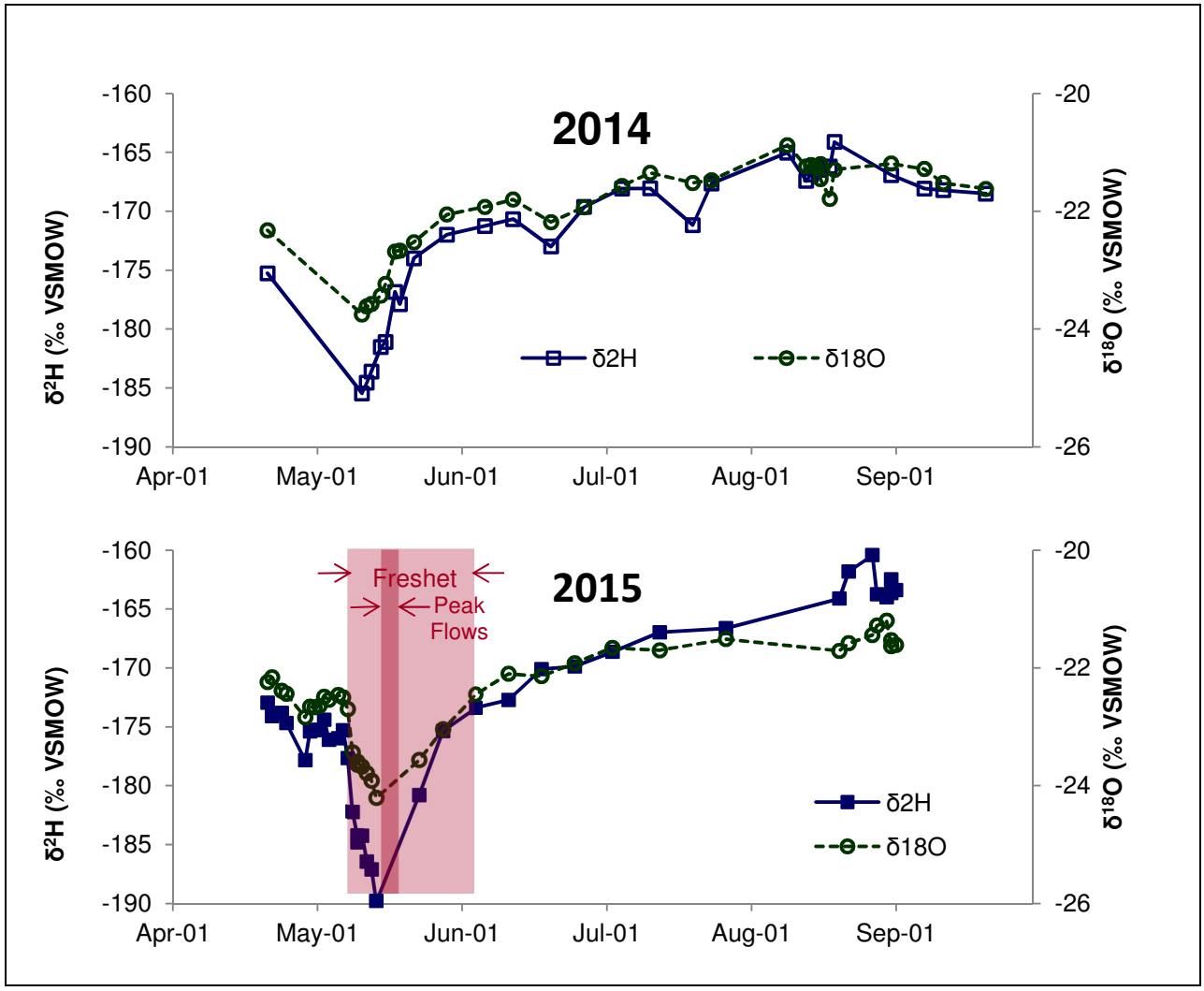

Figure 7 Stable Isotopes, Ogilvie River at sampling site (2014, 2015)

The most depleted values were reached at the peak of the freshet when the depleted snowmelt waters were a major contributor to the flow. The $\delta^{18}O$ values ranged from -24.2‰ to -20.9‰ and δ^2H values ranged from -189.8‰ to -160.4‰. The average winter (pre-freshet) $\delta^{18}O$ values representing groundwater were consistent in 2014 and 2015 at -22.3‰.

7.1.4 Anions/cations

The Ogilvie River waters were high in weathering solutes such as Ca^{2+}, Mg^{2+}, bicarbonate and sulphate, in the winter when the river is fully fed by groundwater. There was a spike in concentrations of Ca^{2+}, SO_4^{2-}, and Na^{+} just prior to the start of the freshet. Later these solutes were diluted by the spring freshet and the concentrations slowly increased as the summer progressed and low-flow autumn conditions approached. Figure 8 shows the time series of the major cations in the upper Ogilvie River waters (Ca^{2+}, Mg^{2+}, and SO_4^{2-}) and Figure 9 shows anions (Na^{+} and Cl-). The groundwater-fed Ca^{2+}-HCO_3^{-} winter waters evolve into (Na^{+}+Ca^{2+})-(HCO_3^{-}+Cl^{-}) waters during freshet (Figure 21).

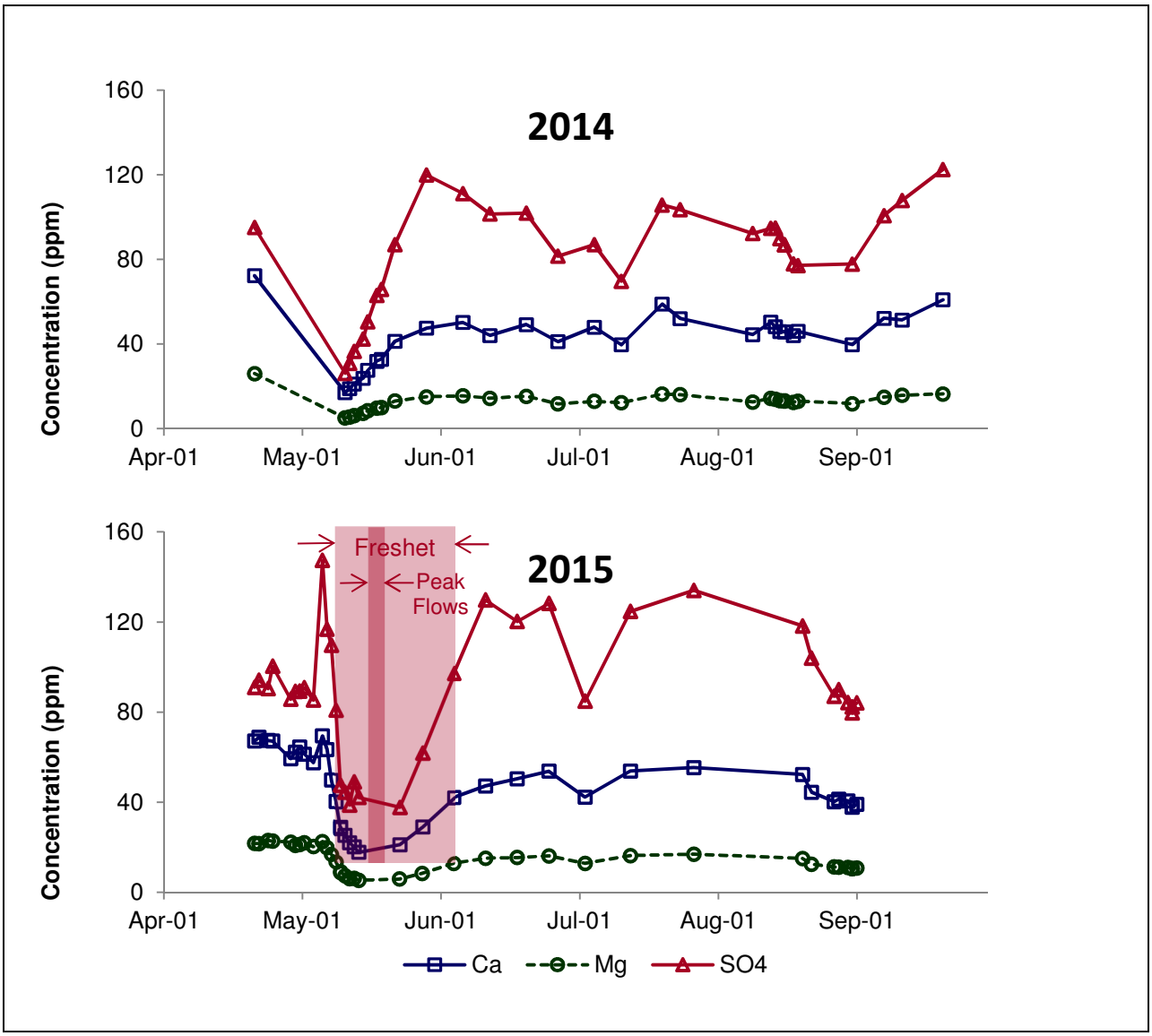

Figure 8 **Major Cations, Ogilvie River at sampling site (2014, 2015)**

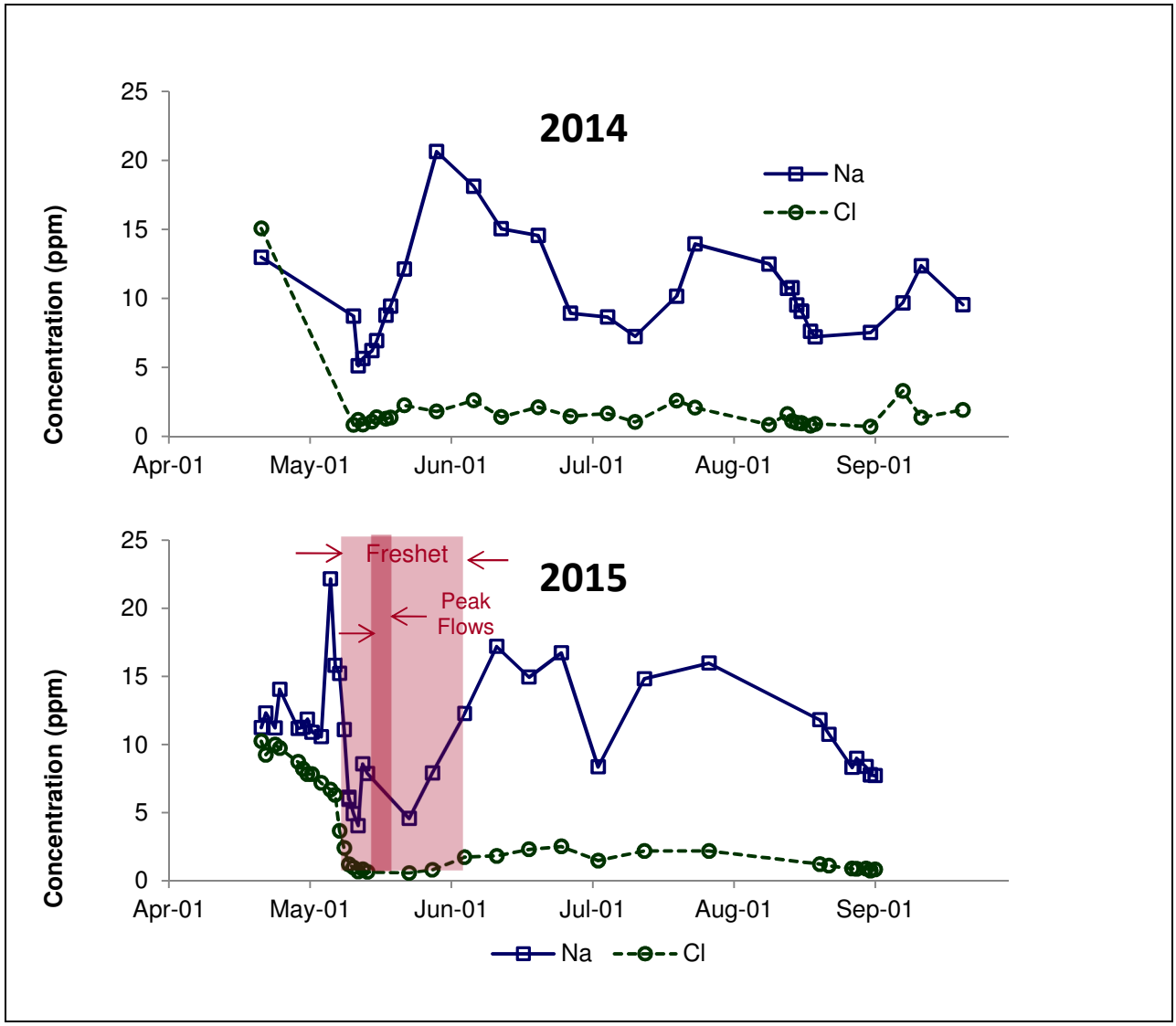

Figure 9 **Na^+ and Cl^-, Ogilvie River at sampling site (2014, 2015)**

The biogenic solutes such as K^+ (paired with DOC in Figure 10) remained generally low throughout 2015. The pre-freshet winter concentration around 0.9 ppm increased to the maximum annual value of 1.14 ppm at the start of the freshet but before the maximum flows. Summer concentrations of K+ may be less reliable due to unfiltered and unrefrigerated storage of those samples (similar to DOC described in Section 7.1.2). The more reliable late summer concentrations reached levels higher than those during early freshet (up to 1.23 ppm) reflecting high biological activity in the watershed and in the river.

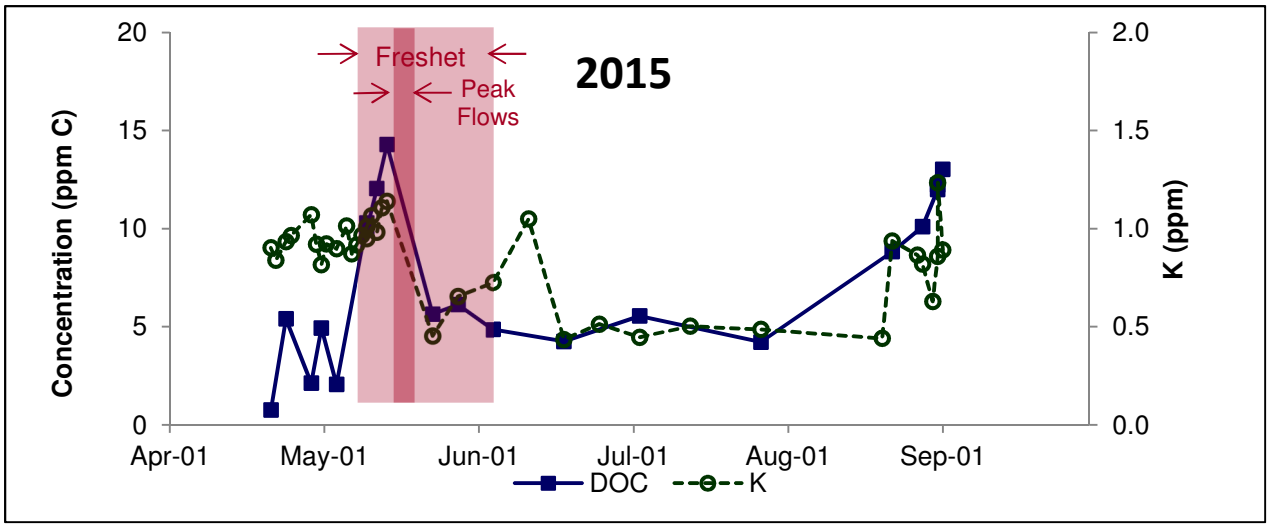

Figure 10 **K^+ and DOC, Ogilvie River at sampling site (2015)**

7.1.5 Tritium

The tritium activities in the Ogilvie River are shown in Figure 11 with associated analytical uncertainties. Based on the 2014 and 2015 analysis, the winter baseflow tritium activity averaged 9.0 TU. The activity dropped to the average value of 7.8 TU during freshet when diluted with low activity snowmelt waters (6.6 TU). In the summer, the tritium activity increased to the average of 11.1 TU in response to the increased input of more enriched rain waters (12.7 TU).

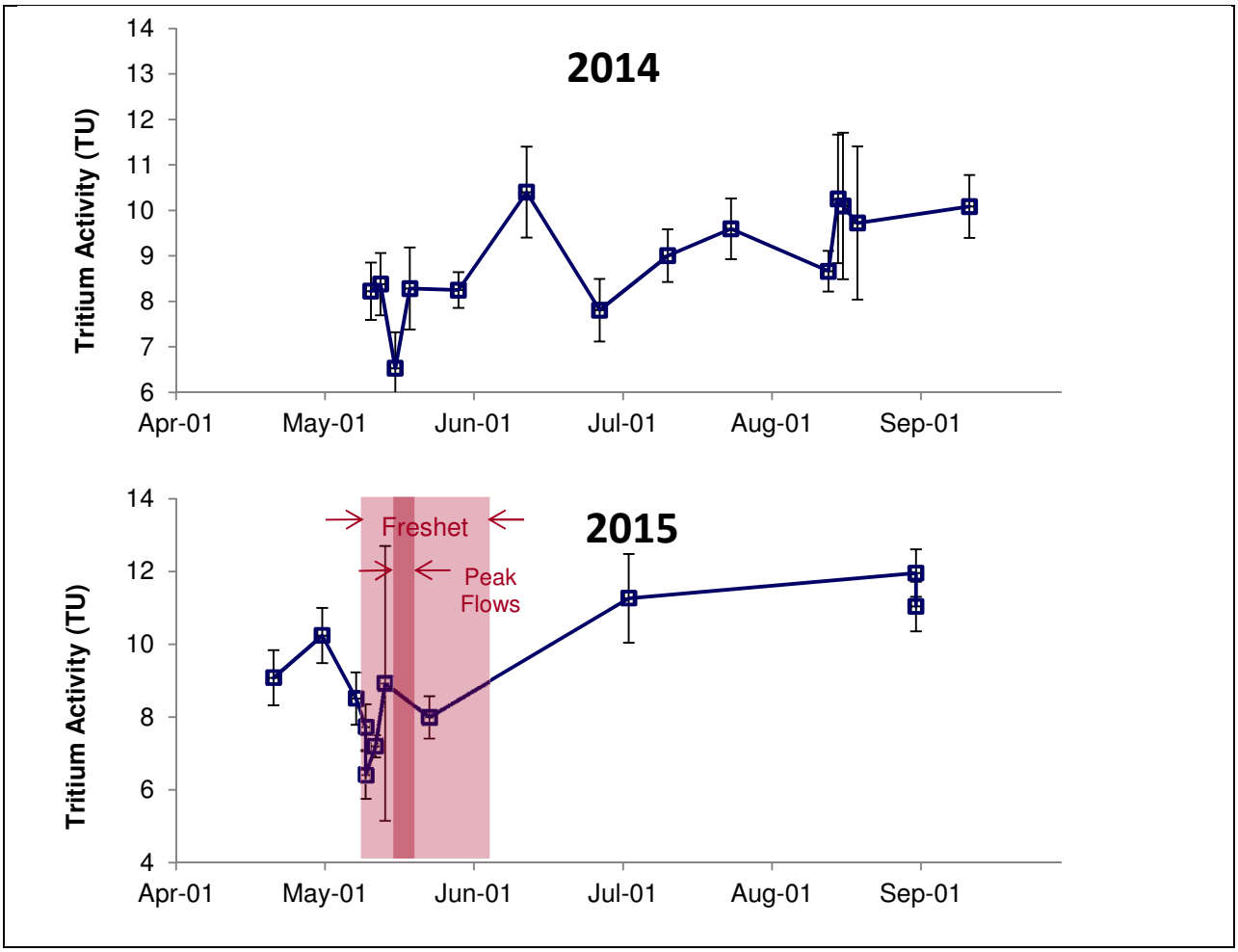

Figure 11 Tritium in Ogilvie River at Sampling Site (2014, 2015)

7.2 Runoff

Sampling of the three analogue tributaries provided signatures of the surface runoff generated in the watershed at different times of the year. The geochemical and isotopic evolution was similar between different runoff streams, but even on such a small geographical scale (up to tens of kilometers) there were differences. It is only logical to assume that heterogeneity on the upper Ogilvie Watershed scale would be greater.

Complete results of the analysis on the tributaries samples (C1, C2, and C3) are included in Appendix D. The ranges of encountered values are summarized in Table 7. Two distinct signatures were identified as freshet and summer runoff.

Table 7 Range of Runoff Values encountered at sampling points C1, C2, and C3 (2014, 2015)

Parameter	Units	Freshet			Summer		
		Average	Min	Max	Average	Min	Max
Conductivity	µS/cm	179.8	93.1	291	370.5	295	429
Alkalinity	ppm C	18.8	8.7	36.6	37	27.7	42.3
pH	pH units	7.69	5.26	8.13	7.97	8.15	8.37
DIC	ppm C	22.0	12.5	39.2	47.8	39.2	56.2
DOC	ppm C	17.3	3.9	41.7	7.5	4.0	10.4
$\delta^{13}C$ (DIC)	‰ VPDB	-5.98	-11.21	-1.29	-7.1	-8.66	-5.32
$\delta^{13}C$ (DOC)	‰ VPDB	-27.24	-28.44	-26.42	-25.97	-27.60	-21.47
$F^{14}C$ (DIC)	-	0.98	0.96	1.02	0.87	0.84	0.89
$F^{14}C$ (DOC)	-	1.05	0.99	1.07	0.93	0.92	0.93
$\delta^{2}H$	‰ VSMOW	-188.65	-197.83	-176.50	-166.96	-173.76	-161.89
$\delta^{18}O$	‰ VSMOW	-24.47	-25.64	-22.23	-21.63	-22.68	-20.82
Ca	ppm	26.42	14.42	42.02	49.01	30.54	60.26
K	ppm	0.92	0 (non-detect)	2.32	0.79	0 (non-detect)	1.65
Mg	ppm	8.85	4.91	18.29	13.55	10.2	19.03
Na	ppm	0.2	0 (non-detect)	0.38	0.06	0 (non-detect)	0.14
Sr	ppm	0.04	0 (non-detect)	0.09	0.08	0.02	0.15
Cl	ppm	0.29	0.15	0.74	0.35	0.17	0.96
SO_4	ppm	13.81	0.28	51.96	35.87	0.33	63.87
NO_3	ppm	0.16	0 (non-detect)	0.41	0.29	0.02	0.74
Tritium	TU	7.8	5.7	9.2	11.1	9.0	12.1

In general, in the spring, the tributary signatures reflected the snow input altered by the interactions with the organic material. The runoff evolution began prior to the freshet in the upper Ogilvie River and continued as the freshet progressed. For example, the runoff waters evolved towards less depleted $\delta^{2}H$ and $\delta^{18}O$ values (Figure 13) and lower DOC concentrations with less depleted $\delta^{13}C$ (Figure 12). The DIC concentrations decreased steadily prior to the freshet and recovered slightly likely in response to flow fluctuations. The $\delta^{13}C$ of DIC did not appear to be directly related to the concentrations.

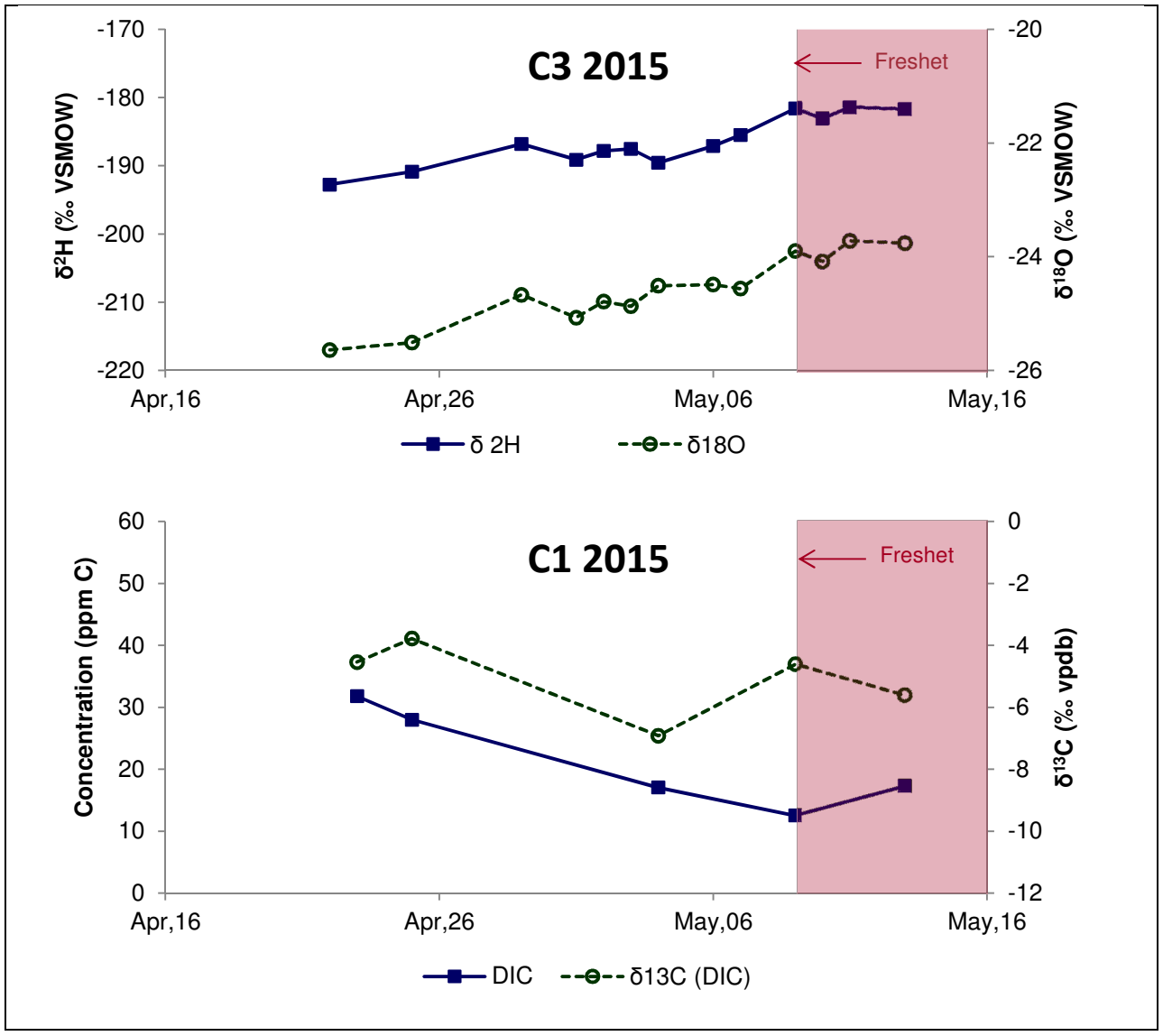

Figure 12 **Freshet evolution of δ^2H, $\delta^{18}O$, DIC, and $\delta^{13}C$ in selected surface runoff streams, 2015**

The biogenic K decreased throughout the freshet matching the DOC pattern indicating that the early spring runoff is rich in organic matter (Figure 13). Smaller quantities of meltwater spent longer in contact with the organic material at the surface. As the freshet progressed, the higher snowmelt volumes passed through the system faster unable to dissolve as much organic material. The weathering solutes either remained constant or fluctuated without an obvious pattern.

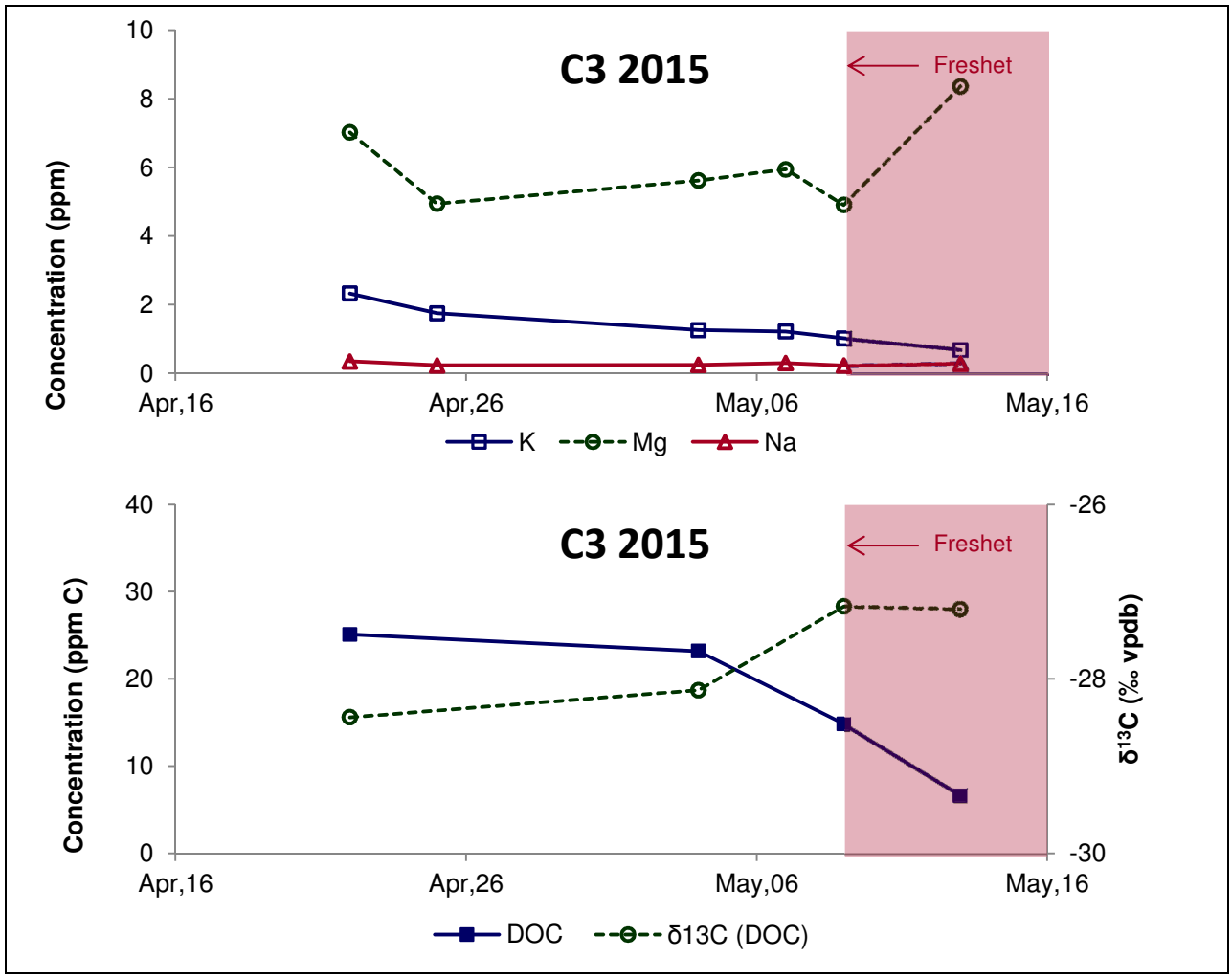

Figure 13 **Freshet evolution of the DOC, $\delta^{13}C$, and some solutes in selected surface runoff streams, 2015**

In the summer, older carbon stocks were accessed by the runoff waters via deepening active layer as evidenced by the reduction of $F^{14}C$ signature of DOC from modern (1.05) to 0.93. Similarly, the DIC $F^{14}C$ signature, mainly generated by soil weathering with the CO_2 derived from the biological activity in soil, became progressively lower throughout the season reducing from 0.98 during freshet to 0.87 in late summer. Other changes from freshet to summer included enrichment of δ^2H and $\delta^{18}O$ isotopes, increase of weathering solutes such as Ca^{2+}, Mg^{2+}, Na^+, SO_4^{2-}, and DIC, and decrease of the biogenic solutes such as DOC and K.

7.3 Active Layer

In the absence of a detailed profile of active layer waters, the surface seeps sampled in late August 2014 and 2015 were considered to be representative of the flowing active layer water. Surface seep sampling locations R3 and R5 were sampled in both years and a direct sample of active layer water AL-BH-SN8 was collected from a test pit dug to drill BH-SN8 in August 2015 (see Map D for sampling locations). Some variability between the samples was present; however, the spatial heterogeneity was most evident in the measurements of DOC and low concentration parameters such as F^-, Cl^-, and NO_3^-. Full results are presented in Appendix D and summary of the results is included in Table 8.

Table 8 Summary of the Active Layer Results (2014, 2015)

Parameter	Units	Average	Min	Max
Conductivity	µS/cm	392.5	291	569
Alkalinity	ppm C	36.6	27.5	45.4
pH	pH units	7.28	6.96	7.66
DIC	ppm C	39.9	28.6	56.3
DOC	ppm C	7.6	3.7	27.6
$\delta^{13}C$ (DIC)	‰ VPDB	-10.4	-12.8	-9.4
$\delta^{13}C$ (DOC)	‰ VPDB	-24.9	-27.5	-22.1
$F^{14}C$ (DIC)		0.66	0.63	0.7
$F^{14}C$ (DOC)		0.88	0.87	0.89
δ^2H	‰ VSMOW	-168.7	-172.19	-162.72
$\delta^{18}O$	‰ VSMOW	-22.32	-22.45	-22.05
Ca	ppm	60.4	43.7	66.7
K	ppm	0.6	0 (non-detect)	0.8
Mg	ppm	13.5	4.5	16.3
Na	ppm	8.0	0.4	9.4
Sr	ppm	0.2	0.1	0.3
P	ppm	0.03	0 (non-detect)	0.14
F	ppm	0.09	0.06	0.18
Cl	ppm	2.9	1.2	4.7
SO_4	ppm	90.6	75.5	138.2
NO_3	ppm	0.2	0.02	0.36
Tritium	TU	9.57	9.28	9.85

Figure 14 shows comparative concentrations of DIC, DOC, and select solutes in active layer samples. The sulphate concentrations in R3 and R5 seeps were significantly higher in 2015 (138 and 116 ppm) compared to 2014 (76 and 80 ppm). Other parameters varied much less between the two consecutive years of sampling and between sampling locations. The active layer water sampled directly had significantly higher DOC concentration of 28 ppm C than the average of 5 ppm C across other samples. It is likely that the DOC oxidized and degassed once the active layer water breached the ground surface and became aerated.

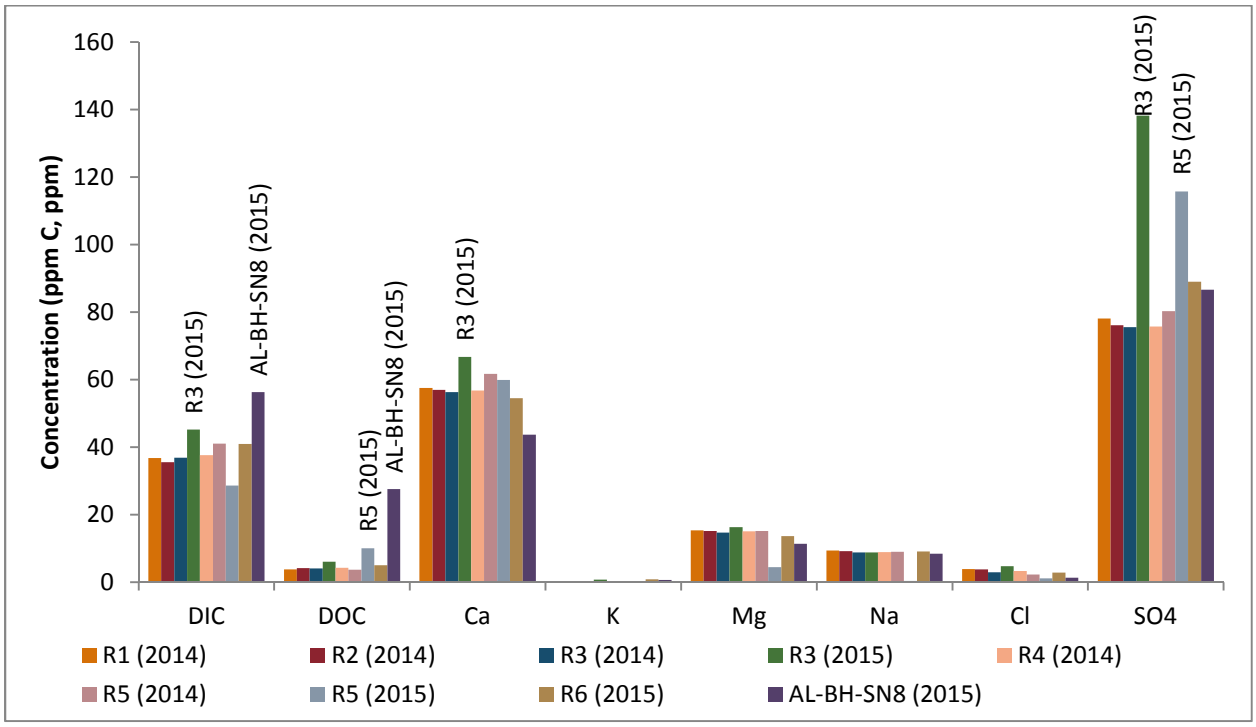

Figure 14 DIC, DOC and solute concentrations in the active layer samples (2014, 2015)

7.4 Soil Water and Gas

The stable isotopes (δ^2H and $\delta^{18}O$) were analyzed in the samples of water extracted from the soil samples collected and stored frozen and unfrozen (Appendix D). The δ^2H values ranged -190.8‰ to -132.4‰ and the $\delta^{18}O$ values ranged from -25.2‰ to -14.9‰. There was no direct correlation of the isotope values with depth.

The $\delta^{13}C$ of the CO_2 in 10 active layer soil samples from depths between 0 and 30 cm was found to be very variable, ranging from -31.1‰ to -18.9‰. The average value was -25.4‰ in line with the expected soil CO_2 signatures between -25‰ and -18‰ (Clark, 2015).

7.5 Shallow Groundwater

Opportunistic samples collected from the drinking water well at the Ogilvie Highway Maintenance Camp provided a signature of shallow groundwater that is not frozen in the winter. The depth to the water at the well ranges from approximately 2 to 3.6 metres below grade (see Section 5.4). Either the well is located in an area of no permafrost or within a talik. If latter, the talik must extend to at least that depth and likely up to at least 5.6 metres as no permafrost was encountered during well installation, albeit, at an unknown time of year.

Samples collected showed a consistent signature over time. The full sampling results are included in Appendix D. A total of 13 samples were analyzed for some or all of the parameters listed in Table 5. The average values for these parameters are summarized in Table 9.

Table 9 Drinking Water Well Analytical Summary (2014, 2015)

Parameter	Units	Average	Parameter	Units	Average
Conductivity	µS/cm	502.33	Ca	ppm	65.20
Alkalinity	ppm C	43.33	K	ppm	0.69
pH	pH units	7.43	Mg	ppm	17.20
DIC	ppm C	50.13	Na	ppm	10.34
DOC	ppm C	2.24	Sr	ppm	0.22
$\delta^{13}C$ (DIC)	‰ VPDB	-10.84	P	ppm	0.04
$\delta^{13}C$ (DOC)	‰ VPDB	-24.84	F	ppm	0.05
$F^{14}C$ (DIC)		0.67	Cl	ppm	3.98
$F^{14}C$ (DOC)		0.87	SO_4	ppm	90.56
$\delta^{2}H$	‰ VSMOW	-172.33	NO_3	ppm	0.04
$\delta^{18}O$	‰ VSMOW	-22.47	Tritium	TU	10.41

In general, the shallow groundwater was characterized by high concentrations of calcite dissolution products such as Ca^{2+} and HCO_3^- expressed as DIC and alkalinity. Magnesium and sulphate were other dominant ions in the solution. The samples plot close to the winter baseflow defined groundwater and to the active layer samples on the Piper Diagram (Figure 21).

7.6 Precipitation

Rain and snowpack isotopic signatures are summarized in Appendix D.

The depth of the measured snowpack on April 23 and 24, 2015, ranged from 40 to 60 cm. The isotopic signatures across the depth profiles exhibited a similar pattern in all sampling locations

(SN1 to SN11). The top and bottom of the snowpack were both more enriched in δ^2H and $\delta^{18}O$ compared to the middle of the pack (Table 10). Very generally, the bottom snowpack is representative of the early winter snowfall (November-December), the middle of the snowpack of the January-February snow and the top of the snow of the March-April snow. As the detailed snowfall records are not available for the region it is not possible to be more precise.

Table 10 **Average snowpack isotopic signature and snow depth profiles**

Snowpack depth	Average δ^2H (‰ VSMOW)
Top	-208.8
Middle	-216.9
Bottom	-199.4

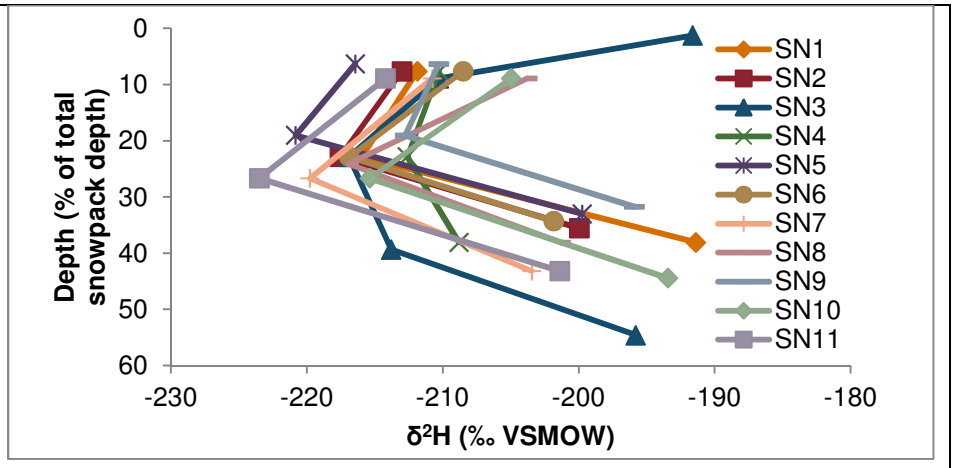

	Average $\delta^{18}O$ (‰ VSMOW)
Top	-26.7
Middle	-28.4
Bottom	-26.1

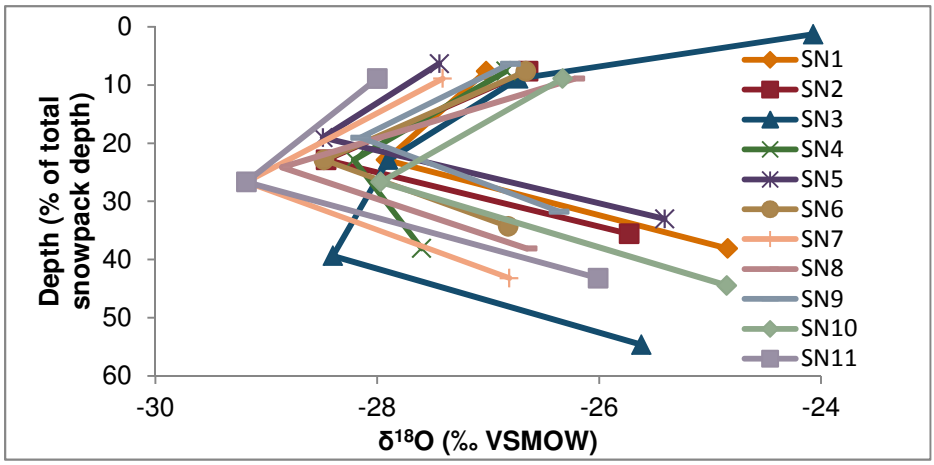

The rain and snow precipitation signatures were corrected to account for the altitude effect. The rain gauge station and most of the snow samples were collected at an elevation of approximately 600 m amsl. The average elevation of the watershed is approximately 1,000 m amsl. The precipitation becomes depleted by 0.15 to 0.5‰ $\delta^{18}O$ and by 1 to 4‰ δ^2H per 100 m in elevation gain (Clark, 2015). The global average value of -0.28‰ $\delta^{18}O$ per 100 m (Poage and Chamberlain, 2001) was selected to correct $\delta^{18}O$. This value is also close to the elevation effect of -0.25‰ per 100 m identified at Mount Meager, 120 km north of Vancouver (Clark et al.,

2011) and elevation gradient of -0.29‰ per 100 m determined for the mainland US states (Dutton et al., 2005).

Because elevation effect does not affect the slope of the meteoric water line, the δ^2H elevation gradient was calculated using the local meteoric water line slope determined from the precipitation values not yet corrected for the altitude. The δ^2H elevation gradient of -1.9‰ per 100 m was used to correct the precipitation values.

Based on the precipitation samples from 2014 and 2015 the average ($\delta^{18}O$, δ^2H) values for rain and snow were (-19.2‰, -154.0‰) and (-28.2‰, -216.0‰) respectively.

The local meteoric water line (LMWL) equation $\delta^2H=6.77\cdot\delta^{18}O-24.54$ ($R^2=0.98$) was developed using rain sample signatures from 2014 and 2015 and snowpack signatures from spring 2015, all corrected for elevation (Figure 15). The LMWL has a shallower slope than GMWL and a much lower d-intercept. The narrow 99.7% confidence interval constrain the LMWL, the wider 99.7% (3σ) prediction intervals reflect the intrinsic variability of the precipitation signatures. International Atomic Energy Agency (IAEA) methodology was used to determine that there were no outliers. The methodology excludes samples that are more than 3 standard deviations away from the regression line (i.e. outside the 99.7% prediction interval) (IAEA, 1992). Some studies exclude values that have d-excess values that are either outside of a certain range such as below -2‰ and above 15‰ (Benjamin et al., 2004) or extreme d-excess values (Streletskiy et al., 2015). There are 24 out of 78 values that have d-excess outside of the abovementioned range. All of the values outside of the d-excess range were present in the rain samples. This makes sense as the rain samples are more likely to be affected by evaporation. However, none of these points plotted outside the 3σ prediction interval envelope and, therefore, were retained.

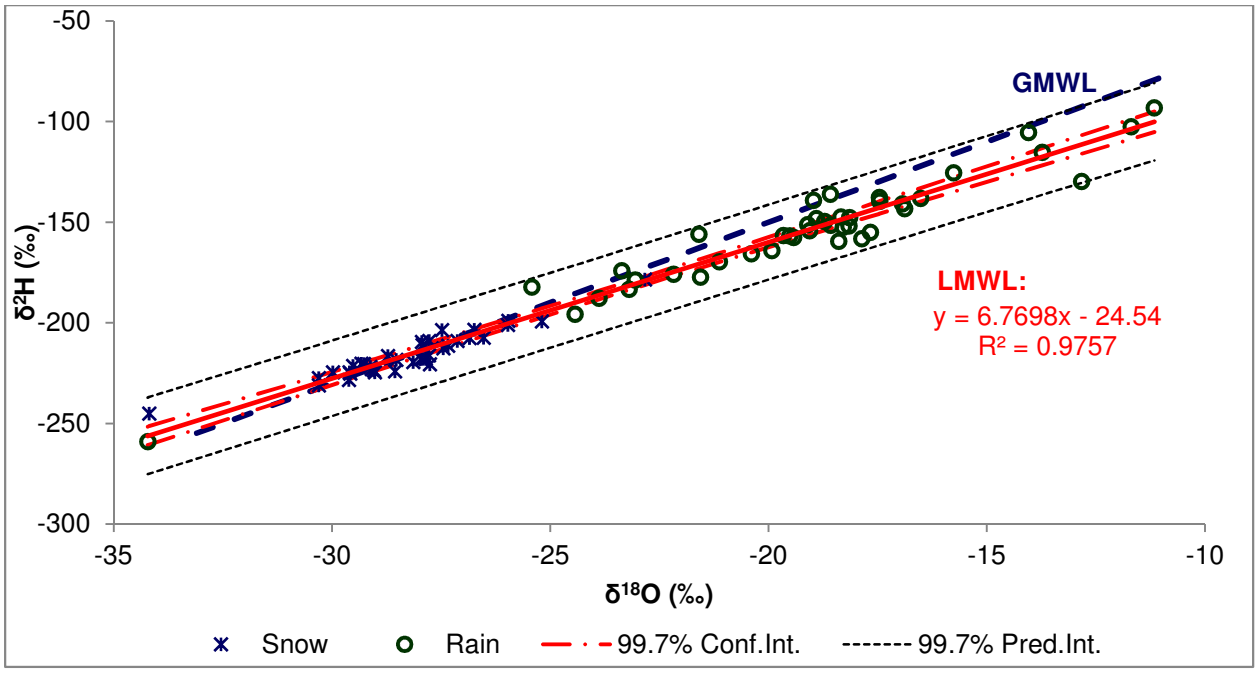

Figure 15 Local Meteoric Water Line (precipitation corrected for elevation)

As discussed in Section 3.1.1, the isotopic signature of the snowpack is not always representative of the fresh precipitation. At the study site, the slopes of the LMWLs derived from rain samples only and from rain and snowpack samples (LMWL) are very close ($\delta^2H=6.71\cdot\delta^{18}O-25.37$ and $\delta^2H=6.77\cdot\delta^{18}O-24.54$ respectively) indicating that the snowpack was sampled prior to any major alterations of the isotope content.

Similarly to the most depleted signature of the snowpack corresponding to the coldest months of the year, the most enriched rain precipitation is observed in July corresponding to the warmest month of the year.

7.7 Radiocarbon

Both DIC and DOC fractions of the water samples were analyzed for radiocarbon. The $F^{14}C$ in various flow components are summarized in Table 11. The winter baseflow had the lowest $F^{14}C$ DIC signature of 0.57, followed in increasing order by active layer, shallow groundwater, Ogilvie summer flows, Ogilvie freshet flow, summer runoff, and finally spring runoff which had almost modern signature of 0.98. The DOC fractions not influenced by addition of the $F^{14}C$ dead sedimentary rock has $F^{14}C$ values ranged from 0.68 in the winter baseflow in the Ogilvie River to modern values of the Ogilvie flow at freshet (1.04) and spring runoff (1.05). The lower DOC

fractions in active layer and shallow groundwater (0.88 and 0.86 respectively) were indicative of the water accessing old organic carbon stocks stored in the soil.

Table 11 Summary of Radiocarbon Signatures

	DIC	Samples Analyzed	DOC	Samples Analyzed
Baseflow (Ogilvie Winter)	0.57	2	0.68	1
Ogilvie Freshet	0.79	4	1.04	4
Ogilvie Summer	0.73	3	0.92	3
Shallow Groundwater	0.67	2	0.86	2
Runoff Spring	0.98	6	1.05	7
Runoff Summer	0.86	3	0.93	3
Active Layer	0.66	2	0.88	2

Note:

DIC Radiocarbon sample result for 21-Apr-2014 was discarded. The $F^{14}C$ value of 0.9123 was not considered representative of the baseflow based on the 2015 and 2016 baseflow samples.

8 Discussion

8.1 Precipitation and Local Meteoric Water Line

The snowpack isotopic trend shows that the middle of the pack is the most depleted in a snow profile corresponding to the coldest temperatures of the January-February. The d-excess values in snowpack range from 0.1‰ to 15.0‰ with the middle of the pack having the highest values.

The LMWL provides a reference point to evaluate components of the hydrological system with respect to the main input – precipitation (Figure 15). The soil water samples generally fall on the LMWL (lc-excess of – 1.0‰) reflecting the precipitation input (Figure 16).

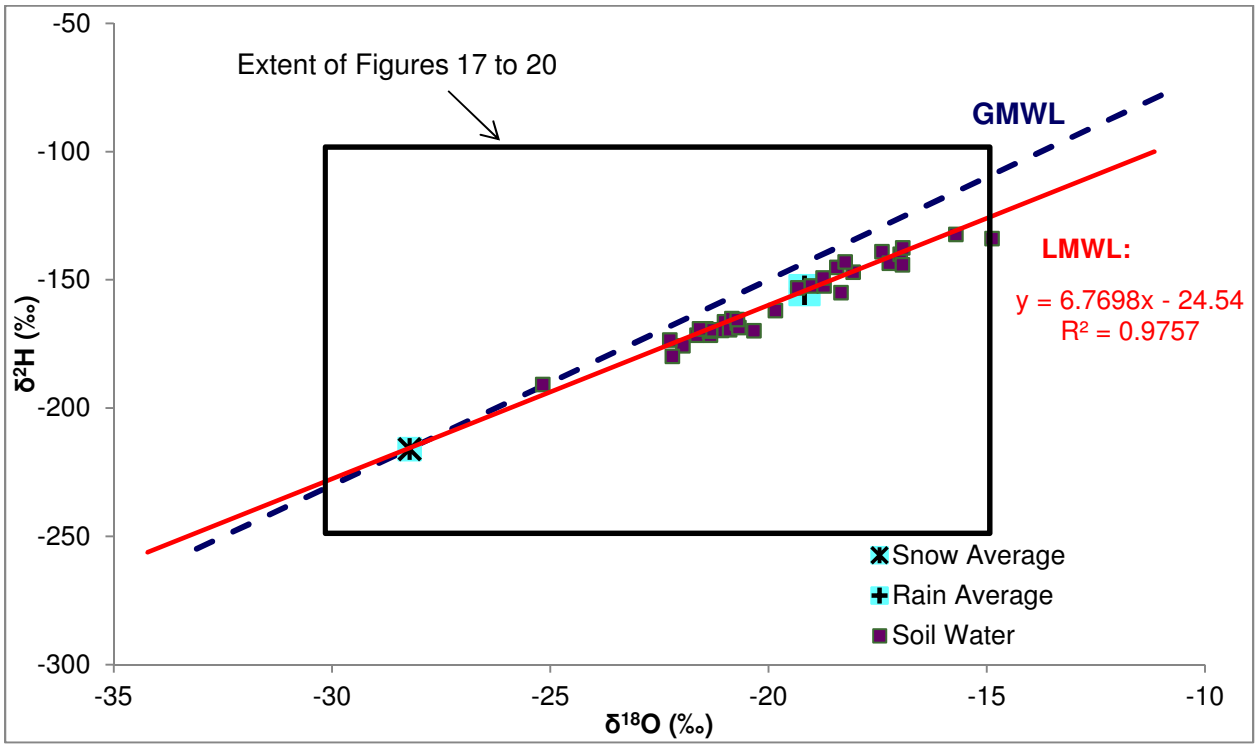

Figure 16 Soil water isotopic signature

The deep groundwater signature plots slightly above the LMWL and shallow groundwater plots further above the water line (Figure 17). However, both groundwaters plot in the same region of the LMWL. Using the LMWL as a mixing line with the snow and rain average signatures as the end-members the groundwater recharge mixing ratio is calculated to originate from 65% rain and 35% snowmelt.

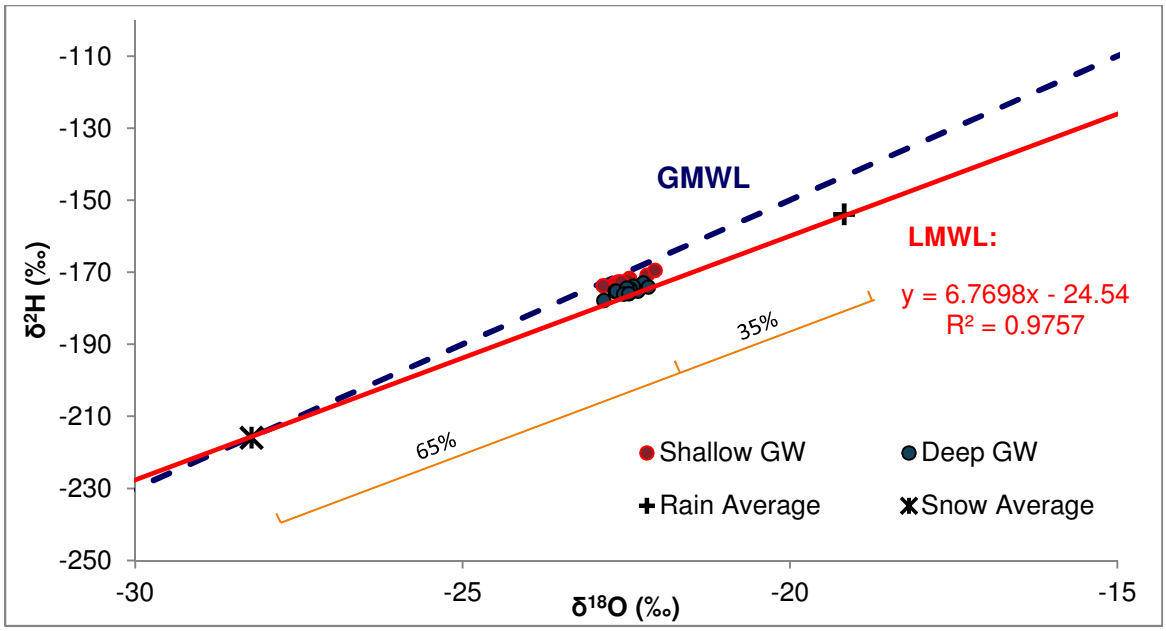

Figure 17 Groundwater isotopic signatures

The shallow groundwater and active layer waters have similar signatures suggesting similar origins of the water (Figure 18). Shallow groundwater signatures vary between different times in the season between April and August. The active layer samples were only collected in late summer (August) from ground seeps. It is, therefore, possible that some temporal and vertical variations in the active layer signature may exist. The active layer waters plot above the LMWL closer to GMWL similar to shallow groundwater.

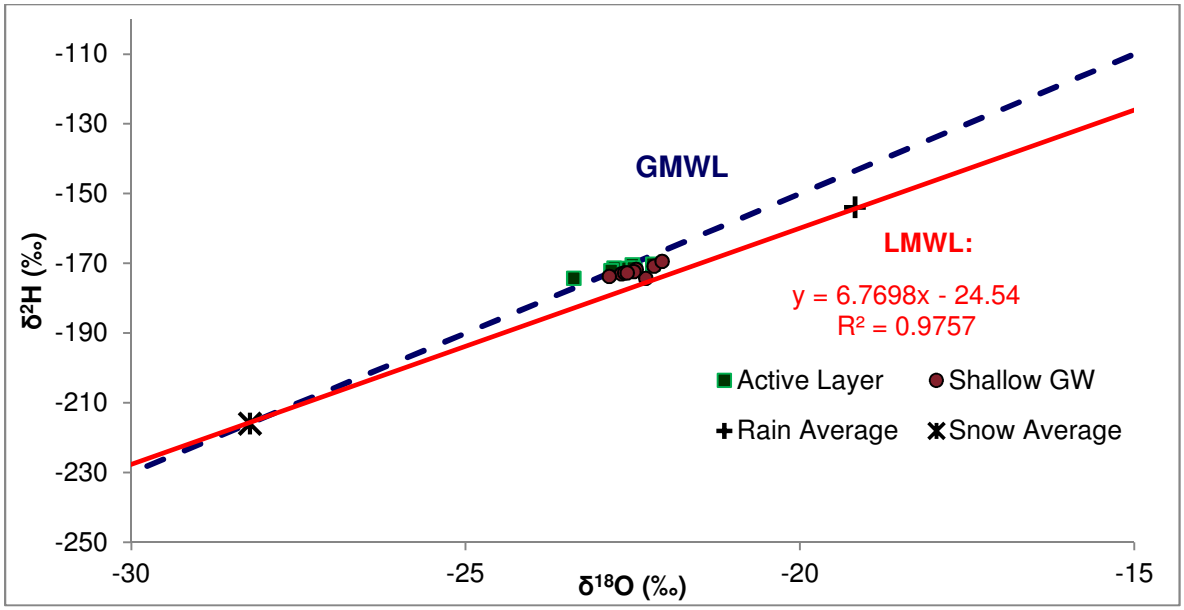

Figure 18 Shallow groundwater and active layer isotopic signatures

During freshet in May, the upper Ogilvie River signature is a mixture dominated by spring runoff with, at times, significant influence of the groundwater (Figure 19). The $\delta^{18}O$ variation of up to 3.4‰ in the flow input signatures is attenuated down to 2.2‰ range in the Ogilvie stream values. The snowpack isotope signature is much more depleted then the actual small stream runoff generated by the snowmelt (Figure 19).

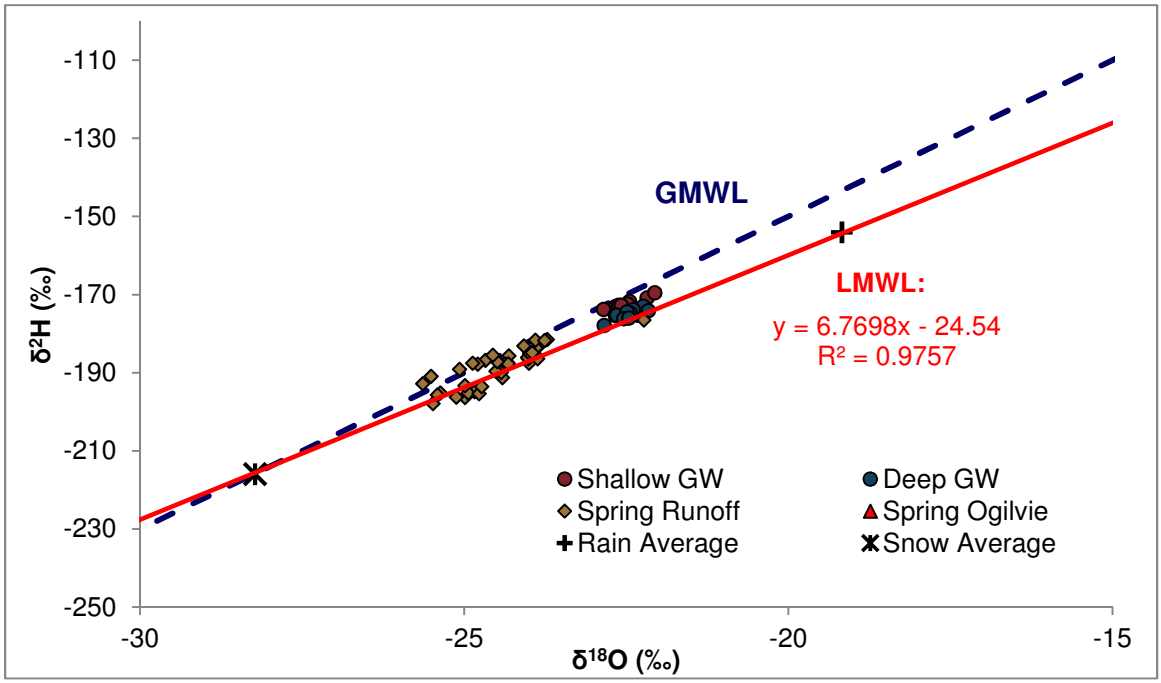

Figure 19 Spring isotope signatures

In the summer time, the flow input components are shallow and deep groundwater, active layer and surface runoff. As can be seen from Figure 20, the summer Ogilvie River isotopic signatures are within the range of the input values showing less attenuation (from 2.6‰ to 1.6‰ $\delta^{18}O$) than in the spring.

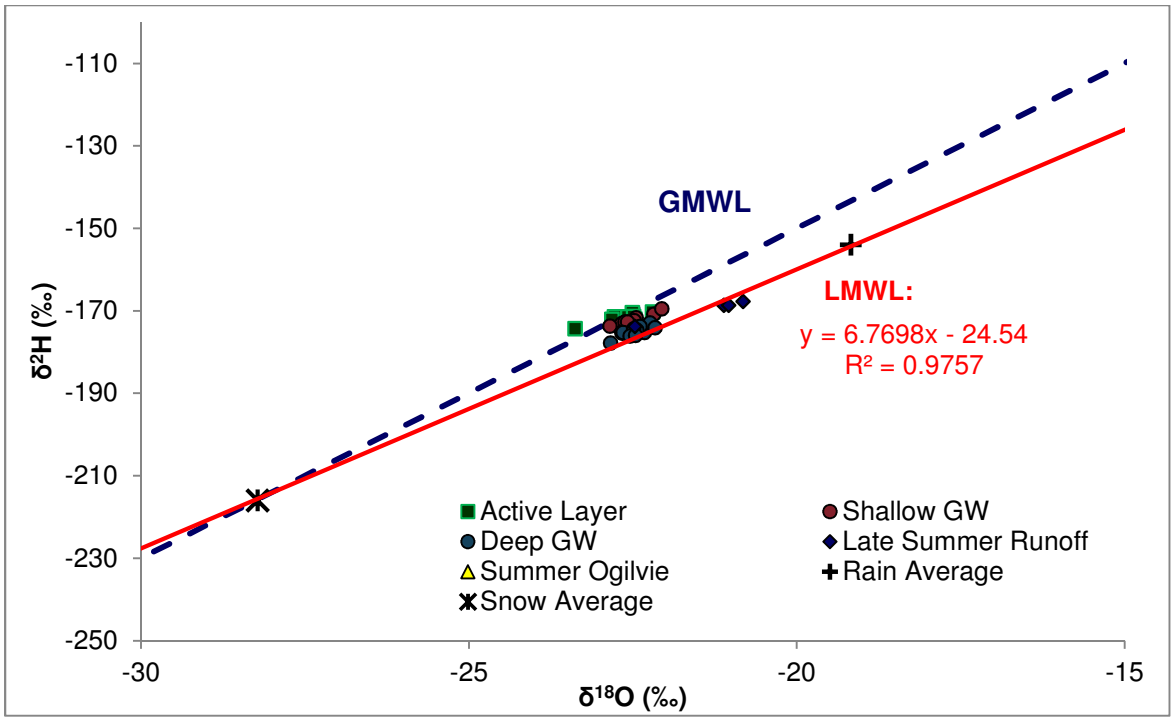

Figure 20 Summer isotopic signatures

The average $\delta^{18}O$ signature of Ogilvie River during the freshet (-23.2‰) was more depleted than in the summer time (-21.6‰) due to the more depleted input of snowmelt generated runoff.

The lc-excess values, summarized in Table 12, show that soil water and Ogilvie River at freshet plot close to the LMWL (i.e. lc-excess values are close to 0‰). Other flow components plot above the LMWL (lc-excess>0‰) with late summer runoff, shallow groundwater and active layer waters plotting the furthest. These three components affect the Ogilvie river flow in the late summer increasing the river lc-excess from 0.9‰ in the spring to 3.4‰ in the summer.

Table 12 Line conditioned excess (lc-excess)

Flow Component	Average local excess values (lc-excess)
Ogilvie (spring)	0.9‰
Ogilvie (summer)	3.4‰
Groundwater (deep)	1.7‰
Groundwater (shallow)	4.3‰
Active layer (late summer)	6.3‰
Runoff (spring)	1.6‰
Runoff (late summer)	4.0‰
Soil Water	-1.0‰

The limitations of this analysis, of course, stem from the assumption that the precipitation at the sampling location is representative of the type, quantity, and isotopic signature of precipitation across the entire watershed. Using the available limited precipitation information and stream discharge records it is clear that the heterogeneity of the rain and snow is high (see discussion in Section 7.1). It is also assumed that the snow precipitation signature was adequately preserved in the sampled snowpack (see discussion in Section 7.6).

8.2 Ogilvie River Chemical and Isotope Trends

The Piper diagram of the upper Ogilvie River samples and other flow components is shown in Figure 21.

The general trends of solute concentrations in the upper Ogilvie River indicate that weathering solutes such as DIC, calcium, magnesium, and sulphate are high during the winter when the deep groundwater is the single constituent of the river flow. Just prior to the onset of the freshet the weathering solutes peak at levels above the winter concentrations. Similar effect was observed in North Klondike River in Yukon (Lapp, 2015) and in Wolf Creek Basin (Herod, 2015). These solutes are diluted during the freshet when the inflow of snowmelt water becomes a significant flow component. The weathering solutes slowly recover their concentrations throughout the summer time subject to rain event induced fluctuations. As the autumn low flow conditions settle in, it is assumed that the solute concentrations continue to increase until only the groundwater is feeding the river during the winter. The $\delta^{13}C$ of DIC was more depleted at low DIC concentrations which occurred at periods of high discharge when large organic loads with very depleted $\delta^{13}C$ (-28.4‰ to -26.4‰) were oxidized to inorganic carbon.

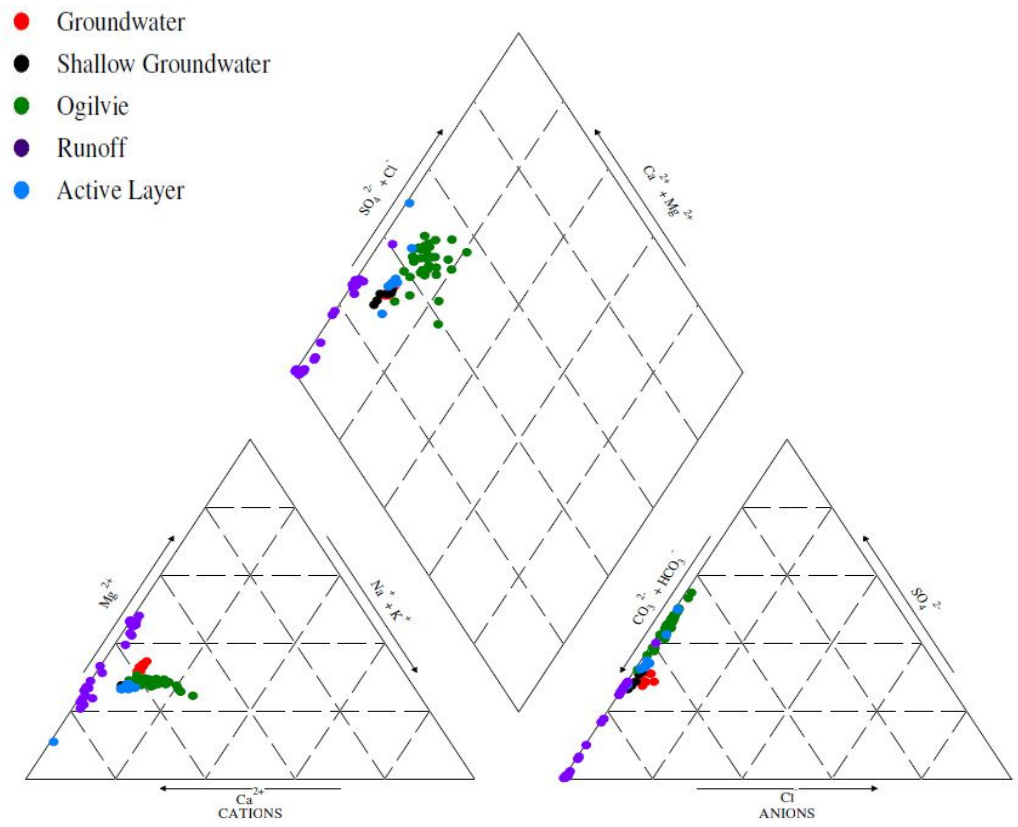

Figure 21 Piper Diagram of the Flow Components

Opposite to the weathering solutes, the biogenic solutes such as DOC and potassium are lowest during the winter when low temperatures and low light levels inhibit biological activity. These solutes peak at the start of freshet when the early snowmelt water is able to pick up high loads of organics from the surficial organic materials. This is similar to findings by Carey et al. (2013) in the Granger Creek basin near Whitehorse, Yukon. At the early snowmelt water accumulates under snowpack, it is in direct contact with the organic matter. In some case, surface 2-5 cm of organics was observed to be fully drained prior to freshet. This layer would also act as thin early season active layer. The contact with organics allows for dissolution of organic matter into waters that form spring runoff. Larger volumes of peak freshet flows flush out easily soluble organic matter and also reduce the contact time of meltwater with the organics resulting in the biogenic solutes peak concentrations occurring prior to the river flow peak. As the summer progresses, the biogenic solutes fluctuate at medium levels responding to increased biological activity on land and in the water and to diluting effect of rain events. The $\delta^{13}C$ of DOC was most depleted at high DOC concentrations corresponding to the input of fresh organic matter with the most depleted isotopic signatures.

The calcite saturation index and partial pressure of CO_2 in the Ogilvie River were calculated using solution calculations in PhreeqC. The input parameters included major ions, pH, temperature, and bicarbonate concentrations derived from the field alkalinity measurements. Figure 22 shows the evolution of the calcite saturation and pCO_2 prior to and through the rising limb of the freshet (2015), during the falling limb of the hydrograph (2014), and during the late summer (2014 and 2015). The calcite was slightly undersaturated during the winter flow conditions (logSI~ -1.5 to -1) and rose close to the fully saturated point (logSI~0) prior to the start of freshet. This saturation peak coincides with the pH rise and peak of the weathering solutes concentrations. As the flows approach peak the calcite saturation returns to the winter levels as the groundwater input is greatly diluted by the surface runoff. After the peak flow calcite saturation increased solely due to increasing proportion of the groundwater in the Ogilvie discharge and associated weathering solutes without pH affecting the solubility. In late summer the calcite was close to full saturation in both 2014 and 2015 owing to higher pH values (~7.9-8.2).

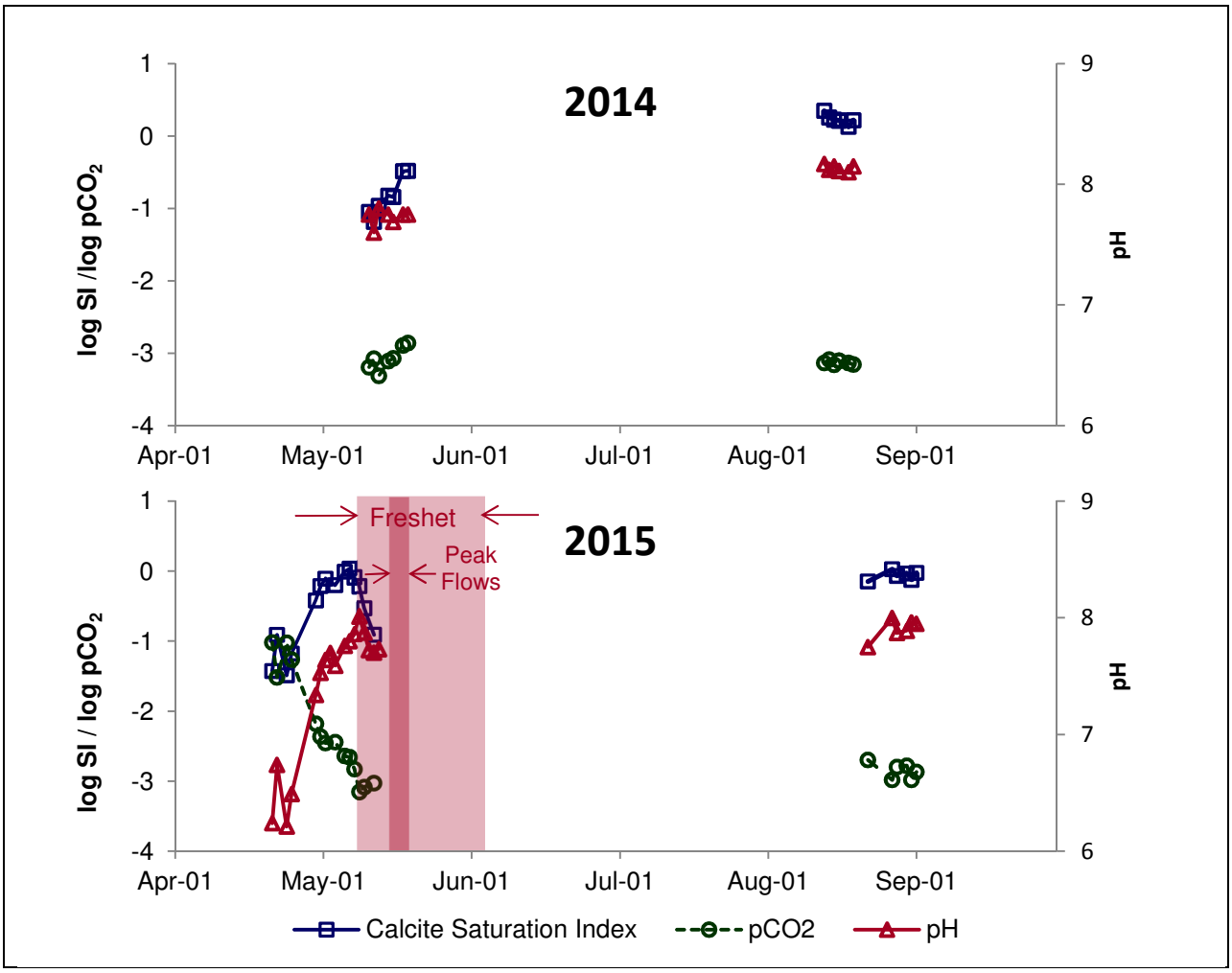

Figure 22 **Calcite Solubility and Partial Pressure of CO_2, Ogilvie River at sampling site (2014, 2015)**

The pCO_2 follows the opposite trend to the calcite saturation. In the winter baseflow the river water was oversaturated with the CO_2 ($pCO_2 \sim 10^{-1}$) compared to the atmospheric CO_2 ($10^{-3.4}$). With the onset of the freshet the CO_2 levels decreased to only slightly above atmospheric levels ($\sim 10^{-3.2}$ to 10^{-3}). The major reason for such a rapid pCO_2 decrease was removal of ice cover from the river and initiation of turbulent flows which allowed for equilibration of dissolved gases with the ambient air. As the freshet flows decreased the pCO_2 rose slightly to approximately $10^{-2.85}$. In the late summer the dissolved CO_2 concentrations remained saturated slightly above the atmosphere ($pCO_2 \sim 10^{-3.1}$ in 2014 and $\sim 10^{-3.0}$ to $10^{-2.7}$ in 2015).

The annual evolution trends of all solutes in Ogilvie River were generally consistent between 2014 and 2015. These trends are also consistent with the available historical information from the late 1970s investigations (Schreier, 1979) suggesting long term consistency.

8.3 Groundwater Residence Times

The tritium activities in deep and shallow groundwaters (Figure 23) are indicative of the residence times of the deep and shallow groundwaters.

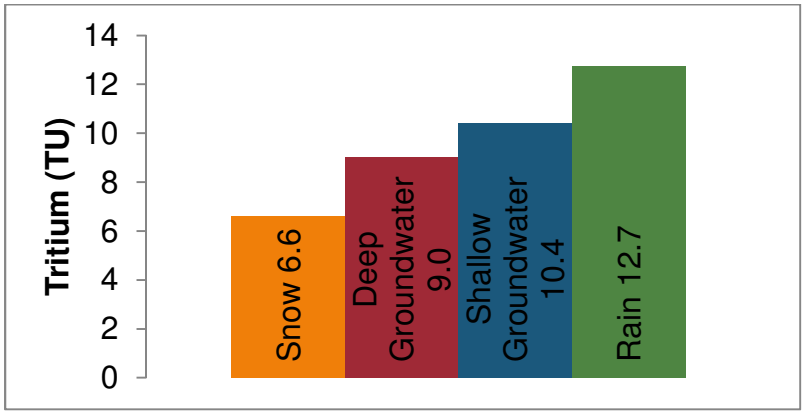

Figure 23 Average tritium activities

The 65% rain – 35% snow mixing ratio of deep and shallow groundwater recharge provides the average tritium activity of recharge waters of 10.6 TU. Using the radioactive decay formula (Equation (4) the groundwater ages were estimated.

$$t = \ln(\frac{N_A}{N_o}) \cdot \frac{-T_{1/2}}{\ln(2)} \qquad \textbf{(4)}$$

where:

t	is the age of groundwater (yr)
N_A	is the activity of groundwater (TU)
No	is the activity of recharge waters (TU)
$T_{1/2}$	is tritium half-life (12.32 yr).

Shallow groundwater age is calculated to be 0.3±1.4 years and deep groundwater age is 2.9±1.1 years. Such low tritium derived ages point to rapidly circulating groundwater systems. Large uncertainties in the calculations are reflective of both the variations in tritium concentrations in flow components and uncertainties associated with the laboratory analysis.

8.4 Sub-surface Interactions at Recharge

The carbon signature of the spring recharge waters is characterized by the surface runoff during freshet when the recharge occurs. At this time of the year, the runoff has a signature of the snowmelt augmented by the interactions of the snowmelt water with the surface organic below

the snowpack and within the surficial organic matter that has been fully drained in the preceding autumn. Based on the field observations prior to the freshet, the surface organic material was well drained and consisted of mosses, lichens, and roots - a highly porous substrate for the snowmelt to flow through. This is especially evident in the levels of DOC in the runoff. The concentrations reached were as high as 41.7 ppm C. The early snowmelt likely spends a certain period of time filling the porous organics prior to generating runoff. It is at the early stages of runoff generations that the high DOC concentrations are present in the runoff streams similar to other subarctic streams (Carey et al., 2013). The concentrations quickly drop off, and by mid-freshet the DOC concentrations are only slightly higher than in the late summer.

The $\delta^{13}C$ isotopes of the DIC and DOC also evolve throughout the freshet. Similarly to the Ogilvie River, The $DI^{13}C$ generally follows the DIC concentrations and $DO^{13}C$ inversely follows the DOC concentrations. The $\delta^{13}C$ of the DOC in the surface runoff ranged from -28.4‰ to -26.4‰ indicating that the organics contributing to the DOC are C_3 vegetation which has an expected signature of around -27‰ (Clark, 2015). The dissolved CO_2 in the soil water is generated from the bacterial respiration that uses organic material as food source and as such should reflect the organic carbon signature. Based on the completed soil gas analysis, the $\delta^{13}C$ of the soil CO_2 is, on average, -25.4‰. Through weathering, the dissolved CO_2 reacts with the carbonate bedrock producing inorganic carbon compounds such as bicarbonate HCO_3^-. The $^{13}CO_2$ signature gets diluted with the ~0‰ $\delta^{13}C$ of the carbonate. The groundwater $\delta^{13}C$ of the DIC is ~7.7‰ which falls on the heavier end of the groundwater DIC range of -19‰ to -7‰ (Clark, 2015).

8.5 Active Layer Water vs. Shallow Groundwater

The shallow groundwater appears to be very similar in composition to the active layer water (Sections 7.3 and 7.5). The geochemical characters of these flow components are very similar as can be seen from the Piper diagram (Figure 21). However, concentrations of weathering solutes such as DIC, calcium and magnesium are slightly higher in the shallow groundwater. The groundwater appears to be more evolved active layer water where the DOC is mostly converted to DIC. The stable carbon isotopes and $F^{14}C$ of DIC and DOC are the same.

8.6 Hydrograph

8.6.1 Comparison to Historical Hydrographs

The 2015 hydrograph for the Ogilvie River at the historical gauging location is similar to the historical hydrographs. The freshet occurred within the previously observed time frame and the peak flow was also within range. The frequency and magnitude of the summer discharge peaks in 2015 were comparable to the historical observations. The noticeable difference occurred in the fall. As can be seen on Figure 24, none of the historical hydrographs had flow peaks past late September. However, there was a large flow spike in the beginning of November 2015 and it took a long time for the Ogilvie River to return to baseflow. It is possible that the active phase of the hydrological cycle is extending further into the autumn.

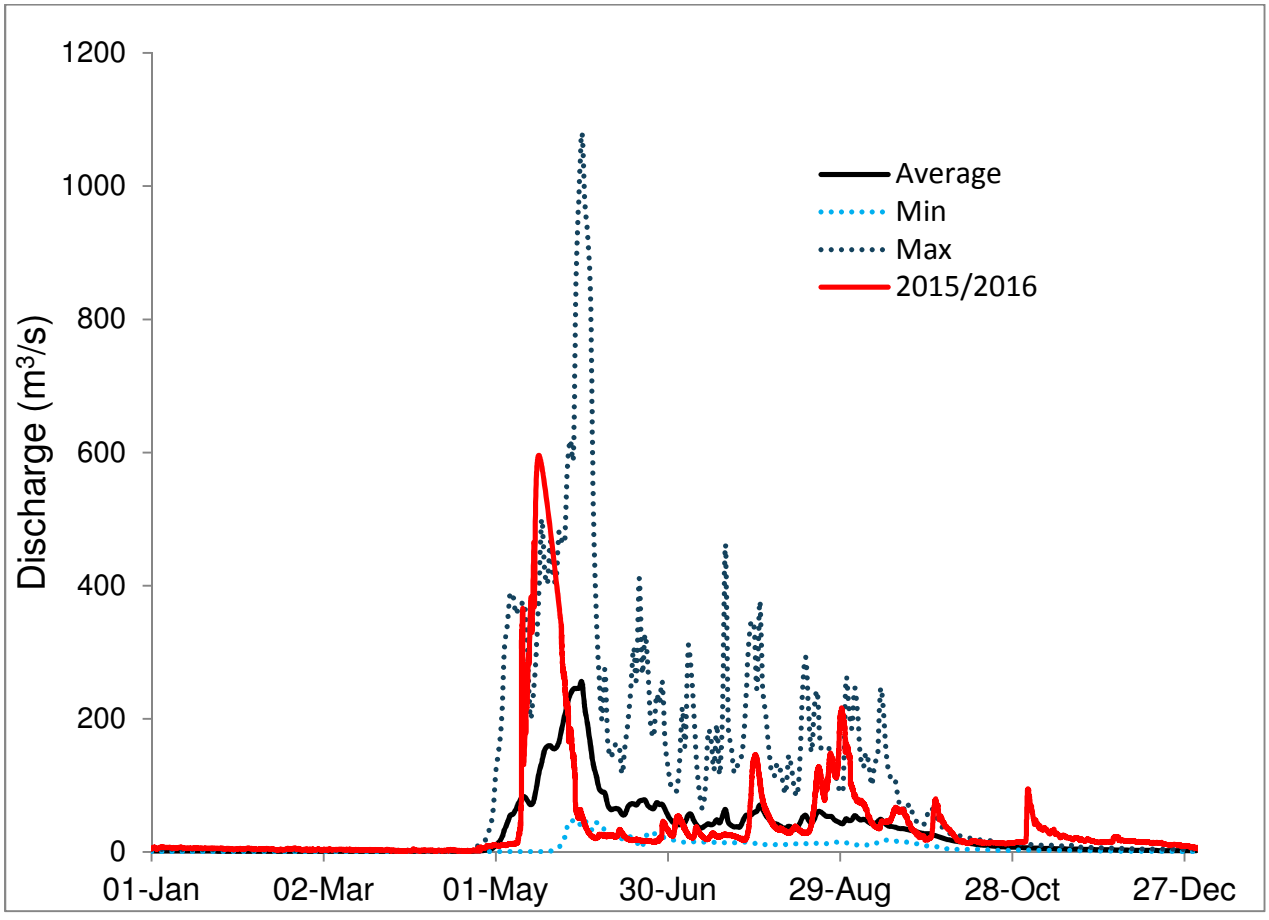

Figure 24 **Comparison of 2015/2016 Hydrograph to 1974-1996 Flow Ranges at 10MA002 location**

8.6.2 Hydrograph Separation

The EMMA hydrograph separation technique was used to quantitatively estimate the amount of deep groundwater contribution to the overall flow of Ogilvie River at sampling point. Stable isotopes (^{18}O and ^{2}H) are considered to be suitable tracers of the meteoric water cycling through the system. As ^{18}O and ^{2}H are dependent on each other, only ^{18}O was used for hydrograph separation.

The mass balance approach was used in this two-member hydrograph separation to calculate the groundwater in the river discharge as shown in the following equations (Equation (5) using groundwater and surface runoff as endmembers.

$$Q_{Ogilvie} \cdot C_{Ogilvie} = Q_{GW} \cdot C_{GW} + Q_{Runoff} \cdot C_{Runoff} \qquad \textbf{(5)}$$

$$Q_{Ogilvie} = Q_{GW} + Q_{Runoff}$$

where:

Q is the flow

C is the concentration of tracer

GW is groundwater.

The hydrograph separation was only performed on the 2015 data based on the discharge data availability. The hydrograph of the Ogilvie River above Engineer Creek was used for separation. The signatures of the endmembers were also derived from the 2015 sampling results. The runoff signature was obtained via averaging the concentrations of the three analogue tributaries C1, C2, and C3. The signatures were divided into two time periods: freshet and summer. Table 13 summarizes the values used in the hydrograph separation and Figure 25 shows the results of the separation for the period of April 24 to August 31, 2015 – the period for which both the required geochemical and hydrometric data were available.

Table 13 Summary of the endmember $\delta^{18}O$ signatures (2015)

Endmember	$\delta^{18}O$ value	Source
Groundwater	-22.31‰	Average of April 21 to 25, 2015 values (Ogilvie River)
Runoff (freshet) April 22 – May 13	Value fluctuates (-25.56‰ to -23.89‰)	Average of C1, C2, C3 values as measured. For days with no samples the values were linearly interpolated between known values.
Runoff (freshet) May 14 – June 4	-24.53‰	Average of April 22 to May 13 (C1, C2, C3)
Runoff (summer) June 5 – August 21	-21.30‰	Average of August 22 to 31 (C1, C2, C3)
Runoff (summer) August 22 – August 31	Value fluctuates (-21.40‰ to -21.15‰)	Average of C1, C2, C3 values as measured. For days with no samples the values were linearly interpolated between known values.

Based on the hydrograph separation results the groundwater constituted 44% of the flow at the peak volumetric flow on May 23 (129 m^3/s out of 295 m^3/s), a week after the river peak flow on May 16. The lowest fraction of the groundwater flow in the analyzed period was 12-14% corresponding to the local minimum river flows on May 12-13. The groundwater fully sustained the river discharge before and right after the freshet. As the summer flows developed, the groundwater contribution steadily dropped to as low as 20% in late July and continued to remain below 40% until the end of August when the groundwater fraction dropped to its minimum of 11% on August 28.

On annual basis for the available record period the overall discharge was $7.1 \cdot 10^8$ m^3 on par with the historical average of $9.6 \cdot 10^8$ m^3. Normalized to the catchment area, the groundwater comprised 77 mm of 157 mm or 48% of the annual discharge.

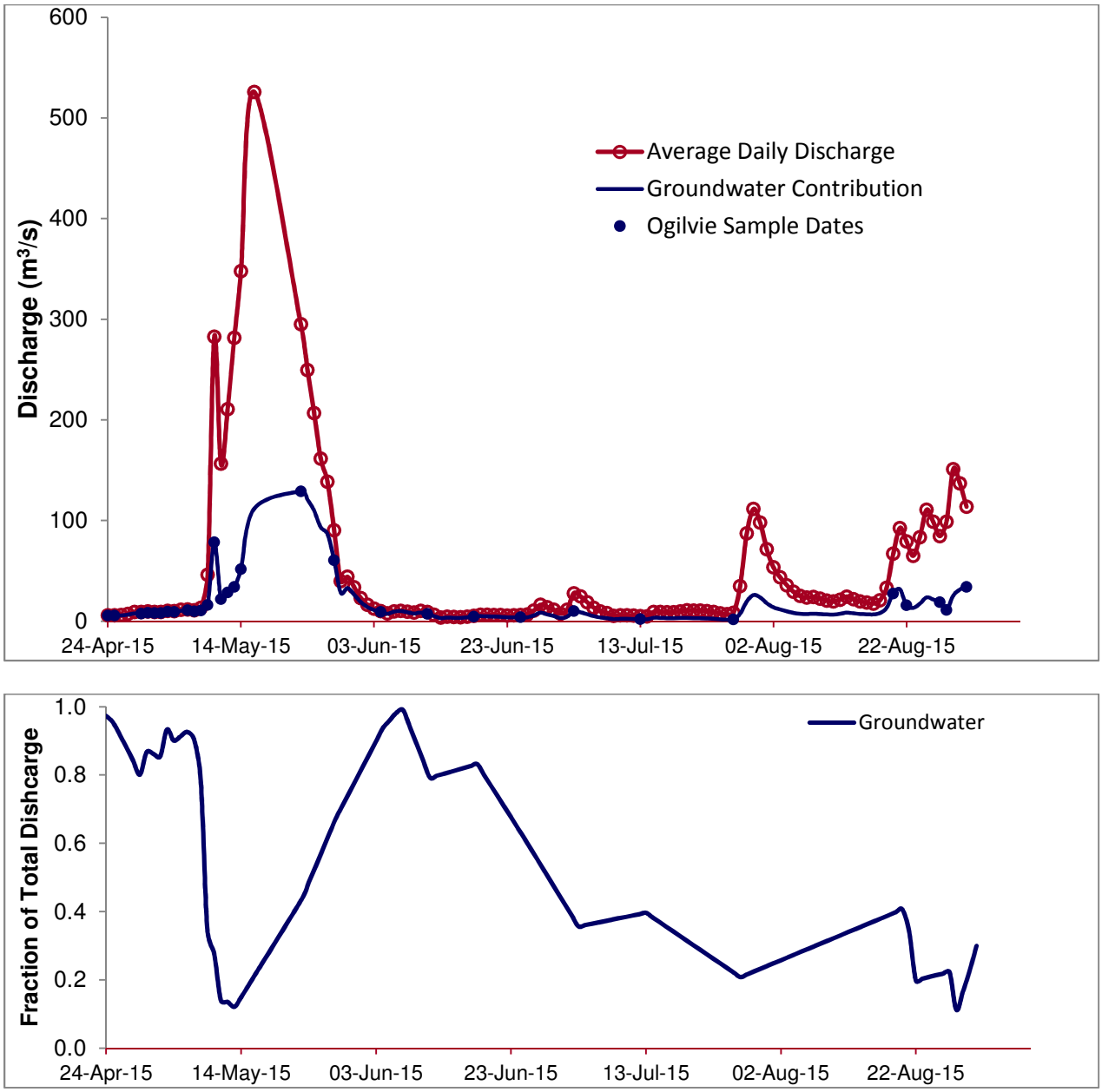

Figure 25 Hydrograph Separation using $\delta^{18}O$, 2015

8.7 Principal Component Analysis

The principal component analysis (PCA) is a technique that uses linear algebra principles in order to identify underlying simplified structure of a dataset which can help identify main factors responsible for observed variability (Shlens, 2005). To reduce the dimensions of the dataset, the technique transforms the dataset in a way that maximizes the variance of the first principal component. The principal components are then uncorrelated orthogonal variables that are essentially the eigenvectors of the covariance (Malkin, 2008; Shlens, 2005).

Statistical package R was used to perform the PCA using the in-built function prcomp(). The analyzed matrix consisted of rows representing individual sampling dates and columns representing analytes. A total of fifteen (15) analytes were used in the analysis including DIC, DOC and their $\delta^{13}C$ values, major cations and anions, $\delta^{18}O$, and $\delta^{2}H$. Fifty samples of the Ogilvie River collected in 2014 and 2015 that had complete results for all 15 analytes were used for the PCA. Because the analytes used in the PCA have different units, the data was standardized using mean center value normalized to the standard deviation (Pittard, 2012).

The full PCA results are included in Appendix E. The first three principal components (PCs) account for a total of 75.6% of the total variance (47.8%, 18.3%, and 9.6% respectively). The remaining PCs account for small portions of total variance and are, therefore, not further examined. The eigenvalues (or loadings) for the first three PCs are shown in Table 14. The PC1 is characterized by DIC, DOC, Ca^{2+}, Mg^{2+}, and SO_4^{2-}. The PC2 is characterized by K^{+}, NO_3^{-}, $\delta^{18}O$, and $\delta^{2}H$. The PC3 is characterized by $\delta^{13}C$ DOC and K^{+}. Some of the analytes contribute significantly to variability in more than one PC.

Table 14 PC eigenvalues, Ogilvie River dataset (2014, 2015)

	PC1	PC2	PC3
DIC	**-0.32924**	0.19367	-0.18503
DOC	**0.30565**	-0.10044	0.10062
δ^{13}C DIC.	-0.21747	0.00539	0.2784
δ^{13}C DOC.	-0.08664	0.10699	**0.72304**
Ca	**-0.36136**	0.05872	-0.06556
K	0.0981	**0.34368**	**-0.38418**
Mg	**-0.35158**	0.17125	-0.0727
Na	-0.27087	-0.08671	-0.2156
Sr	**-0.33046**	-0.18736	0.12962
F	0.00217	-0.05771	-0.1726
Cl	-0.23238	**0.45428**	-0.0315
SO4	**-0.32244**	-0.22529	-0.18723
NO3	-0.18914	**0.41788**	0.25639
δ^{2}H	-0.21497	**-0.39617**	0.00329
δ^{18}O	-0.23882	**-0.39418**	0.05749

The biplot of the PCs 1 and 2 is shown in Figure 26. The arrows indicate the influence each analyte has on PC1 and PC2. It can be seen that K^+ and DOC are more related to each other and the rest of the analytes group more closely. The numbers refer to individual sampling dates in the data set (see Appendix E). There are three general groupings of samples that are evident from this biplot. Group in the top left corner, consisting of samples #31-35, correspond to the winter baseflow samples. Group starting from the centre of the plot and extending to the right contains freshet samples. Lastly, samples extending from the bottom left and wrapping around the bottom to the centre of the plot are summer flow samples. Such grouping indicates that various flow components have distinct enough signatures supporting the use of EMMA hydrograph separation technique. At different times of the year the flow components vary and with distinct signatures it is possible to attribute the in-stream chemistry changes to changes in the individual flow components and their signatures.

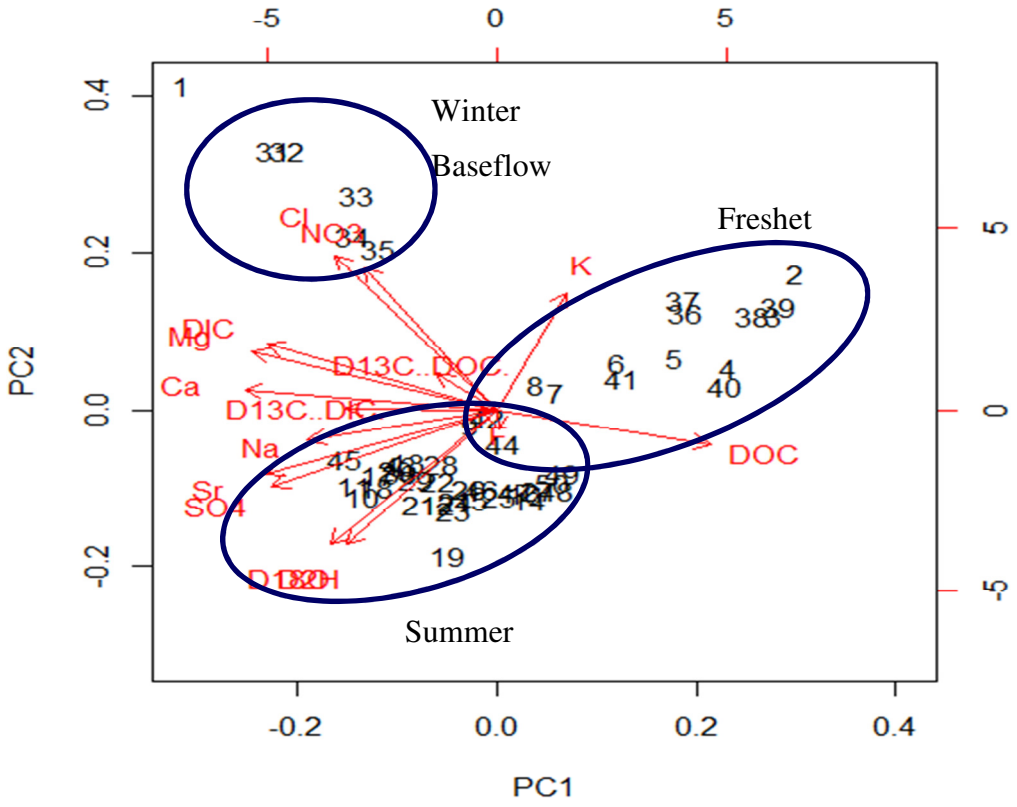

Figure 26 PCA Output Biplot (Ogilvie River dataset, 2014-2015)

8.8 Soil/Water Interactions and Weathering

In order to assess the soil/water interactions and weathering processes in the watershed, the 2014-2015 average values of carbon (DIC and DOC) concentrations, $\delta^{13}C$, and $F^{14}C$ are used. In this section theoretical calculations of these parameters expected based on the proposed wreathing regime are compared to the average measured values.

The external system input of rain and snow is assumed to contain no appreciable concentrations of carbon. Snowmelt interacts with the surface soils to generate spring runoff flow component that is characterized by DIC of 22 ppm C ($\delta^{13}C$ ~ -6.0‰) and DOC of 11.9 ppm C ($\delta^{13}C$ ~ -26.9‰). The DIC component is generated by weathering of inorganic soil potentially augmented by oxidation of organic compounds which is expected to be low due to cold temperatures and corresponding low biological activity. The $\delta^{13}C$ of DIC ranged from -11.2‰ to -1.3‰ reflecting varying degrees of weathering of carbonate minerals in soils via open system

weathering. In the spring the major weathering drivers are the atmospheric CO_2 with the $\delta^{13}C$ of ~ -8.3‰ (Clark, 2015) and the biogenic CO_2 with $\delta^{13}C$ of ~ -25.4‰. An approximately 50-50 mixture of these two CO_2 sources would have $\delta^{13}C$ of ~ -16.9‰ yielding soil DIC of -6.0‰ when a fractionation factor $\varepsilon^{13}C_{DIC\text{-}CO2}$ of 10.9‰ (at 0°C) is applied (Clark, 2015).

The DOC of the spring runoff is solely derived from the dissolution of the pre-existing organic matter at the soil surface and within shallow surficial soils. It was noted during field observations that prior to freshet the top 2-7 cm of organic material were fully drained, thus providing high contact surface area for the surface runoff waters. The $\delta^{13}C$ signature of surface runoff of -26.9‰ is typical of the C_3 plants (Clark, 2015).

In the summer, when the biogenic activity is present, the soil CO_2 $\delta^{13}C$ is -25.4‰. The CO_2 is then the single major driver of open system carbonate weathering resulting in soil water DIC $\delta^{13}C$ of -13.6‰ in late summer and -15.2‰ at freeze-up (theoretically: -25.4‰+ $\varepsilon^{13}C_{DIC\text{-}CO2}$ (9.7‰ at 10°C) = -15.7‰).

The summer runoff waters are generated from rain precipitation that undergoes higher level of interactions with the organic material than the snowmelt waters due to thickening of the active layer. The Summer Runoff component is characterized by DIC of 48 ppm C ($\delta^{13}C$ ~ -7.1‰) and DOC of 7.5 ppm C ($\delta^{13}C$ ~ -26.0‰). Compared to spring runoff, it has higher inorganic carbon and lower organic carbon concentrations. The longer residence time of the water means that the dissolved organic matter is able to oxidize to inorganic carbon (increase in pCO_2) and this, in turn, leads to higher rates of weathering. More depleted $\delta^{13}C$ signature of DIC in summer than spring runoff is likely due to higher proportion of biogenic CO_2 responsible for weathering.

The deep groundwater is recharged with a mixture of spring runoff (i.e. snowmelt) and active layer water (i.e. rainfall) in a 35:65 proportion (Section 8.1). Almost all DOC is oxidized to CO_2 and is then reacted with the carbonate bedrock via closed system weathering. Consequently, DIC concentration increase is equal to double of the molar concentration of DOC, the $\delta^{13}C$ of DIC increases by the halved $\delta^{13}C$ of DOC, and $F^{14}C$ of DIC increases by half of the DOC $F^{14}C$, assuming all DOC is oxidized.

$$DIC_{DGW} = 0.65 \cdot [DIC_{AL} + 2 \cdot DOC_{AL}] + 0.35 \cdot [DIC_{SR} + 2 \cdot DOC_{SR}]$$

$$DI13C_{DGW} = \frac{0.65 \cdot [DIC_{AL} \cdot DI13C_{AL} + DOC_{AL} \cdot (DO13C_{AL} \cdot 0.5)] + 0.35 \cdot [DIC_{SR} \cdot DI13C_{SR} + DOC_{SR} \cdot (DO13C_{SR} \cdot 0.5)]}{DIC_{DGW}}$$

$$DI14C = \frac{0.65 \cdot [DIC_{AL} \cdot DI14C_{AL} + DOC_{AL} \cdot (DO14C_{AL} \cdot 0.5)] + 0.35 \cdot [DIC_{SR} \cdot DI14C_{SR} + DOC_{SR} \cdot (DO14C_{SR} \cdot 0.5)]}{DIC_{DGW}}$$

where DGW is deep groundwater, AL is active layer, SR is spring runoff, DIC is dissolved inorganic carbon, $DI^{13}C$ is the $\delta^{13}C$ of DIC, $DI^{14}C$ is the $F^{14}C$ of DIC, DOC is dissolved organic carbon, $DO^{13}C$ is $\delta^{13}C$ of DOC, and $DO^{14}C$ is the $F^{14}C$ of DOC. As seen from Table 15, the theoretical values of DIC concentration and its isotopes are in line with the observed parameters confirming the groundwater evolution process of DOC oxidation and closed system weathering.

Table 15 Deep Groundwater DIC Values

Input Parameters			
DIC_{AL} = 40 ppm C	DOC_{AL} = 8 ppm C	DIC_{SR} = 22 ppm C	DOC_{SR} = 11.9 ppm C
$DI13C_{AL}$ = -10.4‰	$DO13C_{AL}$ = -24.9‰	$DI13C_{SR}$ = -6‰	$DO13C_{SR}$ = -26.9‰
$DI14C_{AL}$ = 0.66	$DO14C_{AL}$ = 0.87	$DI14C_{SR}$ = 0.98	$DO14C_{SR}$ = 1.05
Calculated (Theoretical)		**Observed Parameters**	
DIC_{DGW} = 52.9 ppm C		DIC_{DGW} = 55 ppm C	
$DI13C_{DGW}$ = -8.3‰		$DI13C_{DGW}$ = -7.7‰	
$DI14C_{DGW}$ = 0.51		$DI14C_{DGW}$ = 0.55	
Assumption: all DOC is oxidized			

In the summer, the active layer water is further evolved into the shallow groundwater by similar principle as above via oxidation of organic matter to CO_2 and closed system bedrock weathering. Because there is appreciable residual DOC in the shallow groundwater, only the converted portion of DOC is used in the calculations. The calculated and observed DIC parameters show good correlation (Table 16).

Table 16 Shallow Groundwater DIC Values

Input Parameters			
DIC_{AL} = 40 ppm C	DOC_{AL} = 8 ppm C		DOC_{SGW} = 2.2 ppm C
$DI13C_{AL}$ = -10.4‰	$DO13C_{AL}$ = -24.9‰		
$DI14C_{AL}$ = 0.66	$DO14C_{AL}$ = 0.87		
Calculated (Theoretical)		**Observed Parameters**	
DIC_{SGW} = 52 ppm C		DIC_{SGW} = 50 ppm C	
$DI13C_{SGW}$ = -10.9‰		$DI13C_{SGW}$ = -10.8‰	
$DI14C_{SGW}$ = 0.61		$DI14C_{SGW}$ = 0.66	
Assumption: Amount of DOC oxidized = DOC_{AL}-DOC_{SGW} = 8-2.2 = 5.8 ppm C			

8.9 Recharge pathways

Based on the recharge mixing ratio of snowmelt to rainfall, a large portion (35%) of recharge is occurring in the springtime. The rest of the recharge (65%) must occur during the summer rain periods, likely during larger rain events.

Because of the high degree of interaction of the recharge waters with soil, the large portion of recharge is expected to take place over vegetated areas. This excludes the more obvious recharge pathways through the fractures of exposed limestone. However, these bedrock exposures are usually located at the ridge peaks where the snow accumulation is low and the rain runoff is high due to steep slopes.

The actual recharge pathways cannot be examined on a large watershed scale using available data. However, some potential pathways may include recharge through thermal contraction cracks and bedrock fractures. It is known that the thin permafrost observed nearby the watershed may be due to the shallow groundwater circulation providing additional heat input to degrade permafrost from the underside (Idrees et al., 2015). Based on the presence of thin permafrost and thick talik at the maintenance camp (at least 5.4 m based on the drinking water well installation details), there are possibilities for through taliks to exist throughout the discontinuous permafrost of the study watershed.

While not covered by this research, the historical study that examined water quality along the Ogilvie River (albeit mostly downstream of the study watershed) found that there may be some recharge occurring in-stream due to the syncline-anticline bedrock systems (Schreier, 1979). It should be also noted that without regional scale groundwater watershed delineation, it is not

known if all the groundwater discharged in the upper Ogilvie watershed is actually recharged within the surficial basin.

8.10 DIC/DOC Exports

The one year of full discharge data for the upper Ogilvie River was collected for the period of April 24, 2015 to April 23, 2016. A data gap of 7 days in the middle of the freshet was filled in by data interpolation. The total discharge for this period was 0.71 km^3/yr or 15.8 cm/yr when normalized to the watershed area of 4,500 km^2.

The upper Ogilvie runoff is 15.6 cm/yr which is within the range of the Mackenzie River runoff values (15-20 cm/yr); however, the DIC runoff of 5.6 gC/m^2/yr is closer to the Yukon River watershed exports (5-6 gC/m^2/yr) compared to the Mackenzie River exports (4-5 gC/m^2/yr) (Tank et al., 2012).

The DOC exports from the basin are 2.1 gC/m^2/yr which is on the higher end of the DOC exports from the Big Six Arctic rivers ranging from 0.75 to 2.6 gC/m^2/yr (Raymond et al., 2007). While Raymond et al. (2007) argues that the DOC released during freshet passes through the riverine systems largely unchanged due to cold temperatures, it is unlikely that the DOC export from Ogilvie watershed will directly reach Arctic Ocean because of the long distance between the Ogilvie watershed and the Mackenzie River delta. The DOC exported during the summer is expected to be biologically or chemically consumed prior to discharging in the ocean.

The seasonality of the DIC and DOC exports exhibits somewhat opposite trends. Due to high weathering DIC concentrations in the groundwater, the majority of DIC is exported during the fall/winter months; however, the DOC concentrations are highest during freshet coinciding with high river discharge. Figure 27 shows the comparison of the DIC and DOC exports by flow periods of 2015-2016: freshet from April 22 to June 4; summer from June 5 to August 31, and fall/winter from September 1 to April 21. The DOC exports correspond well with the discharge volumes while the DIC export is disproportionately higher in the fall/winter due to low freshet exports.

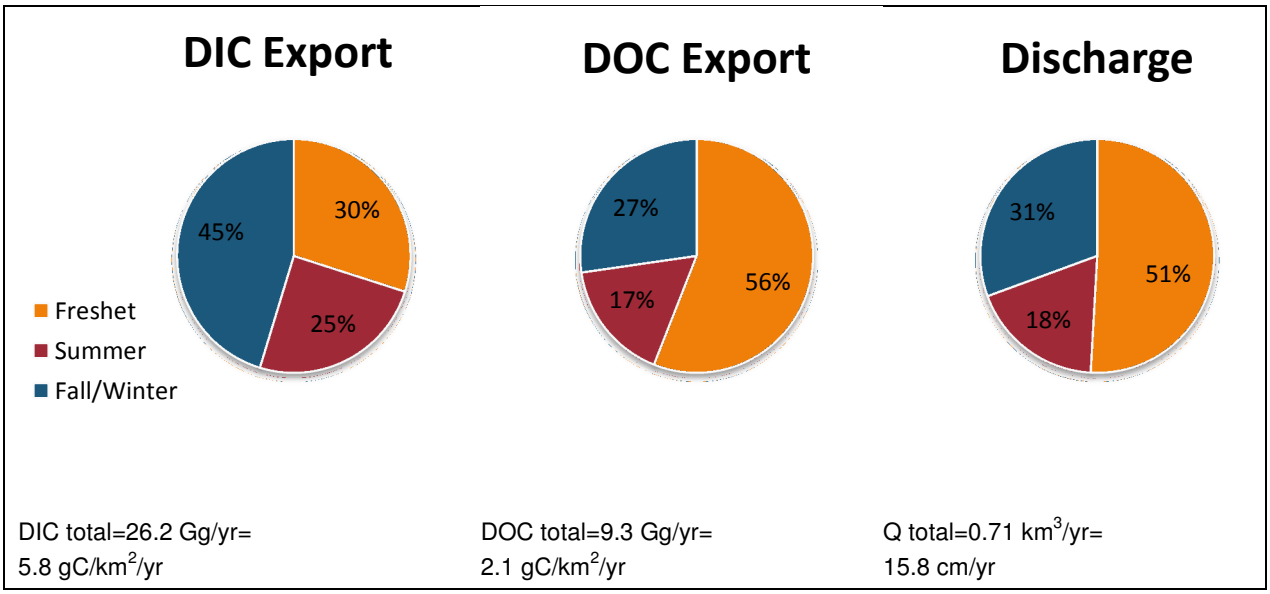

Figure 27 Seasonality of DIC and DOC exports from upper Ogilvie River (2015/2016)

The DIC:DOC ratio of 2.8 falls above the global average of 2 but is below the North American ratio of 3.8 (Tank et al., 2012).

9 Conclusions

This study examines hydrology and geochemistry of the upper Ogilvie watershed based on the data collected in 2014 and 2015 and based on the available historical weather and discharge data.

The 4,475 km^2 study watershed is located at the northern extent of the discontinuous permafrost region. The permafrost thickness is highly variable (2.1 to 244 m) and is poorly defined. The active layer ranges from 35 to 80 cm. Sedimentary bedrock such as limestone, dolostone and shales comprise approximately two thirds of the watershed. The study area is characterized by MAAT of -8°C and average annual precipitation of 343 mm comprising of 63% rain and 37% snow. Limited meteorological and hydrometric historical data consists of 36 years of frequently incomplete year-round precipitation records at the Ogilvie Highway Maintenance Camp (1971-2006) and 22 years of flow gauging of Ogilvie River downstream of its junction with Engineer Creek at Dempster Highway (1974-1996). The average annual flow of the historically gauged watershed (5,410 km^2) was $9.6 \cdot 10^8$ m^3. The average runoff coefficient of 0.52 is typical for the low Arctic. Ogilvie River exhibits subarctic nival flow regime characteristic of the discontinuous permafrost areas.

The seasonal variations of chemistry of the upper Ogilvie River were governed by mass balance of the discharge contributions at different times of the year. In the winter the flow is fully fed by deep groundwater characterized by high levels of weathering solutes (calcium, magnesium, sulphate and DIC). The concentrations of these solutes peak prior to freshet. During the freshet the river is fed by spring snowmelt runoff and groundwater. This translates to dilution of the weathering solutes throughout the freshet and spike of the biogenic solutes such as K^+ and DOC at the start of freshet. The groundwater-fed Ca^{2+}-HCO_3^- winter waters evolve into (Na^++Ca^{2+})-(HCO_3^-+Cl^-) waters during freshet. During the summer the active layer and shallow groundwater are additional sources of water in the Ogilvie River. At this time, the weathering solutes fluctuate in response to the flow changes; however, no direct correlation to the precipitation and/or flows is evident. In general, the $\delta^{13}C$ isotope signatures are dependent on the carbon source. The $\delta^{13}C$ of DIC follows the DIC concentration pattern – more depleted isotope values correspond to lower DIC concentrations. The DIC concentrations are diluted at times of increased discharge which generally corresponds to the increased organic load with much more depleted $\delta^{13}C$ signature (-28.4‰ to -26.4‰). As the organic matter is oxidized to DIC, the groundwater $\delta^{13}C$ of

~-8‰ is lowered. The $\delta^{13}C$ of DOC exhibited a trend opposite of DIC – more depleted isotope values corresponded to higher DOC concentrations. The fresh DOC input into the system has the lowest $\delta^{13}C$ values. Due to the large size of the upper Ogilvie watershed (~4,500 km^2), the minor changes are attenuated and only large-scale hydrological events such as freshet can be directly traced through the system.

The LMWL, established for the watershed based on the local precipitation samples collected and corrected for altitude, is $\delta^2H=6.77\cdot\delta^{18}O-24.54$ ($R^2=0.98$). All components of the hydrological system except for the soil water plot above the LMWL showing lc-excess between 0.9‰ in the spring Ogilvie flow and 6.3‰ in the active layer water. This lc-excess is not currently explained. The stable oxygen and hydrogen isotopes in the flow inputs are attenuated in the river, more so in the spring compared to the summer.

Two groundwater components were identified in the study watershed: deep groundwater corresponding to the winter baseflow and shallow groundwater corresponding to the water found in deep talik in the vicinity of the river. Shallow groundwater is in many ways similar to the active layer waters; however, the shallow groundwater is distinguished by higher weathering solutes and lower DOC concentrations. The higher DIC concentrations in shallow groundwater than in active layer reflect the oxidation of DOC to DIC and more advanced weathering. Shallow and deep groundwater components in the study area are likely separated by permafrost that may be thin in the area due to actively circulating groundwater.

Discharge records were collected for the Ogilvie River above Engineer Creek (upper Ogilvie) and below Engineer Creek (corresponding to historical gauging station catchment area) for the period of April 24, 2015, to April 24, 2016. The hydrograph compared well to the historical records with respect to freshet peak flows and timing and to the late summer peak magnitudes. An unusual November flow peak recorded in 2015 may indicate extension of the active hydrological cycle into the fall. The upper Ogilvie River maximum flow of 526 m^3/s was recorded on May 16, 2015. Due to uncertainties of the records during the very peak of the freshet, it is possible that higher flows were reached.

In order to assess the deep groundwater contribution to the overall stream discharge, two-component EMMA was completed using $\delta^{18}O$ as a stable isotopic tracer. Based on this hydrograph separation the largest groundwater contribution of 129 m^3/s occurred on May 23

during the freshet when it comprised 44% of the flow. The groundwater was the sole flow component in upper Ogilvie River during the winter baseflow as well as during some of the low flow of the early summer. During the middle and late summer the groundwater contribution remained below 40% of the total flow. On the annual basis, the deep groundwater comprised almost half (48%) of the total river discharge.

Based on the LMWL, shallow and deep groundwaters are recharged with the mixture of snowmelt (35%) and rain (65%). All sampled flow components contained tritium pointing to short residence times. Taking into account the mixing ratio of low tritium snow (6.6 TU) and high tritium rain (12.7 TU), shallow groundwater circulates very rapidly in the order of months and the residence time of deep groundwater was about 3 years.

At the time of recharge the water interacts greatly with the subsurface: with the soil at the recharge and with carbonate bedrock as the water travels form recharge to discharge zone. Open system carbonate weathering takes place as the surface runoff infiltrates the active layer driven by high biogenic CO_2 concentrations with depleted $\delta^{13}C$ signatures (-25.4‰). As the deep groundwater recharges, the DOC is oxidized to CO_2 which, in turn, drives closed system carbonate weathering. This results in reduction of DOC concentrations to very low levels, increase in the DIC concentrations, and dilution of the $\delta^{13}C$ and $F^{14}C$ signatures of the DIC. Shallow groundwater component is an evolved active layer water generated by further closed system weathering which converts DOC to DIC. Because the groundwater age was constrained by the presence of tritium activity, low radiocarbon levels aided in identifying closed system weathering conditions demonstrating carbon dilution. The radiocarbon signatures of the dissolved organic matter traced the access to fresh modern organics ($F^{14}C$=1.05) during the spring and to older carbon stocks ($F^{14}C$=0.88) during the late summer. Even older organic stocks are accessed by deep groundwater ($F^{14}C$=0.68).

The exact groundwater recharge pathways cannot be directly identified based on the collected data. The summer recharge (65%) likely occurs during high precipitation events. High degree of interactions with soil during recharge suggests that majority of recharge occurs over vegetated areas. Potential recharge pathways include thermal contraction cracks in permafrost and bedrock fractures with the possibility of some of the recharge occurring within the stream.

The annual DIC catchment export was estimated to be 5.6 $gC/m^2/yr$. The DIC exports were disproportionately higher in the winter (45% of total) compared to freshet (30%) and summer (25%). The DOC export of 2.1 $gC/m^2/yr$ was proportional to the discharge throughout the year. The DIC:DOC export ratio was 2.8, below the North American ratio of 3.8.

The conclusions summarized above allow for better understanding of the hydrological and geochemical processes in the upper Ogilvie River watershed. However, many potential improvements may be made to the general understanding and specific calculations by refining the inputs and quantifying assumptions. One of largest sources of uncertainty is the spatial heterogeneity of the inputs, especially precipitation type, quantity, and distribution. Due to limited access to the watershed, the runoff was characterized based on three small analogue streams outside of the study catchment area. The runoff throughout the watershed is likely to be more varied. There are some small gaps in the discharge record which could be filled and the overall record improved by updating the historical rating curve relied upon. Longer and fuller records of geochemical and isotopic composition of the Ogilvie River and its flow inputs would allow for better understanding of trends in the middle of the summer and during the fall/winter period and for long-term trend analysis.

10 References

Albright, L., 1980. Microbial dynamics of two sub-Arctic Canadian rivers. Water Res. 14, 1353–1362. doi:10.1016/0043-1354(80)90196-7

Albright, L.J., Masuda, K. V., Ennis, G.L., Lake, E., 1980. Effects of streambank materials additions upon microbial activities of two sub-Arctic Canadian rivers. Water Res. 14, 1363–1366.

Andersen, D.T., Pollard, W.H., Mckay, C.P., Heldmann, J., 2002. Cold springs in permafrost on Earth and Mars. J. Geophys. Res. 107, 4-1-7. doi:10.1029/2000JE001436

Anderson, L.G., Olsson, K., Chierici, M., 1998. A carbon budget for the Arctic Ocean 12, 455–465.

Benjamin, L., Knobel, L.L., Hall, L.F., Cecil, L.D., Green, J.R., 2004. Development of a Local Meteoric Water Line for Southeastern Idaho, Western Wyoming, and South-Central Montana, USGS.

Beta Analytic Limited, 1990. Introduction to Radiocarbon Determination by the Accelerator Mass Spectrometry Method.

Bond, J., 2004. Late Wisconsinan McConnel glaciation of the Whitehorse map area (105D), Yukon., in: Edmond, D.S., Lewis, L.L. (Eds.), Yukon Exploration and Geology 2003. Yukon Geological Survey, pp. 73–88.

Boyer, C., Vichot, L., Fromm, M., Losset, Y., Tatin-Froux, F., Guetat, P., Badot, P.M., 2009. Tritium in plants: A review of current knowledge. Environ. Exp. Bot. 67, 34–51. doi:10.1016/j.envexpbot.2009.06.008

British Columbia Ministry of the Environment, n.d. Water quality: definitions, concepts and analytical measurements [WWW Document]. URL http://www.env.gov.bc.ca/wat/wq/BCguidelines/orgcarbon/definitions.html (accessed 5.5.16).

Brook, G.A., Ford, D.C., 1980. Hydrology of the Nahanni Karst, Northern Canada, and the Importance of Extreme Summer Storms. J. Hydrol. 46, 103–121.

Brown, J., Ferrians, O.J., Heginbottom, J.A., Melnikov, E.S., 1998. (rev. Feb 2001). Circum-Arctic Map of Permafrost and Ground Ice Conditions [digital cartographic material]. Boulder, CO. National Snow and Ice Center.

Burn, C.R., Moore, J.L., Neill, H.B.O., 2015. Permafrost characterization of the Dempster Highway , Yukon and Northwest Territories, in: 68e Conférence Canadienne de Géotechnique et 7e Conférence Canadienne Sur Le Pergélisol, 20 Au 23 Septembre 2015, Québec, Québec.

Canadian Parks and Wilderness Society, 2004. Peel Watershed Atlas (Working Draft).

Carey, S.K., Boucher, J.L., Duarte, C.M., 2013. Inferring groundwater contributions and pathways to streamflow during snowmelt over multiple years in a discontinuous permafrost subarctic environment - Yukon, Canada. Hydrogeol. J. 21, 67–77. doi:10.1007/s10040-012-0920-9

Carey, S.K., Pomeroy, J.W., 2009. Progress in Canadian Snow and Frozen Ground Hydrology,

2003-2007. Can. Water Resour. J. 34, 127–138. doi:10.4296/cwrj3402127

Clark, I.D., 2015. Groundwater Geochemistry and Isotopes, Groundwater. CRC Press, New York. doi:10.1111/gwat.12377

Clark, I.D., Fritz, P., 1997. Environmental Isotopes in Hydrogeology. CRC Press/Lewis Publishers, Boca Raton, FL.

Clark, I.D., Fritz, P., Michel, F.A., Souther, J.G., 2011. Isotope hydrogeology and geothermometry of the Mount Meager geothermal area. Can. J. Earth Sci. 1473, 1454–1473.

Clark, I.D., Lauriol, B., 1997. Aufeis of the Firth River Basin, Northern Yukon, Canada: Insights into permafrost hydrogeology and karst. Arct. Alp. Res. 29, 240–252. doi:10.2307/1552053

Craig, H., 1961. Isotopic Variations in Meteoric Waters. Science (80-.). 133, 1702–1703.

Cruickshank, A., 2014. Yukon missing essential groundwater information: hydrologist. Whitehorse Dly. Star.

Dietermann, N., Weiler, M., 2013. Spatial distribution of stable water isotopes in alpine snow cover. Hydrol. Earth Syst. Sci. 17, 2657–2668. doi:10.5194/hess-17-2657-2013

Duk-Rodkin, A., 1999. Glacial Limits of Yukon Territory [cartographic material] 1:1,000,000. Geological Survey of Canada, Open File 3694, Indian and Northern Affairs Canada Geoscience Map 1999-2.

Dutton, A., Wilkinson, B.H., Welker, J.M., Bowen, G.J., Lohmann, K.C., 2005. Spatial distribution and seasonal variation in 18O/16O of modern precipitation and river water across the conterminous USA. Hydrol. Process. 19, 4121–4146. doi:10.1002/hyp.5876

Ekaykin, A.A., Hondoh, T., Lipenkov, V.Y., Miyamoto, A., 2009. Post-depositional changes in snow isotope content : preliminary results of laboratory experiments. Clim. Past Discuss. 5, 2239–2267. doi:10.5194/cpd-5-2239-2009

Ennis, G.L., Albright, L.J., 1982. Distribution and abundance of periphyton and phytoplankton species in two subarctic Canadian rivers. Can. J. Bot. 60, 224–236. doi:10.1139/b82-030

Fisheries and Environment Canada, 1978. Hydrologic Atlas of Canada [cartographic material] 1:10,000,000.

Fraser, M., 2016. Personal communication with Michael Fraser, Northern Area Superintendent, Highways and Public Works, Government of Yukon.

Gat, J.R., 2010. Isotope Hydrology: A Study of the Water Cycle. Imperial College Press, London.

Geyh, M.A., 2000. An Overview of 14C Analysis in the Study of Groundwater. Radiocarbon 42, 99–114.

GIN, 2014. Cordillera Hydrogeological Region [WWW Document]. Groundw. Inf. Netw. URL http://gin.gw-info.net/service/api_ngwds:gin2/en/hydroreg/cord.html (accessed 5.28.16).

Government of Yukon, 2016. Weather Data, Ogilvie Station, January 2014 - April 2016 provided by Transportation Maintenance Branch, Department of Public Works.

Gruber, S., 2012. Derivation and analysis of a high-resolution estimate of global permafrost zonation. Cryosphere 6, 221–233. doi:10.5194/tc-6-221-2012

Haldorsen, S., Heim, M., S.E., L., 1996. Subpermafrost groundwater, western Svalbard. Nord.

Hydrol. 27, 57–68.

Healy, R.W., 2010. Estimating Groundwater Recharge. Cambridge University Press, New York.

Heginbottom, J.A., Dubreuil, M.A., Harker, P.A., 1995. Canada - Permafrost in: National Atlas of Canada, 5th Edition, National Atlas Information Service [cartographic material] 1:7,500,000. Natural Resources Canada.

Heginbottom, J.A., Radburn, L.K., 1992. Permafrost and ground ice conditions of northwestern Canada [cartographic material] 1:1,000,000. Geological Survey of Canada, Map 1691A.

Hernes, P.J., Holmes, R.M., Raymond, P.A., Spencer, R.G.M., Tank, S.E., 2014. Fluxes, processing, and fate of riverine organic and inorganic carbon in the Arctic Ocean, in: Bianchi et al. (Ed.), Biogeochemical Dynamics at Large River-Coastal Interfaces: Linkages with Global Climate Change. Cambridge University Press.

Herod, M.N., 2015. Tacing the Transport, Geochemical Cycling and Fate of Iodine-129 in Earth Surface Reseroirs. University of Ottawa.

Holmes, R.M., Coe, M.T., Fiske, G.J., Gurtovaya, T., McClelland, J.W., Shiklomanov, A.I., Spencer, R.G.M., Tank, S.E., Zhulidov, A. V., 2013. Climate change impacts on the hydrology and biogeochemistry of Arctic rivers, in: Goldman, C.R., Kumagai, M., Robards, R.D. (Eds.), Climatic Change and Global Warming of Inland Waters: Impacts and Mitigation for Ecosystems and Societies. John Wiley & Sons, Ltd.

Hua, Q., 2009. Radiocarbon: A chronological tool for the recent past. Quat. Geochronol. 4, 378–390. doi:10.1016/j.quageo.2009.03.006

IAEA, 1992. Statistical treatment of data on environmental isotopes in precipitation. Techinal Rep. Ser. No. 331.

Idrees, M., Burn, C.R., Moore, J.L., Calmels, F., 2015. Monitoring permafrost conditions along the Dempster Highway. 68e Conférence Can. Géotechnique 7e Conférence Can. sur le Pergélisol, 20 au 23 Sept. 2015, Québec, Québec.

Kane, D.L., Stein, J., 1983. Field Evidence of Groundwater Recharge in Interior Alaska, in: Permafrost Fourth International Conference Proceedings. pp. 572–577.

Kane, D.L., Yoshikawa, K., McNamara, J.P., 2012. Regional groundwater flow in an area mapped as continuous permafrost, NE Alaska (USA). Hydrogeol. J. 21, 41–52. doi:10.1007/s10040-012-0937-0

Kang, S., Kreutz, K.J., Mayewski, P.A., 2002. Stable-Isotopic Composition of Precipitation Over the Northern Slope of the Central Himalaya 48, 519–526.

Kern, Z., Kohan, B., Leuenberger, M., 2014. Precipitation isoscape of high reliefs: Interpolation scheme designed and tested for monthly resolved precipitation oxygen isotope records of an Alpine domain. Atmos. Chem. Phys. 14, 1897–1907. doi:10.5194/acp-14-1897-2014

Khan, E., Subramania-Pillai, S., 2006. Effect of leaching from filters on laboratory analyses of collective organic constituents. Proc. Water Environ. Fed. 901–918. doi:http://dx.doi.org/10.2175/193864706783749747

Klaus, J., McDonnell, J.J., 2013. Hydrograph separation using stable isotopes: Review and evaluation. J. Hydrol. 505, 47–64. doi:10.1016/j.jhydrol.2013.09.006

Kwong, Y.T.J., Whitley, G., Roach, P., 2009. Natural acid rock drainage associated with black

shale in the Yukon Territory, Canada. Appl. Geochemistry 24, 221–231. doi:10.1016/j.apgeochem.2008.11.017

Lacelle, D., 2011. On the d18O, dD and D-excess relations in meteoric precipitation and during equilibrium freezing: Theoretical approach and field examples. Permafr. Periglac. Process. 22, 13–25. doi:10.1002/ppp.712

Lacelle, D., St-Jean, M., Lauriol, B., Clark, I.D., Lewkowicz, A., Froese, D.G., Kuehn, S.C., Zazula, G., 2009. Burial and preservation of a 30,000 year old perennial snowbank in Red Creek valley, Ogilvie Mountains, central Yukon, Canada. Quat. Sci. Rev. 28, 3401–3413. doi:10.1016/j.quascirev.2009.09.013

Landwehr, J., Coplen, T., 2006. Line-conditioned excess: a new method for characterizing stable hydrogen and oxygen isotope ratios in hydrologic systems. Isot. Environ. Stud. IAEA-CN-11, 132–135. doi:10.8/S

Lapp, A., 2015. Seasonal Variability of Groundwater Contribution to Watershed Discharge in Discontinuous Permafrost in the North Klondike River Valley, Yukon. University of Ottawa.

Lauriol, B., Lacelle, D., St-Jean, M., Clark, I.D., Zazula, G.D., 2010. Late Quaternary paleoenvironments and growth of intrusive ice in eastern Beringia (Eagle River valley, northern Yukon, Canada). Can. J. Earth Sci. 47, 941–955. doi:10.1111/j.1574-6941.2006.00198.x

Lechler, A.R., Niemi, N.A., 2012. The influence of snow sublimation on the isotopic composition of spring and surface waters in the southwestern United States: Implications for stable isotope-based paleoaltimetry and hydrologic studies. Bull. Geol. Soc. Am. 124, 318–334. doi:10.1130/B30467.1

Leibundgut, C., Maloszewski, P., Kulls, C., 2009. Tracers in Hydrology, 1st ed. Wiley-Blackwell.

Li, T., 2013. The Geochemistry and Runoff Process in Wolf Creek Research Basin, Whitehorse, Yukon Territory. University of Ottawa.

Malkin, E., 2008. Principal Components Analysis: A How-To Manual for R.

Mazor, E., 2004. Chemical and Isotopic Groundwater Hydrology, 3rd ed. Marcel Dekker, Inc., New York.

McGuire, A.D., Anderson, L.G., Christensen, T.R., Dallimore, S., Guo, L., Hayes, D.J., Heimann, M., Lorenson, T.D., Macdonald, R.W., Roulet, N., 2009. Sensitivity of the carbon cycle in the Arctic to climate change. Ecol. Monogr. 79, 523–555. doi:10.1890/08-2025.1

McGuire, A.D., Macdonald, R.W., Schuur, E.A.G., Harden, J.W., Kuhry, P., Hayes, D.J., Christensen, T.R., Heimann, M., 2010. The carbon budget of the northern cryosphere region. Curr. Opin. Environ. Sustain. 2, 231–236. doi:10.1016/j.cosust.2010.05.003

Mook, W., Gat, J., Meijer, H., 2001. Environmental isotopes in the hydrological cycle: principles and applications. Vol.2. Atmospheric Water, Environmental Isotopes in The Hydrological Cycle.

Mougeot, C.M., Walton, L.A., 1996. Yuokon Geoprocess File (2002), Geological Processes and Terrain Hazards of Ogilvie River 116G & 116F (E1/2) [cartographic material] 1:250,000.

Exploration and Geological Services Division, Yukon Region, Indian and Northern Affairs Canada.

Natural Resources Canada, 2000. EOSD Land Cover Classification [digital cartographic material]. Canadian Forest Service - Pacific Forestry Centre.

Norris, D.K., 1982. Geology, Ogilvie River, Yukon Territory [cartographic material] 1:250,000. Geological Survey of Canada, Map 1526A.

Peel, M.C., Finlayson, B.L., McMahon, T.A., 2006. Updated world map of the K¨oppen-Geiger climate classification. Meteorol. Zeitschrift 15, 259–263. doi:10.1127/0941-2948/2006/0130

Pittard, S., 2012. Using prcomp and varimax for PCA in R (YouTube Video sponsored by the Department of Biostatistic and Bioinformatics, Rollins School of Public Health, Emory University, Atlanta, GA) [WWW Document]. URL https://www.youtube.com/watch?v=oZ2nfIPdvjY

Poage, M.A., Chamberlain, C.P., 2001. Empirical relationships between elevation and the stable isotope composition of precipitation and surface waters: Considerations for studies of paleoelevation change. Am. J. Sci. 301, 1–15. doi:10.2475/ajs.301.1.1

Pollard, W., Omelon, C., Andersen, D., McKay, C., 1999. Perennial spring occurrence in the Expedition Fiord area of western Axel Heiberg Island, Canadian High Arctic. Can. J. Earth Sci. 36, 105–120. doi:10.1139/e98-097

Pyle, L., Roots, C., Allen, T., Fraser, T., Bond, J., Jones, A., Gal, L., 2007. Roadside Geology of the Dempster Highway , Northwest Territories and Yukon. NWT Open File 2007-05 / YGS Open File 2007-10.

Raymond, P.A., McClelland, J.W., Holmes, R.M., Zhulidov, A. V., Mull, K., Peterson, B.J., Striegl, R.G., Aiken, G.R., Gurtovaya, T.Y., 2007. Flux and age of dissolved organic carbon exported to the Arctic Ocean: A carbon isotopic study of the five largest arctic rivers. Global Biogeochem. Cycles 21, 1–9. doi:10.1029/2007GB002934

Schreier, H., 1979. Winter Watrer Quality Sampling and its Use in Determening Hydrological Conditions in the Ogilvie River System in the Yukon Territory, in: Hydrology Symposium Proceedings. pp. 559–569.

Schreier, H., Erlebach, W., Albright, L., 1980. Variations in water quality during winter in two Yukon rivers with emphasis on dissolved oxygen concentration. Water Res. 14, 1345–1351. doi:10.1016/0043-1354(80)90195-5

Shlens, J., 2005. A Tutorial on Principal Component Analysis.

Smith, C.A.S., Metkle, J.C., Roots, C.F. (Eds.), 2004. Ecoregions of the Yukon Territory: Biophysical Properties of Yukon Landscapes. Agriculture and Agri-Food Canada, PARC Technical Bulletin No. 04-01, Summerland, British Columbia.

Smith, I.R., Lesk-Winfield, K., 2012. An updated assessment of ground ice and permafrost geology-related observations based on seismic shothole drillers' log records, Nortwest Territories and northern Yukon [digital cartographic material]. Geological Survey of Canada, Open File 7061. doi:10.4095/290974

Smith, S., Burgess, M.M., 2002. A Digital Database of Permafrost Thickness in Canada.

Geological Survey of Canada, Open File 4173.

Smith, S., Burgess, M.M., 2000. Ground Temperature database for northern Candada [data set]. Geological Survey of Canada, Open File 3954. doi:10.4095/211804

Sokolov, B.L., 1991. Hydrology of Rivers of the Cryolithic Zone in the U.S.S.R. The Present State and Prospects for Investigations. Nord. Hydrol. 22, 211–226.

Sokratov, S.A., Golubev, V.N., 2009. Snow isotopic content change by sublimation. J. Glaciol. 55, 823–828. doi:10.3189/002214309790152456

Streletskiy, D.A., Tananaev, N.I., Opel, T., Shiklomanov, N.I., Nyland, K.E., Streletskaya, I.D., Tokarev, I., Shiklomanov, A.I., 2015. Permafrost hydrology in changing climatic conditions: seasonal variability of stable isotope composition in rivers in discontinuous permafrost. Environ. Res. Lett. 10, 95003. doi:10.1088/1748-9326/10/9/095003

Striegl, R.G., Dornblaser, M.M., Aiken, G.R., Wickland, K.P., Raymond, P.A., 2007. Carbon export and cycling by the Yukon, Tanana, and Porcupine rivers, Alaska, 2001-2005. Water Resour. Res. 43, 2001–2005. doi:10.1029/2006WR005201

Tamocai, C., Kimble, J.M., Swanson, D., Goryachkin, S., Naumov, Y.M., Stolbovoi, V., Jakobsen, B., Broll, G., Montanarella, L., Amoldussen, A., Amalds, O., Yli-Halla, M., 2002. Northern Circumpolar Soils [digital cartographic material] 1:10,000,000. Ottawa, Canada: Research Branch, Agriculture and Agri-Food Canada, Distributed by the National Snow and Ice Data Center, Boulder, CO.

Tank, S.E., Raymond, P.A., Striegl, R.G., McClelland, J.W., Holmes, R.M., Fiske, G.J., Peterson, B.J., 2012. A land-to-ocean perspective on the magnitude, source and implication of DIC flux from major Arctic rivers to the Arctic Ocean. Global Biogeochem. Cycles 26, 1–15. doi:10.1029/2011GB004192

Taylor, A.E., Burgess, M.M., Judge, A.S., Allen, V., Wilkinson, A., 1998. Deep permafrost temperatures and thickness of permafrost [report and data set]. National Snow and Ice Data Center.

Thompson, R.I., 1995. Geological Compilation of Dawson map area (116B,C) (northeast of Tintina Trench) [cartographic material] 1:250,000. Geological Survey of Canada, Open File 3223. doi:10.4095/207488

USGS, 2012. Alkalinity and acid neutralizing capacity, in: Rounds, S.A. (Ed.), TWRI Book 9 Alkalinity and Acid Neutralizating Capacity. pp. 1–45.

van der Ploeg, M.J., Haldorsen, S., Leijnse, A., Heim, M., 2012. Subpermafrost groundwater systems: Dealing with virtual reality while having virtually no data. J. Hydrol. 475, 42–52. doi:10.1016/j.jhydrol.2012.08.046

Walvoord, M. a., Striegl, R.G., 2007. Increased groundwater to stream discharge from permafrost thawing in the Yukon River basin: Potential impacts on lateral export of carbon and nitrogen. Geophys. Res. Lett. 34. doi:10.1029/2007GL030216

Williams, J.R., 1970. Ground Water in the Permafrost Regions of Alaska, Geological Survey Professional Paper 696. Washington. doi:10.1016/0022-1694(71)90061-8

Williams, P.J., Smith, M.W., 1989. The Frozen Earth. Cambridge University Press, New York.

Woo, M., 2012. Permafrost Hydrology, Permafrost Hydrology. doi:10.1007/978-3-642-23462-0

Yukon Ecoregions Working Group, 2004. North Ogilvie Mountains, Taiga Cordillera Ecozone, in: Smith, C.A.S. Meikle, J.C. Roots, C.F. (Ed.), Ecoregions of the Yukon Territory: Biophysical Properties of Yukon Landscapes. Agriculture and Agri-Food Canada, PARC Technical Bulletin No. 04-01, Summerland, British Columbia, pp. 123–130.

Yukon Geological Survery, 2001. Bedrock Geology [digital cartographic material].

Yukon Placer Secretariat, n.d. Yukon Placer Watershed Atlas [WWW Document]. URL http://www.yukonplacersecretariat.ca/placer_atlas.html (accessed 3.15.16).

Data Sources

Environment Canada, Climate. Daily Data Report, Station Ogilvie River, 1971-2008. Accessed on May 28, 2014. http://climate.weather.gc.ca/

Environment Canada, Climate. Climate Normals, Station Dawson A, 1981-2010. Accessed February 27, 2015. http://climate.weather.gc.ca/

Environment Canada, Water Survey of Canada (2010), Historical Hydrometric Data, Station 10MA002, accessed via ECDataExplorer V1.2.30, HYDAT Version 1.0 (Nov 15, 2012)

Environment Yukon, Water Resources Branch, Yukon Snow Survey Bulletin & Water Supply Forecast: 2014: March 1, April 1, May 1; 2015: March 1, April 1, May 1; 2016: March 1, April 1, May 1

Government of Yukon, Department of Highways and Public Works, Transportation Maintenance Branch, Ogilvie Station Weather Records March 1, 2014 to May 15, 2016 via personal communication with Ben Gaetz (May 16, 2016) and via on-site records (August 14, 2014)

Digital Data Sources

Environment Yukon Geomatics (2006) 50K Canadian Digital Elevation Data for Yukon, 1:50,000

Geomatics Yukon (2014) Geographic Feature Names

Geomatics Yukon (2014) Transportation Line & Annotation – 50K, 1:50,000 National Topographic Data Base

Government of Canada (2014) Canadian Geopolitical Boundaries, ed. 2.4. Ottawa, Ontario. Natural Resources Canada, Surveyor General Branch

Government of Canada (rev. 2008) Hydrology – Major River Basin, Atlas of Canada, 1:1,000,000 National Framework Data. Natural Resources Canada, Canada Centre for Mapping and Earth Observation

Yukon geological Survey (2014) Bedrock Geology, 1:250,000

Appendix A

Summary of Permafrost Information, upper Ogilvie River watershed

Table 1 Permafrost Distribution Summary

Source	Area Covered	Permafrost Type
Heginbottom, J.A., Radburn, L.K., 1992. Permafrost and ground ice conditions of northwestern Canada [cartographic material] 1:1,000,000. Geological Survey of Canada, Map 1691A.	Eastern portion of the watershed (approximately east of Mount Chambers)	Extensive discontinuous permafrost with ice content ranging from nil to low to moderate. Intermediate discontinuous permafrost along the Ogilvie River valley with low to moderate ice content.
Fisheries and Environment Canada, 1978. Hydrologic Atlas of Canada [cartographic material] 1:10,000,000.	Entire study watershed	Discontinuous permafrost area
Brown, J., Ferrians, O.J., Heginbottom, J.A., Melnikov, E.S., 1998. (rev. Feb 2001). Circum-Arctic Map of Permafrost and Ground Ice Conditions [digital cartographic material]. Boulder, CO. National Snow and Ice Center.	Entire study watershed	Continuous permafrost across the eastern portion of the watershed with low ice content (<10%) in the mountainous regions with thin overburden (<5-10 m) or bedrock outcrops in the north and south and medium ice content (10-20%) along the river valley with thick overburden (>5-10 m). Discontinuous permafrost across the western portion of the watershed with medium ice content (10-20%).
Smith, I.R., Lesk-Winfield, K., 2012. An updated assessment of ground ice and permafrost geology-related observations based on seismic shothole drillers' log records, Nortwest Territories and northern Yukon [digital cartographic material]. doi:10.4095/290974	Entire study watershed	Continuous permafrost across most of the watershed, extensive discontinuous permafrost at the very southern extent of the watershed.
Heginbottom, J.A., Dubreuil, M.A., Harker, P.A., 1995. Canada - Permafrost in: National Atlas of Canada, 5th Edition, National Atlas Information Service [cartographic material] 1:7,500,000. Natural Resources Canada.	Entire study watershed	Continuous permafrost across most of the watershed, extensive discontinuous permafrost at the very southern extent of the watershed (same as Smith and Lesk-Winfield, 2012). Low to medium ice content, sparse ice wedges and massive ice.

Table 2 Permafrost Thickness Summary

Source	Area Covered	Permafrost Thickness
Smith, I.R., Lesk-Winfield, K., 2012. An updated assessment of ground ice and permafrost geology-related observations based on seismic shothole drillers' log records, Nortwest Territories and northern Yukon [digital cartographic material]. doi:10.4095/290974	Three areas in the watershed where historical seismic investigation have been completed	Minimum permafrost thickness: 2.1 to 27.4 meters
Taylor, A.E., Burgess, M.M., Judge, A.S., Allen, V., Wilkinson, A., 1998. Deep permafrost temperatures and thickness of permafrost [report and data set]. National Snow and Ice Data Center.	Closest borehole North Cath B-62 (66°11.2′N, 138°41.6′W) located 80 km north of the watershed	Permafrost thickness based on temperature data from the thermistor cables installed in 4 boreholes: 79 - 89 metres below ground surface (0°C isotherm).
Smith, S., Burgess, M.M., 2000. Ground Temperature database for northern Candada [data set]. Geological Survey of Canada, Open File 3954. doi:10.4095/211804		MAGT <=4.3°C
Smith, S., Burgess, M.M., 2002. A Digital Database of Permafrost Thickness in Canada. Geological Survey of Canada, Open File 4173.		Discontinuous permafrost zone Base of ice-bearing permafrost – 244 m Depth of 0°C isotherm – 89 m
Idrees, M., Burn, C.R., Moore, J.L., Calmels, F., 2015. Monitoring permafrost conditions along the Dempster Highway. 68e Conférence Can. Géotechnique 7e Conférence Can. sur le Pergélisol, 20 au 23 Sept. 2015, Québec, Québec.	Borehole at Chapman airstrip at km. 124 of Dempster Highway (64°54′10.8″N, 138°16′40.8″W) located 15 km east of the watershed	Bottom of permafrost at 7 m; Permafrost temperatures at 1 m: -4.7, -4.5, and -5.0°C; Unfrozen ground and free water were encountered; Thin permafrost thought to be due to convective heat from shallow groundwater.
Lacelle, D., St-Jean, M., Lauriol, B., Clark, I.D., Lewkowicz, A., Froese, D.G., Kuehn, S.C., Zazula, G., 2009. Burial and preservation of a 30,000 year old perennial snowbank in Red Creek valley, Ogilvie Mountains, central Yukon, Canada. Quat. Sci. Rev. 28, 3401–3413. doi:10.1016/j.quascirev.2009.09.013	Borehole at Red Creek (65°9′N, 138°21′W) located 8 km east of the watershed	Average ground temperature of -2.5°C; Estimated permafrost depth between 75 and 150 m

Appendix B

Precipitation

Table shows summary of the annual precipitation at Ogilvie River weather station. The weather station was operational between 1971 and 2008. Only 17 years with full records are included in the Table.

Table 1 Summary of Precipitation Records at Ogilvie River

Year	Precipitation as Rain (mm)	Precipitation as Snow (cm)	Total Ppt (mm)	%Snow	%Rain
1982	167.5	95.5	263	36%	64%
1984	265.9	150	415.9	36%	64%
1985	218.4	80	298.4	27%	73%
1986	172.9	126	298.9	42%	58%
1987	279	107	386	28%	72%
1988	321.8	124	445.8	28%	72%
1989	227.6	161	388.6	41%	59%
1991	183.4	128	311.4	41%	59%
1992	140.5	176.5	317	56%	44%
1993	215.3	142.6	357.9	40%	60%
1994	277	136.5	413.5	33%	67%
1995	203.3	73.6	276.9	27%	73%
1997	245.9	104.8	350.7	30%	70%
1998	256.4	117.5	373.9	31%	69%
2002	235.3	120	355.3	34%	66%
2004	104.4	176.5	280.9	63%	37%
2005	171	126	297	42%	58%
Average	**216.8**	**126.2**	**343.0**	**37%**	**63%**

Appendix C

Discharge Measurements

Table 1 and Figure 1 show Ogilvie River rating curve as provided by Wade Hannah, Hydrometric Supervisor of Water Survey of Canada (personal communication, April 30, 2014).

Table 1 Ogilvie River Rating Curve Equations, Hydrometric Station 10MA002

Stage	Discharge	Equation	Stage	Discharge	Equation
m	m^3/s		m	m^3/s	
6.1	12	-----	8.1	491	X = -2668.000 + 390.000 * Y
6.2	14.5	X = -140.500 + 25.000 * Y	8.2	532	X = -2830.000 + 410.000 * Y
6.3	18	X = -202.500 + 35.000 * Y	8.4	616	X = -2912.000 + 420.000 * Y
6.4	25	X = -423.000 + 70.000 * Y	8.5	659	X = -2996.000 + 430.000 * Y
6.5	34.5	X = -583.000 + 95.000 * Y	8.6	703	X = -3081.000 + 440.000 * Y
6.6	46	X = -713.000 + 115.000 * Y	8.8	793	X = -3167.000 + 450.000 * Y
6.7	60.5	X = -911.000 + 145.000 * Y	9.1	934	X = -3343.000 + 470.000 * Y
6.8	76.5	X = -1011.500 + 160.000 * Y	9.3	1030	X = -3434.000 + 480.000 * Y
6.9	96.5	X = -1283.500 + 200.000 * Y	9.4	1080	X = -3620.000 + 500.000 * Y
7	119	X = -1456.000 + 225.000 * Y	7.6	301	X = -2359.000 + 350.000 * Y
7.1	144	X = -1631.000 + 250.000 * Y	7.8	375	X = -2511.000 + 370.000 * Y
7.2	171	X = -1773.000 + 270.000 * Y	7.9	413	X = -2589.000 + 380.000 * Y
7.3	201	X = -1989.000 + 300.000 * Y	8.1	491	X = -2668.000 + 390.000 * Y
7.4	233	X = -2135.000 + 320.000 * Y	8.2	532	X = -2830.000 + 410.000 * Y
7.5	266	X = -2209.000 + 330.000 * Y	8.4	616	X = -2912.000 + 420.000 * Y
7.6	301	X = -2359.000 + 350.000 * Y			
7.8	375	X = -2511.000 + 370.000 * Y			
7.9	413	X = -2589.000 + 380.000 * Y			

Notes:

(a) X – Flow, Y – Stage

Site datum: Control benchmark (top of large vertical nut in the footing on upstream end of the left bank pier) has elevation of 11.890 m, as per the original hydrometric station installation.

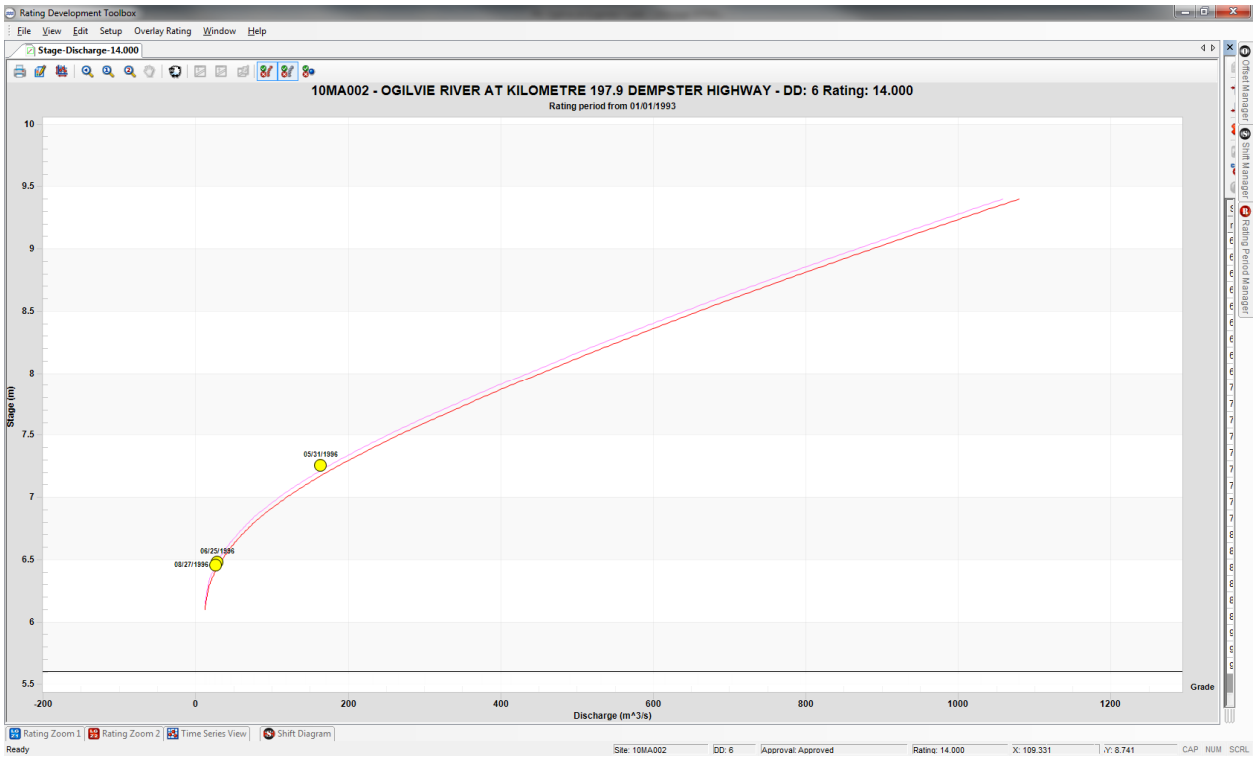

Figure 1 Ogilvie River Rating Curve, Hydrometric Station 10MA002

Engineer Creek rating curve was developed by conducting flow measurements in the spring and late summer of 2015. At lower water levels the area-velocity method was used. At higher water levels, when wading was unsafe, flow estimates were made using surface velocity measurements. These estimates were used in conjunction with the cross-sectional depth profile at the probe installation location measured in April 2015 when the creek was not yet flowing. Table 2 summarizes the flow measurements. Figure 2 and Table 3 show the developed rating curve.

Table 2 Engineer Creek Flow Measurements

	Measurement					
Date	**Start Time**	**Finish Time**	**Date+Time of Probe Reading**	**Stage(m)**	**Flow (m3/s)**	**Measurement Method**
30-Apr-15	4:50 PM	5:24 PM	30/04/2015 17:00	0.577	0.54	In-stream 20%&80%
01-May-15	2:00 PM		01/05/2015 14:00	0.582	0.64	In-stream 60%
02-May-15	4:05 PM	4:26 PM	02/05/2015 16:30	0.509	0.82	In-stream 60%
04-May-15	9:30 AM	10:00 AM	04/05/2015 9:30	0.522	0.59	In-stream 60%
07-May-15	8:30 AM	9:00 AM	07/05/2015 8:30	0.64	1.24	In-stream 60%
08-May-15	5:00 PM	6:00 PM	08/05/2015 17:30	0.712	4.23	In-stream 60%
09-May-15	9:00 AM	9:40 AM	09/05/2015 9:30	0.878	10.26	Surface velocity estimate
10-May-15	2:55 PM	3:10 PM	10/05/2015 15:00	1.444	39.05	Surface velocity estimate
11-May-15	10:15 AM	10:40 AM	11/05/2015 10:30	1.73	73.57	Surface velocity estimate
12-May-15	11:00 AM	11:40 AM	12/05/2015 11:30	1.928	91.78	Surface velocity estimate
13-May-15	7:20 AM	8:00 AM	13/05/2015 7:30	1.919	105.26	Surface velocity estimate
27-Aug-15	4:00 PM	4:45 PM	27/08/2015 4:30	1.322	30.65	Surface velocity estimate
29-Aug-15	9:20 AM	9:45 AM	29/08/2015 9:30	1.729	65.80	Surface velocity estimate
30-Aug-15	12:30 PM	1:00 PM	30/08/2015 12:30	1.544	43.39	Surface velocity estimate

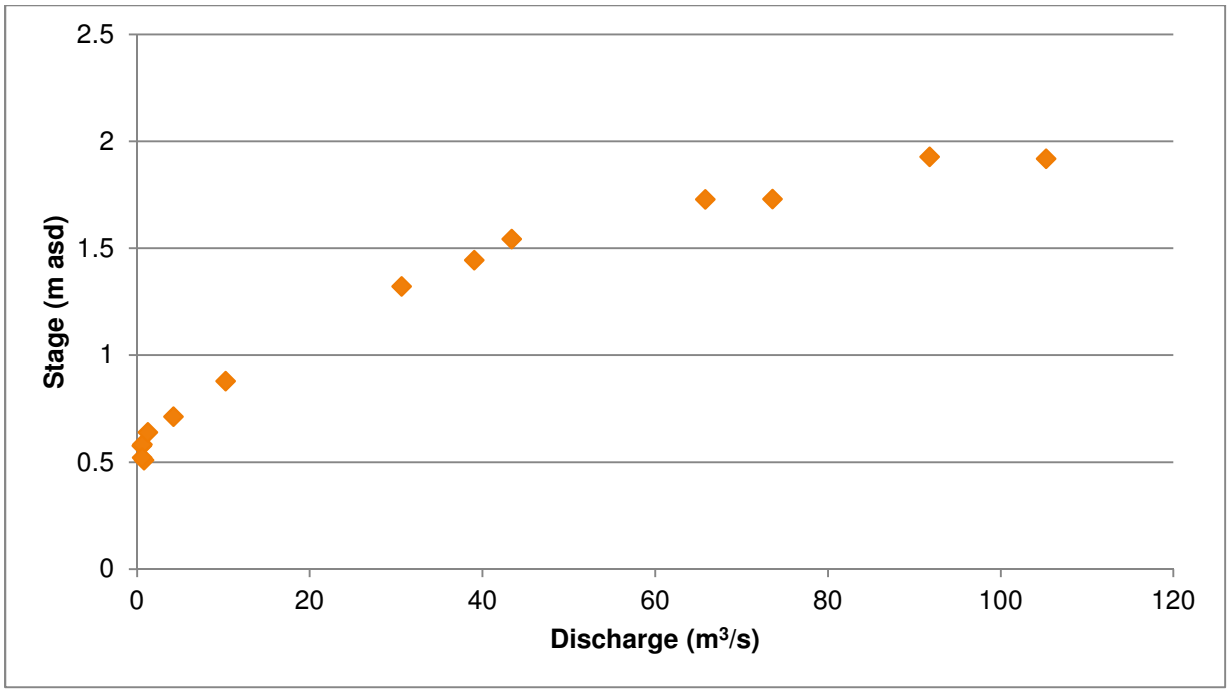

Figure 2 **Engineer Creek Rating Curve**

Table 3 Engineer Creek Rating Curve Equations

Stage	Discharge	Equation
m	**m^3/s**	
0	0	
0.1	0.06	X= 1.667*Y+0.00
0.2	0.12	X= 1.818*Y+-0.01
0.3	0.19	X= 1.429*Y+0.04
0.4	0.29	X= 1.000*Y+0.12
0.5	0.35	X= 1.538*Y+-0.04
0.55	0.51	X= 0.313*Y+0.39
0.6	0.73	X= 0.233*Y+0.43
0.7	3.6	X= 0.035*Y+0.57
0.8	7	X= 0.029*Y+0.59
0.9	11	X= 0.025*Y+0.63
1	14.5	X= 0.029*Y+0.59
1.1	18.5	X= 0.025*Y+0.64
1.2	23	X= 0.022*Y+0.69
1.3	28.5	X= 0.018*Y+0.78
1.4	34	X= 0.018*Y+0.78
1.5	41.5	X= 0.013*Y+0.95
1.6	49.5	X= 0.013*Y+0.98
1.7	61	X= 0.009*Y+1.17
1.8	72	X= 0.009*Y+1.15

Notes:

(a) X – Flow, Y – Stage

(b) Site datum – 0 m assumed to be pressure transducer elevation at its first deployment on April 24, 2015. Elevation continuity was maintained during the probe deployment period.

The measured discharge hydrographs for the Ogilvie River at the old monitoring station and at Engineer Creek are shown on Figure 3 are shown together with the derived hydrograph for the sampling site.

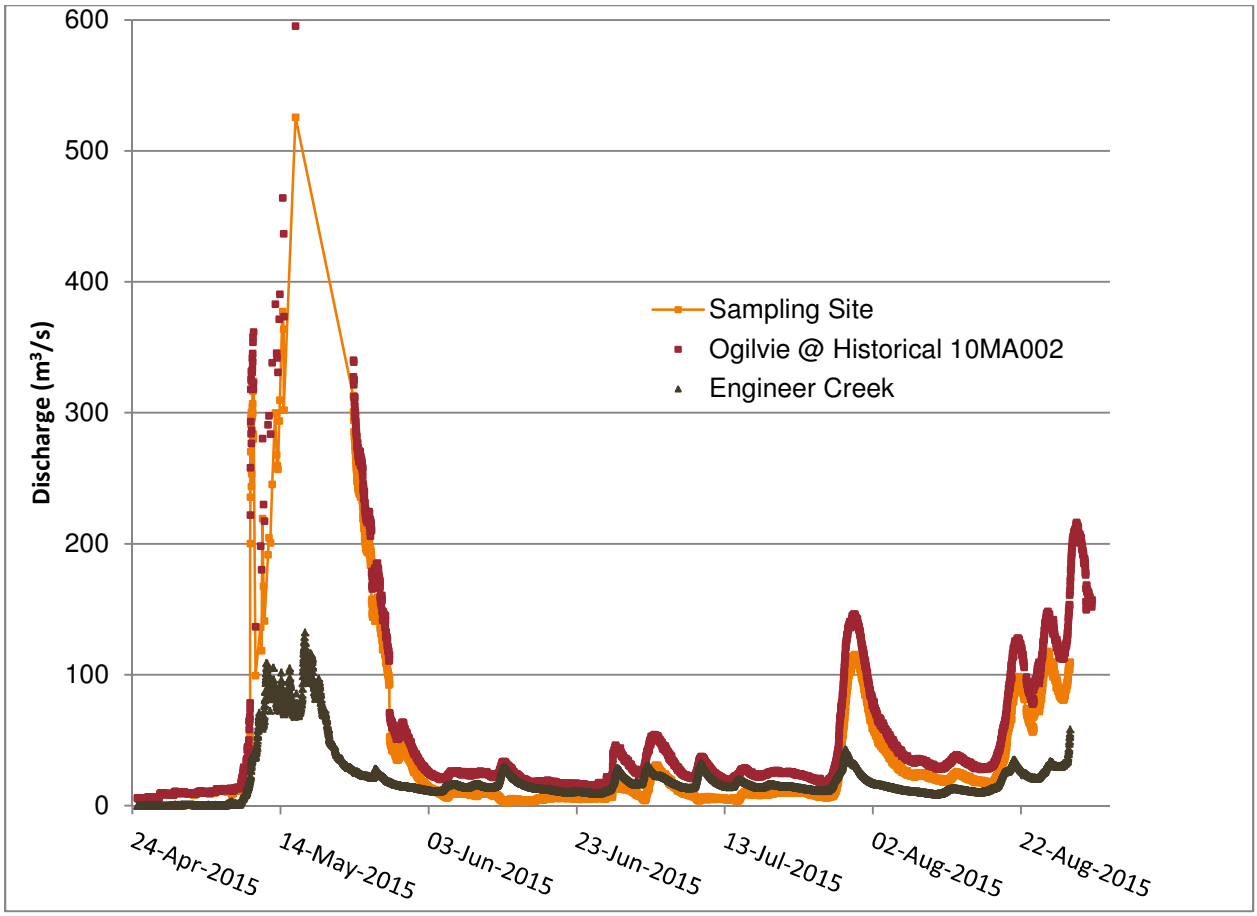

Figure 3 Hydrographs

The hydrographs are subject to several potentially large sources of uncertainty. The Ogilvie River hydrograph is developed based on the rating curve that is at least 19 years old. The gravel river channel had almost certainly shifted over the years altering the cross section. The Engineer Creek hydrograph is based on the flow estimates obtained via surface velocity estimates. It is recognized that the discharge values cannot be relied upon for detailed hydrological investigations. However, the main flow trends and major hydrological events are evident and bulk estimates of watershed exports may be derived using these hydrographs.

Appendix D

Analytical Results

Table D1 Ogilvie River Analytical Results

Date:	Conductivity	Temperature	pH	Alkalinity	DIC	DOC	$\delta^{13}C$ (DIC)	$\delta^{13}C$ (DOC)	$F^{14}C$ (DIC)	±	$F^{14}C$ (DOC)	±	Ca	K	Mg	Na	Sr	P	F	Cl	SO_4	NO_3	$\delta^{2}H$	$\delta^{18}O$	Tritium
Units	µS/cm	℃	-	ppm C	ppm C	ppm C	‰ vpdb	‰ vpdb					ppm	ppm	ppm	ppm	ppm	ppm	ppm	ppm	ppm	ppm	‰ VSMOW	‰ VSMOW	TU
	Field Parameters																								
21-Apr-14	482				54.35	1.05	-7.69	-24.53	0.9123	0.0049			72.29	0.72	25.93	12.98	0.34		0.10	15.07	95.06	0.51	-175.26	-22.32	7.70
11-May-14	122.5	4	7.75	9.1	10.56	13.79	-11.21	-27.74	0.7755	0.0044	1.0496	0.0057	17.00	1.61	4.98	8.71	0.09		0.05	0.82	26.10	0.11	-185.47	-23.75	8.22
12-May-14		4.5	7.6	8.4	10.60	11.67	-11.39	-27.40					18.84	0.73	5.45	5.10	0.11		0.04	1.19	30.81	0.10	-184.56	-23.62	
13-May-14	153	5.4	7.8	7.7	12.28	11.83	-9.70	-27.03	0.79	0.00			21.11	0.02	6.07	5.64	0.12		0.05	0.85	36.53	0.07	-183.61	-23.57	8.38
15-May-14		5.2	7.75	11.0	14.12	9.85	-8.02	-26.99					23.82	0.36	7.29	6.21	0.14		0.06	1.06	42.28	0.07	-181.52	-23.43	
16-May-14	193	5.7	7.69	10.5	15.21	8.68	-6.98	-27.07					27.53	0.06	8.38	6.93	0.16		0.05	1.37	50.54	0.14	-181.10	-23.23	6.53
18-May-14		6.8	7.75	18.0	17.69	7.58	-7.05	-26.69			0.9954	0.0025	31.81	0.00	9.64	8.78	0.19		0.06	1.27	62.92	0.18	-176.84	-22.68	
19-May-14	253	3.7	7.75	20.2	18.08	6.45	-6.65	-26.52					32.75	0.00	9.87	9.44	0.19		0.06	1.37	65.83	0.19	-177.89	-22.67	8.28
22-May-14					26.86	5.15	-7.98	-27.79					41.22	0.00	13.05	12.12	0.24		0.07	2.24	86.95	0.12	-173.99	-22.52	
29-May-14	377				30.36	3.93	-7.91	-27.59					47.49	0.00	15.01	20.63	0.31		0.08	1.80	119.90	0.07	-171.99	-22.05	8.25
6-Jun-14					33.63	3.11	-7.44	-27.41	0.6951	0.0022	0.8953	0.0058	50.16	0.00	15.46	18.12	0.31		0.08	2.61	111.14	0.03	-171.25	-21.92	
12-Jun-14	327				29.05	5.79	-8.48	-27.70					44.02	0.00	14.29	15.04	0.26		0.08	1.40	101.45	0.02	-170.66	-21.80	10.40
20-Jun-14					32.24	4.65	-8.09	-27.54					49.18	0.00	15.23	14.55	0.29		0.09	2.10	101.86	0.06	-172.99	-22.18	
27-Jun-14	276				25.48	7.71	-9.76	-27.94					41.12	0.00	11.67	8.92	0.24		0.08	1.45	81.47	0.00	-169.63	-21.93	7.81
5-Jul-14					29.15	7.15	-9.17	-27.83					47.95	0.00	12.86	8.65	0.28		0.10	1.65	86.89	0.06	-168.08	-21.57	
11-Jul-14	244				27.37	6.92	-9.28	-27.54					39.62	0.00	12.17	7.24	0.21		0.07	1.04	69.61	0.04	-168.06	-21.35	9.00
20-Jul-14					35.63	4.17	-8.53	-27.58					58.88	0.00	16.28	10.15	0.33		0.11	2.60	105.69	0.07	-171.17	-21.52	
24-Jul-14	367				35.46	4.29	-8.64	-27.55					52.03	0.00	16.00	13.95	0.30		0.08	2.07	103.48	0.10	-167.63	-21.47	9.59
9-Aug-14					27.75	8.02	-8.86	-27.63					44.44	0.00	12.52	12.49	0.29		0.08	0.83	92.20	0.05	-165.01	-20.88	
13-Aug-14	405	13.6	8.17	26.0	26.87	6.30	-7.60	-24.94					50.29	0.00	14.25	10.72	0.30		0.08	1.62	94.68	0.17	-167.42	-21.24	8.66
14-Aug-14	397	11.5	8.12	26.3	25.48	6.48	-7.60	-25.98					48.16	0.00	13.93	10.77	0.28		0.08	1.11	94.84	0.09	-166.88	-21.22	
15-Aug-14	379	11.2	8.15	24.0	23.78	7.27	-7.79	-25.48					45.84	0.00	13.12	9.51	0.27		0.08	0.97	89.76	0.18	-166.25	-21.25	10.25
16-Aug-14	371	12.7	8.11	24.3	24.14	7.78	-7.77	-25.32					45.73	0.00	12.98	9.06	0.27		0.08	0.96	86.96	0.05	-166.47	-21.20	10.1
16-Aug-14	371	12.7	8.11	24.3	24.18	7.63	-7.79	-25.66					45.78	0.00	13.05	9.08	0.27		0.08	0.94	86.79	0.07	-166.47	-21.45	
18-Aug-14	352	10	8.1	22.8	23.05	9.06	-8.14	-25.56	0.7405	0.0023	0.9754	0.0040	43.92	0.00	12.37	7.62	0.25		0.07	0.76	77.82	0.03	-166.20	-21.79	
19-Aug-14	360	9.5	8.15	24.6	24.05	8.28	-8.14	-25.53					46.00	0.00	12.94	7.21	0.26		0.07	0.90	77.08	0.13	-164.11	-21.29	9.72
31-Aug-14					26.14	8.9	-9.10	-27.53					39.68	0.48	11.74	7.53	0.18	0.04	0.11	0.71	77.77	0.04	-166.92	-21.19	
7-Sep-14					30.36	6.1	-8.29	-27.93					52.12	0.61	14.87	9.67	0.23	0.04	0.07	3.29	100.66	0.00	-168.07	-21.28	
11-Sep-14					30.96	5.7	-6.83	-28.15					51.34	0.61	15.72	12.36	0.23	0.05	0.06	1.36	107.81	0.01	-168.21	-21.52	10.09
20-Sep-14					32.38	4.3	-7.95	-28.12					60.86	0.66	16.33	9.53	0.26	0.04	0.08	1.91	122.49	0.00	-168.50	-21.62	
21-Apr-15	528		6.24	45	53.71	0.75	-7.81	-26.62	0.5716	0.0017	0.6848	0.0124	67.19	0.90	21.67	11.24	0.24	0.04	0.06	10.23	91.02	0.46	-172.96	-22.24	9.08
22-Apr-15	534	1.4	6.74	45									68.82	0.84	21.62	12.31	0.25	0.04	0.07	9.24	94.15	0.30	-174.11	-22.16	
24-Apr-15			6.21	42	56.5	5.4	-7.60	-26.69					67.41	0.93	23.03	11.22	0.25	0.06	0.08	9.99	90.42	0.46	-173.82	-22.39	
25-Apr-15			6.49	46									67.16	0.97	22.73	14.05	0.25	0.06	0.06	9.72	100.37	0.38	-174.68	-22.44	
29-Apr-15				43	44.87	2.12	-7.03	-27.58					59.33	1.07	22.28	11.18	0.21	0.05	0.05	8.72	85.70	0.20	-177.85	-22.84	
30-Apr-15	522	1	7.34	39									62.20	0.92	20.82	11.26	0.22	0.04	0.09	8.20	89.18	0.26	-175.40	-22.66	
1-May-15	488	0.6	7.53	40	52.1	4.9	-8.20	-27.20					64.54	0.82	21.24	11.86	0.23	0.03	0.07	7.81	89.35	0.20	-175.26	-22.67	10.24
2-May-15	495	0.7	7.64	42									61.37	0.92	21.97	10.90	0.22	0.03	0.06	7.82	90.79	0.17	-175.26	-22.65	
3-May-15	453	2.6	7.7	40																			-174.40	-22.49	
4-May-15	477	1.7	7.59	38	44.68	2.06	-7.76	-27.08					57.56	0.90	20.30	10.56	0.21	0.03	0.07	7.17	85.33	0.15	-176.12	-22.54	
6-May-15	553	1.6	7.76	36									69.45	1.01	22.54	22.15	0.32	0.02	0.05	6.67	147.37	0.17	-175.98	-22.46	
7-May-15	530	2.2	7.8	37									63.36	0.87	19.81	15.81	0.25	0.03	0.04	6.29	116.79	0.06	-175.31	-22.50	
8-May-15	452	2.9	7.86	29									49.81	0.92	16.86	15.20	0.21	0.04	0.04	3.65	109.67	0.00	-177.66	-22.70	8.51
9-May-15	356	0.5	8.01	19									40.36	0.97	13.60	11.08	0.17	0.03	0.05	2.41	80.95	0.00	-182.19	-23.43	
10-May-15	242	1.7	7.87	16	17.83	10.30	-8.40	-26.69					28.41	0.95	8.69	5.96	0.12	0.03	0.02	1.20	47.68	0.00	-184.18	-23.64	7.73
10-May-15	242	1.7	7.87		18.64	9.95	-9.13	-25.82	0.7846	0.0019	1.0645	0.0026	29.13	1.01	9.06	6.13	0.12	0.03	0.04	1.20	47.69	0.00	-184.76	-23.59	6.42
11-May-15	182	0.6	7.72										25.48	1.07	7.39	4.92	0.12	0.03	0.07	0.98	44.66	0.00	-184.20	-23.67	
12-May-15	188	1.1	7.7	12	12.80	12.05	-8.49	-27.44					22.24	0.98	6.04	4.04	0.10	0.03	0.03	0.68	38.93	0.00	-186.39	-23.78	7.21
13-May-15	204	0.7	7.73						0.8161	0.0022	1.0684	0.0026	20.42	1.11	6.20	8.56	0.09	0.03	0.04	0.84	49.25	0.01	-187.04	-23.91	
14-May-15		-		9	9.86	14.28	-8.61	-27.99					18.03	1.14	5.32	7.87	0.09	0.03	0.05	0.64	42.33	0.00	-189.79	-24.20	8.93
23-May-15					14.5	5.67	-10.54	-27.73					21.37	0.46	5.91	4.57	0.10	0.00	0.41	0.57	37.92	0.01	-180.8	-23.56	8.00
28-May-15					19.83	6.15	-9.33	-27.58					29.17	0.66	8.42	7.91	0.14	0.00	0.09	0.81	61.93		-175.3	-23.04	
4-Jun-15					26.8	4.86	-7.81	-27.32					42.12	0.73	12.86	12.26	0.20	0.00	0.06	1.73	97.26	0.01	-173.4	-22.45	
11-Jun-15													47.23	1.05	15.11	17.20	0.23	0.00	0.06	1.81	129.79	0.00	-172.7	-22.10	

Table D1 Ogilvie River Analytical Results

Date:	Conductivity	Temperature	pH	Alkalinity	DIC	DOC	$\delta^{13}C$ (DIC)	$\delta^{13}C$ (DOC)	$F^{14}C$ (DIC)	±	$F^{14}C$ (DOC)	±	Ca	K	Mg	Na	Sr	P	F	Cl	SO_4	NO_3	$\delta^{2}H$	$\delta^{18}O$	Tritium
Units	µS/cm	℃	-	ppm C	ppm C	ppm C	‰ vpdb	‰ vpdb					ppm	ppm	ppm	ppm	ppm	ppm	ppm	ppm	ppm	ppm	‰ VSMOW	‰ VSMOW	TU
	Field Parameters																								
18-Jun-15					31.84	4.25	-7.51	-27.54					50.37	0.43	15.45	14.94	0.24	0.00	0.10	2.30	120.22	0.00	-170.1	-22.14	
25-Jun-15													53.76	0.51	16.14	16.73	0.26	0.00	0.06	2.51	128.25	0.00	-169.9	-21.92	
03-Jul-15					27.3	5.55	-8.79	-27.55					42.25	0.45	12.82	8.35	0.18	0.00	0.06	1.47	84.81	0.08	-168.6	-21.66	11.26
13-Jul-15													53.85	0.50	16.26	14.82	0.25	0.00	0.06	2.18	124.69	0.07	-167.0	-21.70	
27-Jul-15					35.2	4.22	-8.12	-27.16					55.36	0.49	16.95	15.97	0.26	0.00	0.06	2.18	134.06	0.15	-166.6	-21.51	
20-Aug-15													52.33	0.44	15.00	11.81	0.25	0.04	0.08	1.21	118.24	0.00	-164.1	-21.71	
22-Aug-15	437	9.8	7.75	28	28.9	8.83	-9.55	-27.38					44.39	0.94	12.43	10.74	0.21	0.00	0.07	1.09	103.91	0.00	-161.8	-21.58	
27-Aug-15	383	9.3	8	26									40.19	0.86	11.23	8.30	0.19	0.00	0.07	0.87	87.06		-160.4	-21.44	
28-Aug-15	399	6.7	7.87	30	26.0	10.1	-8.69	-27.42					41.33	0.82	11.16	8.98	0.19	0.00	0.07	0.85	89.97	0.01	-163.8	-21.28	
30-Aug-15	357	5.3	7.89	33									40.61	0.63	11.03	8.37	0.19	0.00	0.07	0.89	84.22	0.00	-164.0	-21.20	
31-Aug-15	357	4.8	7.96	25	23.3	12	-8.73	-27.52	0.7439	0.0101	0.8915	0.0180	37.70	0.86	10.50	7.75	0.18	0.00	0.06	0.77	79.62	0.00	-162.5	-21.63	11.95
31-Aug-15	357	4.8	7.96		23.1	12.23	-8.46	-27.54					37.87	1.23	10.53	7.77	0.18	0.00	0.06	0.74	82.29	0.00	-163.7	-21.53	11.04
01-Sep-15	367	4.6	7.95	31	24.0	13.03	-8.81	-27.42					39.05	0.89	10.81	7.71	0.18	0.00	0.07	0.82	84.05	0.01	-163.4	-21.61	

Table D2 Shallow Groundwater (Drinking Water Well) Analytical Results

Date:	Conductivity	Temperature	pH	Alkalinity		DIC	DOC	$\delta^{13}C$ (DIC)	$\delta^{13}C$ (DOC)	$F^{14}C$ (DIC)	±	$F^{14}C$ (DOC)	±	Ca	K	Mg	Na	Sr	P	F	Cl	SO_4	NO_3	δ2H	δ18O	Tritium	±
Units	**µS/cm**	**°C**	**-**	**ppm C**		**ppm C**	**ppm C**	**‰ vpdb**	**‰ vpdb**					**ppm**	**ppm**	**ppm**	**ppm**	**ppm**	**ppm**	**ppm**	**ppm**	**ppm**	**ppm**	**‰ VSMOW**	**VSMOW**	**TU**	**TU**
	Field Parameters																										
19-Aug-14	498	18.4	7.64			49.83	2.64	-10.50	-19	0.67	0.002			68.48	0.00	17.61	9.15	0.29		0.07	4.29	82.37	0.06	-174.3	-22.3	10.7	1.16
23-Apr-15		-	6.94	44		51.13	0.96	-10.24	-25	0.66	0.0			67.74	0.78	18.39	11.56	0.22	0.06	0.04	4.34	99.45	0.03	-171.71	-22.45		
29-Apr-15				53								0.870	0.002	67.09	0.76	18.33	11.98	0.22	0.05	0.04	4.36	99.66	0.02	-172.39	-22.48		
2-May-15	518	-	7.45	46																				-173.06	-22.67		
7-May-15		-	7.56	42		52.82	1.22	-10.31	-25.67					69.30	0.78	18.61	12.17	0.22	0.08	0.04	4.46	99.16	0.05	-172.72	-22.62		
7-May-15				42										67.41	0.70	17.86	11.90	0.22	0.05	0.04	4.45	99.00	0.03	-172.72	-22.58		
10-May-15				36										67.09	0.71	17.98	11.11	0.21	0.05	0.04	4.45	98.79	0.05	-173.74	-22.85		
13-May-15		-	7.56	40		50.96	1.11	-10.28	-25.16					62.25	0.64	16.61	10.04	0.20	0.05	0.04	3.55	92.63	0.04			10.1	0.79
23-May-15																								-184.17	-22.46		
12-Jun-15																								-178.31	-22.20		
3-Jul-15																								-176.15	-21.35		
27-Aug-15		-	7.46	45		46.0	3.78	-11.01	-27.36			0.840	0.020	58.74	0.83	14.76	7.66	0.20	0.00	0.05	3.19	70.90	0.09	-170.9	-22.2		
31-Aug-15	491	9.7	7.39	43		50.10	3.74	-12.72	-27.58					58.70	1.03	14.71	7.51	0.20	0.00	0.06	2.75	73.12	0.02	-169.5	-22.1		

Table D3 Runoff (C1) Analytical Results

Date:	Conductivity	Temperature	pH	Alkalinity		DIC	DOC	$\delta^{13}C$ (DIC)	$\delta^{13}C$ (DOC)	$F^{14}C$ (DIC)	±	$F^{14}C$ (DOC)	±	Ca	K	Mg	Na	Sr	P	F	Cl	SO_4	NO_3	$\delta^{2}H$	$\delta^{18}O$	Tritium	±
Units	**µS/cm**	**℃**	**-**	**ppm C**		**ppm C**	**ppm C**	**‰ vpdb**	**‰ vpdb**					**ppm**	**ppm**	**ppm**	**ppm**	**ppm**	**ppm**	**ppm**	**ppm**	**ppm**	**ppm**	**‰ VSMOW**	**‰ VSMOW**	**TU**	**TU**
	Field Parameters																										
16-May-14	200	5	8.02			24.61	7.5	-1.63	-26.42			0.99	0.0035	37.47	0.00	9.19	0.00	0.09		0.05	0.34	21.2	0.31	-185.68	-23.89	8.8	0.6
17-Aug-14	387	5.7	8.37			39.15	5.66	-6.56	-23.01	0.87	0.0025	0.93	0.0036	61.07	0.00	13.71	0.00	0.15		0.06	0.20	54.29	0.38	-171.92	-22.66	12.1	1.6
22-Apr-15	93.1	0	5.26																					-197.83	-25.48		
23-Apr-15	107	0	7.32	32		31.8	10.6	-4.54	-27.96	1.02	0.0024	1.06	0.0029	26.02	1.37	12.20	0.19	0.03	0.03	0.01	0.51	2.86	0.18	-195.43	-24.94	8.5	0.7
25-Apr-15	-	-	7.1	25		27.98	19.77	-3.78	-26.79					22.48	1.24	11.73	0.19	0.02	0.03	0.04	0.57	1.64	0.12	-196.30	-24.99		
29-Apr-15																								-194.85	-24.84		
01-May-15	165.3	0	7.8																					-195.14	-24.94		
02-May-15	175	0.1	7.84																					-195.29	-24.77		
03-May-15	147.1	0.1	7.82																					-196.18	-25.12		
04-May-15	107	0	7.8	16		17.04	32.17	-6.92	-28.35					18.98	1.27	8.80	0.25	0.02	0.04	0.01	0.22	4.25	0.04	-195.17	-25.37		
06-May-15																								-193.26	-24.99		
07-May-15	125.1	0.1	7.75	14										15.87	1.09	7.34	0.14	0.02	0.04	0.0035	0.16	3.28	0.02	-191.18	-24.41		
09-May-15	111	0	7.6	9		12.51	15.81	-4.61	-28.10					14.42	0.95	5.93	0.15	0.02	0.04	0.01	0.17	3.47	0.14	-187.35	-24.33	8.04	0.4
10-May-15																								-187.32	-24.47		
11-May-15	145	0.1	7.92																					-187.52	-24.00		
13-May-15	155.5	2.2	8	13		17.3	11.9	-5.62	-26.46	0.97	0.0024	1.07	0.0025	22.01	0.67	6.17	0.16	0.04	0.02	0.02	0.17	7.63	0.13	-185.64	-24.31	7.73	0.7
22-Aug-15	424	5.8	8.08	28		44.4	7.72	-7.73	-27.34					56.03	0.79	12.48	0.13	0.12	0.00	0.05	0.27	60.40	0.03	-164.96	-21.36	9.04	0.5
28-Aug-15	391	1.5	8.14	35										51.86	0.87	11.21	0.09	0.10	0.00	0.05	0.27	57.90	0.02	-163.78	-21.15		
31-Aug-15	398	1.8	8.17	35		36.9	7.64	-6.33	-27.40					53.24	1.02	11.99	0.08	0.11	0.00	0.06	0.28	59.14	0.18	-163.79	-21.31		

Table D3 Runoff (C2) Analytical Results

Date:	Conductivity	Temperature	pH	Alkalinity		DIC	DOC	$\delta^{13}C$ (DIC)	$\delta^{13}C$ (DOC)	$F^{14}C$ (DIC)	±	$F^{14}C$ (DOC)	±	Ca	K	Mg	Na	Sr	P	F	Cl	SO_4	NO_3	$\delta^{2}H$	$\delta^{18}O$	Tritium	±
	µS/cm	℃	-	ppm C		ppm C	ppm C	‰ vpdb	‰ vpdb					ppm	ppm	ppm	ppm	ppm	ppm	ppm	ppm	ppm	ppm	‰ VSMOW	‰ VSMOW	TU	TU
	Field Parameters																										
16-May-14	175	0	7.94			24.94	11.83	-5.76	-26.68	0.9605	0.002	1.04	0.0028	24.02	0.00	12.73	0.00	0.00		0.03	0.39	0.3	0.00	-176.50	-22.23	8.1	1.0
17-Aug-14	304	2.9	8.15			44.67	8.86	-8.46	-24.70	0.87	0.0049	0.93	0.0027	36.44	-0.24	19.03	0.00	0.02		0.02	0.17	0.33	0.48	-173.76	-22.68	12.1	0.9
29-Apr-15																								-195.64	-25.41		
01-May-15																								-193.47	-24.73		
02-May-15																								-187.67	-24.37		
04-May-15	259	0.3	7.99	37		39.2	41.7	-5.67	-27.00	0.98	0.0022	1.06	0.0025	31.90	0.90	18.29	0.38	0.02	0.03	0.01	0.36	0.58	0.26	-186.36	-24.01	7.6	0.7
06-May-15																								-186.07	-24.02		
06-May-15																								-186.34	-23.87		
07-May-15	203	0	7.92	26										24.68	0.68	13.27	0.31	0.01	0.06	0.01	0.28	0.40	0.25	-185.09	-23.99		
09-May-15	146	0.1	7.88	11		18.27	19.96	-7.4	-27.03					17.79	0.59	9.64	0.19	0.01	0.05	0.00	0.18	0.28	0.22	-182.74	-23.83	7.7	0.72
10-May-15																								-183.61	-23.89		
11-May-15	148	0	7.92																					-184.82	-23.95		
13-May-15	133.2	0.9	7.91	19		18.38	14.9	-9.28	-26.47	0.98	0.002	1.07	0.0025	15.73	0.48	8.32	0.13	0.01	0.05	-0.01	0.17	0.57	0.03	-187.67	-24.32	9.2	0.72
22-Aug-15	322	2.7	7.97	42		45.4	10.26	-9.38	-27.40	0.89	0.018	0.92	0.0203	32.57	1.65	16.67	0.10	0.03	0.00	0.05	0.38	1.85	0.48	-168.68	-21.74	10.21	0.6
28-Aug-15	304	1.1	8.06	40										30.78	0.95	15.71	0.02	0.02	0.00	0.03	0.36	1.08	0.43	-167.73	-21.49		
31-Aug-15	295	1.2	8.08	39		41.3	10.43	-8.09	-27.40					30.54	0.96	15.57	0.08	0.02	0.00	0.10	0.96	1.18		-168.64	-21.68		

Table D3 Runoff (C3) Analytical Results

Date:	Conductivity	Temperature	pH	Alkalinity		DIC	DOC	$\delta^{13}C$ (DIC)	$\delta^{13}C$ (DOC)	$F^{14}C$ (DIC)	±	$F^{14}C$ (DOC)	±	Ca	K	Mg	Na	Sr	P	F	Cl	SO_4	NO_3	$\delta^{2}H$	$\delta^{18}O$	Tritium	±
	µS/cm	℃	-	ppm C		ppm C	ppm C	‰ vpdb	‰ vpdb					ppm	ppm	ppm	ppm	ppm	ppm	ppm	ppm	ppm	ppm	‰ VSMOW	‰ VSMOW	TU	TU
	Field Parameters																										
16-May-14	156	2.4	8.02			19.11	3.91	-1.29	-26.42	0.96	0.006	1.06	0.0057	26.02	0.00	7.82	0.00	0.05		0.02	0.20	15.3	0.20	-189.86	-24.43	7.5	0.5
17-Aug-14	409	5.7	8.24			41.32	4.01	-5.32	-21.47	0.84	0.0025			65.26	0.00	13.87	0.00	0.12		0.05	0.20	61.28	0.74	-170.58	-22.47	10.9	1.2
22-Apr-15	235	0	6.5	17		19.3	25.1	-11.21	-28.44					35.77	2.32	7.02	0.35	0.06	0.05	0.01	0.74	51.96	0.06	-192.74	-25.64	5.7	0.8
25-Apr-15				15										29.73	1.75	4.94	0.23	0.05	0.06	0.01	0.32	29.04	0.03	-190.86	-25.51		
29-Apr-15																								-186.80	-24.67		
01-May-15	247	0	7.83																					-189.12	-25.07		
02-May-15	291	0.1	7.85																					-187.81	-24.79		
03-May-15	212	0	7.72																					-187.52	-24.87		
04-May-15	201	0	7.77	17		17.87	23.17	-8.27	-28.13					32.32	1.25	5.62	0.24	0.06	0.05	0.01	0.17	28.68	0.16	-189.55	-24.51		
06-May-15																								-187.09	-24.49		
07-May-15	216	0	7.8	18										34.27	1.21	5.94	0.29	0.06	0.06	0.01	0.27	32.09	0.18	-185.49	-24.56		
09-May-15	188	0	7.92	10		16.64	14.83	-6.38	-27.17					30.38	1.02	4.91	0.23	0.05	0.06	0.01	0.15	21.89	0.25	-181.60	-23.90	7.27	0.5
10-May-15																								-183.13	-24.08		
11-May-15	243	0	8.01																					-181.44	-23.72		
13-May-15	271	2.1	8.13	22		25.6	6.7	-7.29	-27.20					42.02	0.69	8.35	0.29	0.07	0.06	0.02	0.22	37.05	0.41	-181.72	-23.76	7.98	0.8
22-Aug-15	429	5.5	8.18	39		44.4	5.84	-6.86	-27.60					60.35	1.24	11.47	0.06	0.11	0.00	0.07	0.40	63.87	0.03	-163.98	-21.11	12.06	0.8
28-Aug-15	368	1.2	8.16	36										50.56	0.97	10.22	0.04	0.08	0.00	0.01	0.39	7.96		-161.89	-20.82		
31-Aug-15	415	1.7	8.14	39		39.1	6.69	-6.05	-27.42					59.40	1.08	10.63	0.14	0.11	0.35	0.07	0.28	61.13	0.15	-163.80	-21.04		

Table D4 Active Layer Analytical Results

Sample Name	Date	Conductivity	Temperature	pH	Alkalinity	DIC	DOC	$\delta^{13}C$ (DIC)	$\delta^{13}C$ (DOC)	$F^{14}C$ (DIC)	±	$F^{14}C$ (DOC)	±	Ca	K	Mg	Na	Sr	P	F	Cl	SO_4	NO_3	$\delta^{2}H$	$\delta^{18}O$	Tritium	±
		µS/cm	℃	-	ppm C	ppm C	ppm C	‰ vpdb	‰ vpdb					ppm	ppm	ppm	ppm	ppm	ppm	ppm	ppm	ppm	ppm	‰ VSMOW	‰ VSMOW	TU	TU
		Field Parameters																									
R1	16-Aug-14	308	10.6	6.96		36.8	3.7	-9.72	-22.92					57.56	0.05	15.36	9.35	0.27		0.0778	3.91	78.13	0.1	-170.47	-22.51	9.28	1.6
R2	16-Aug-14	-	10.1	7.11		35.6	4.1	-9.4	-22.68	0.63	0.0069	0.87	0.0048	56.97	0.00	15.13	9.15	0.27		0.0753	3.84	76.13	0.36	-172.19	-22.82		
R3	16-Aug-14	291	10	7.18		36.9	4.1	-9.70	-23.03					56.33	0.00	14.74	8.79	0.27		0.08	2.92	75.54	0.25	-171.42	-22.78	9.85	2.1
R4	16-Aug-14	-	9.4	7.23		37.6	4.2	-9.82	-23.33					56.78	0.00	15.03	8.94	0.27		0.08	3.27	75.70	0.23	-171.98	-22.47		
R5	17-Aug-14	314	8	7.56		41.1	3.7	-10.01	-22.12	0.70	0.0024			61.75	0.00	15.12	9.01	0.27		0.07	2.26	80.27		-171.49	-22.57	9.66	1.2
R3	30-Aug-15	473	4.2	7.32	37.0	45.2	6.08	-12.75	-27.54			0.89	0.0187	66.71	0.78	16.28	8.80	0.28	0.00	0.08	4.71	138.18	0.02	-163.58	-22.45		
R5	29-Aug-15	400	4.4	7.66	27.5	28.6	10.04	-9.46	-27.53					59.89	0.30	4.47	0.42	0.08	0.00	0.18	1.15	115.70		-162.72	-22.36		
R6	30-Aug-15	569	3.5	7.22	36.6	40.9	4.99	-10.26	-27.28					54.55	0.84	13.67	9.06	0.21	0.00	0.07	2.83	88.98		-164.32	-22.42	9.47	0.7
AL-BH-SN8	23-Aug-15				45.4	56.3	27.6	-12.37	-27.29					43.70	0.63	11.39	8.43	0.19	0.14	0.06	1.30	86.60		-170.74	-22.05		

Table D5 Soil Water and Gas Analytical Results

Sample Location	Sample Date	Bag or Isojar	Sample Name	Depth for plotting	pH	$\delta^{13}C$ (Gas)	$\delta^{2}H$	$\delta^{18}O$
				cm		‰ vpdb	‰ VSMOW	‰ VSMOW
SN8	24/04/2015	Bag	BH1-SN8 0-3"	3.81	6.16		-175.76	-21.96
SN8	24/04/2015	Bag	BH1-SN8 3-6"	11.43	6.28		-169.04	-21.43
SN8	24/04/2015	Bag	BH1-SN8 6-9"	19.05	6.48		-169.51	-21.33
SN8	24/04/2015	Isojar	BH1-SN8 7-9"	20.32	6.64	-18.86	-173.43	-22.26
SN9	24/04/2015	Bag	BH1-SN9 0-2"	1.00	6.71		-155.02	-18.34
SN9	24/04/2015	Bag	BH1-SN9 2-4.5"	3.25	6.78		-139.01	-17.4
SN9	24/04/2015	Bag	BH1-SN9 4.5-7"	5.75	6.83		-152.42	-19.02
SN9	24/04/2015	Isojar	BH1-SN9 7-9"	8	6.46	-21.52	-153.13	-19.33
C1	23/04/2015	Bag	BH1-C1 4-6"	12.7	5.37		-161.99	-19.84
C1	23/04/2015	Bag	BH1-C1 6-9"	19.05	5.1		-139.98	-16.98
C1	23/04/2015	Isojar	BH1-C1 9-12"	26.67	6.73	-28.37	-144.1	-16.93
C1	23/04/2015	Bag	BH2-C1 0-5"	6.35	6.93		-190.8	-25.17
C1	23/04/2015	Bag	BH2-C1 5-9"	17.78	6.56		-169.1	-21.58
C1	23/04/2015	Isojar	BH2-1C 9-12"	26.67	6.49	-29.17	-147.01	-18.06
C1	23/04/2015	Isojar	BH2a-C1 0-3"	3.81	5.87	-25.38	-137.54	-16.92
C1	23/04/2015	Isojar	BH2a-C1 3-6"	11.43	6.75	-25.68	-149.29	-18.75
C1	23/04/2015	Isojar	BH1-C3 1-3"	5.08	6.33	-31.11	-179.86	-22.2
C3	23/04/2015	Isojar	BH3a-C3 7-10"	21.59	6.78	-25.63	-145.13	-18.43
C3	23/04/2015	Isojar	BH3a-C3 10-12"	27.94	6.48	-22.72	-142.96	-18.24
C3	23/04/2015	Isojar	BH3c-C3 6-9"	19.05	6.45	-27.51	-165.47	-20.71

Table D6 Precipitation Analytical Results

Precipitation Type	Sample ID	Date	δ^2H	$\delta^{18}O$	δ^2H (corrected for elevation)	$\delta^{18}O$ (corrected for elevation
			‰ VSMOW	‰ VSMOW	‰ VSMOW	‰ VSMOW
Rain		07-Jun-14	-145.0	-17.17	-152.57	-18.29
Rain		09-Jun-14	-122.2	-11.71	-129.82	-12.83
Rain		10-Jun-14	-150.6	-16.74	-158.17	-17.86
Rain		11-Jun-14	-151.8	-17.27	-159.43	-18.39
Rain		12-Jun-14	-162.1	-20.00	-169.70	-21.12
Rain		15-Jun-14	-141.9	-17.59	-149.55	-18.71
Rain		17-Jun-14	-180.3	-22.76	-187.86	-23.88
Rain		21-Jun-14	-149.2	-18.39	-156.76	-19.51
Rain		25-Jun-14	-146.6	-17.94	-154.24	-19.06
Rain		26-Jun-14	-171.2	-21.93	-178.77	-23.05
Rain		02-Jul-14	-144.2	-17.04	-151.80	-18.16
Rain		05-Jul-14	-133.3	-15.81	-140.90	-16.93
Rain		10-Jul-14	-143.5	-17.98	-151.14	-19.10
Rain		13-Jul-14	-147.5	-16.55	-155.10	-17.67
Rain		14-Jul-14	-156.4	-18.80	-164.04	-19.92
Rain		18-Jul-14	-130.5	-15.39	-138.10	-16.51
Rain		19-Jul-14	-94.9	-10.57	-102.53	-11.69
Rain		20-Jul-14	-132.0	-16.33	-139.65	-17.45
Rain		24-Jul-14	-107.6	-12.60	-115.25	-13.72
Rain		26-Jul-14	-130.1	-16.34	-137.72	-17.46
Rain		27-Jul-14	-149.0	-18.53	-156.57	-19.65
Rain		30-Jul-14	-168.3	-21.06	-175.91	-22.18
Rain		15-Aug-14	-139.8	-17.22	-147.43	-18.34
Rain		19-Aug-14	-144.0	-17.46	-151.57	-18.58
Rain		20-Aug-14	-150.0	-18.30	-157.62	-19.42
Rain		24-Aug-14	-140.2	-17.02	-147.79	-18.14
Rain		27-Aug-14	-175.7	-22.07	-183.30	-23.19
Rain		28-Aug-14	-169.6	-20.44	-177.24	-21.56
Rain		29-Aug-14	-158.1	-19.27	-165.70	-20.39
Rain		30-Aug-14	-135.6	-15.76	-143.20	-16.88
Rain		31-Aug-14	-188.1	-23.31	-195.67	-24.43
Rain		20-Sep-14	-117.85	-14.64	-125.45	-15.76
Snow		05-Oct-14	-170.79	-21.71	-178.39	-22.83
Rain		31-Oct-14	-251.43	-33.1	-259.03	-34.22
Rain		28-May-15	-85.6	-10.04	-93.21	-11.16
Rain		30-May-15	-97.8	-12.92	-105.44	-14.04
Rain		04-Jun-15	-174.7	-24.30	-182.27	-25.42
Rain		17-Jun-15	-131.6	-17.85	-139.15	-18.97
Rain		02-Jul-15	-148.3	-20.47	-155.91	-21.59
Rain		15-Jul-15	-128.5	-17.46	-136.06	-18.58
Rain		27-Jul-15	-166.5	-22.24	-174.13	-23.36
Rain		12-Aug-15	-140.5	-17.79	-148.13	-18.91
Snow		28-Aug-15	-237.5	-33.07	-245.07	-34.19
Snow	SN-1a 22-Apr-2015	22-Apr-15	-211.87	-27.02	-219.47	-28.14
Snow	SN-1b 22-Apr-2015	22-Apr-15	-215.97	-27.92	-223.57	-29.04
Snow	SN-1c 22-Apr-2015	22-Apr-15	-191.38	-24.84	-198.98	-25.96

Table D6 Precipitation Analytical Results

Precipitation Type	Sample ID	Date	δ^2H	$\delta^{18}O$	δ^2H (corrected for elevation)	$\delta^{18}O$ (corrected for elevation
			‰ VSMOW	‰ VSMOW	‰ VSMOW	‰ VSMOW
Snow	SN-2a 22-Apr-2015	22-Apr-15	-213	-26.64	-220.60	-27.76
Snow	SN-2b 22-Apr-2015	22-Apr-15	-217.56	-28.46	-225.16	-29.58
Snow	SN-2c 22-Apr-2015	22-Apr-15	-199.96	-25.73	-207.56	-26.85
Snow	SN-3a 22-Apr-2015	22-Apr-15	-191.63	-24.07	-199.23	-25.19
Snow	SN-3b 22-Apr-2015	22-Apr-15	-210.3	-26.73	-217.90	-27.85
Snow	SN-3c 22-Apr-2015	22-Apr-15	-216.89	-27.9	-224.49	-29.02
Snow	SN-3d 22-Apr-2015	22-Apr-15	-213.79	-28.4	-221.39	-29.52
Snow	SN-3e 22-Apr-2015	22-Apr-15	-195.8	-25.62	-203.40	-26.74
Snow	SN-4a 22-Apr-2015	22-Apr-15	-210.27	-26.84	-217.87	-27.96
Snow	SN-4b 22-Apr-2015	22-Apr-15	-212.62	-28.21	-220.22	-29.33
Snow	SN-4c 22-Apr-2015	22-Apr-15	-208.81	-27.6	-216.41	-28.72
Snow	SN-5a 22-Apr-2015	22-Apr-15	-216.44	-27.44	-224.04	-28.56
Snow	SN-5b 22-Apr-2015	22-Apr-15	-220.83	-28.49	-228.43	-29.61
Snow	SN-5c 22-Apr-2015	22-Apr-15	-199.75	-25.41	-207.35	-26.53
Snow	SN-6a 23-Apr-2015	22-Apr-15	-208.5	-26.66	-216.10	-27.78
Snow	SN-6b 23-Apr-2015	23-Apr-15	-216.88	-28.48	-224.48	-29.60
Snow	SN-6c 23-Apr-2015	23-Apr-15	-201.84	-26.82	-209.44	-27.94
Snow	SN-7a 23-Apr-2015	23-Apr-15	-210.77	-27.41	-218.37	-28.53
Snow	SN-7b 23-Apr-2015	23-Apr-15	-219.77	-29.18	-227.37	-30.30
Snow	SN-7c 23-Apr-2015	23-Apr-15	-203.44	-26.81	-211.04	-27.93
Snow	SN-8a 24-Apr-2015	24-Apr-15	-203.8	-26.22	-211.40	-27.34
Snow	SN-8b 24-Apr-2015	24-Apr-15	-216.93	-28.86	-224.53	-29.98
Snow	SN-8c 24-Apr-2015	24-Apr-15	-201.34	-26.65	-208.94	-27.77
Snow	SN-9a 24-Apr-2015	24-Apr-15	-210.28	-26.8	-217.88	-27.92
Snow	SN-9b 24-Apr-2015	24-Apr-15	-212.77	-28.15	-220.37	-29.27
Snow	SN-9c 24-Apr-2015	24-Apr-15	-195.9	-26.36	-203.50	-27.48
Snow	SN-10a 24-Apr-2015	24-Apr-15	-204.98	-26.33	-212.58	-27.45
Snow	SN-10b 24-Apr-2015	24-Apr-15	-215.37	-27.97	-222.97	-29.09
Snow	SN-10c 24-Apr-2015	24-Apr-15	-193.44	-24.85	-201.04	-25.97
Snow	SN-11a 24-Apr-2015	24-Apr-15	-214.22	-28	-221.82	-29.12
Snow	SN-11b 24-Apr-2015	24-Apr-15	-223.5	-29.18	-231.10	-30.30
Snow	SN-11c 24-Apr-2015	24-Apr-15	-201.38	-26.01	-208.98	-27.13

Appendix E

Principal Component Analysis

PCA Input:

		DIC	DOC	D13C (DIC)	D13C (DOC)	Ca	K	Mg	Na	Sr	F	Cl	SO4	NO3	D2H	D18O
1	21-Apr-14	54.35	1.05	-7.69	-24.53	72.29	0.72	25.93	12.98	0.34	0.10	15.07	95.06	0.51	-175.26	-22.32
2	11-May-14	10.56	13.79	-11.21	-27.74	17.00	1.61	4.98	8.71	0.09	0.05	0.82	26.10	0.11	-185.47	-23.75
3	12-May-14	10.60	11.67	-11.39	-27.40	18.84	0.73	5.45	5.10	0.11	0.04	1.19	30.81	0.10	-184.56	-23.62
4	13-May-14	12.28	11.83	-9.70	-27.03	21.11	0.02	6.07	5.64	0.12	0.05	0.85	36.53	0.07	-183.61	-23.57
5	15-May-14	14.12	9.85	-8.02	-26.99	23.82	0.36	7.29	6.21	0.14	0.06	1.06	42.28	0.07	-181.52	-23.43
6	16-May-14	15.21	8.68	-6.98	-27.07	27.53	0.06	8.38	6.93	0.16	0.05	1.37	50.54	0.14	-181.10	-23.23
7	18-May-14	17.69	7.58	-7.05	-26.69	31.81	0.00	9.64	8.78	0.19	0.06	1.27	62.92	0.18	-176.84	-22.68
8	19-May-14	18.08	6.45	-6.65	-26.52	32.75	0.00	9.87	9.44	0.19	0.06	1.37	65.83	0.19	-177.89	-22.67
9	22-May-14	26.86	5.15	-7.98	-27.79	41.22	0.00	13.05	12.12	0.24	0.07	2.24	86.95	0.12	-173.99	-22.52
10	29-May-14	30.36	3.93	-7.91	-27.59	47.49	0.00	15.01	20.63	0.31	0.08	1.80	119.90	0.07	-171.99	-22.05
11	6-Jun-14	33.63	3.11	-7.44	-27.41	50.16	0.00	15.46	18.12	0.31	0.08	2.61	111.14	0.03	-171.25	-21.92
12	12-Jun-14	29.05	5.79	-8.48	-27.70	44.02	0.00	14.29	15.04	0.26	0.08	1.40	101.45	0.02	-170.66	-21.80
13	20-Jun-14	32.24	4.65	-8.09	-27.54	49.18	0.00	15.23	14.55	0.29	0.09	2.10	101.86	0.06	-172.99	-22.18
14	27-Jun-14	25.48	7.71	-9.76	-27.94	41.12	0.00	11.67	8.92	0.24	0.08	1.45	81.47	0.00	-169.63	-21.93
15	5-Jul-14	29.15	7.15	-9.17	-27.83	47.95	0.00	12.86	8.65	0.28	0.10	1.65	86.89	0.06	-168.08	-21.57
16	11-Jul-14	27.37	6.92	-9.28	-27.54	39.62	0.00	12.17	7.24	0.21	0.07	1.04	69.61	0.04	-168.06	-21.35
17	20-Jul-14	35.63	4.17	-8.53	-27.58	58.88	0.00	16.28	10.15	0.33	0.11	2.60	105.69	0.07	-171.17	-21.52
18	24-Jul-14	35.46	4.29	-8.64	-27.55	52.03	0.00	16.00	13.95	0.30	0.08	2.07	103.48	0.10	-167.63	-21.47
19	9-Aug-14	27.75	8.02	-8.86	-27.63	44.44	0.00	12.52	12.49	0.29	0.08	0.83	92.20	0.05	-165.01	-20.88
20	13-Aug-14	26.87	6.30	-7.60	-24.94	50.29	0.00	14.25	10.72	0.30	0.08	1.62	94.68	0.17	-167.42	-21.24
21	14-Aug-14	25.48	6.48	-7.60	-25.98	48.16	0.00	13.93	10.77	0.28	0.08	1.11	94.84	0.09	-166.88	-21.22
22	15-Aug-14	23.78	7.27	-7.79	-25.48	45.84	0.00	13.12	9.51	0.27	0.08	0.97	89.76	0.18	-166.25	-21.25
23	16-Aug-14	24.14	7.78	-7.77	-25.32	45.73	0.00	12.98	9.06	0.27	0.08	0.96	86.96	0.05	-166.47	-21.20
24	16-Aug-14	24.18	7.63	-7.79	-25.66	45.78	0.00	13.05	9.08	0.27	0.08	0.94	86.79	0.07	-166.47	-21.45
25	18-Aug-14	23.05	9.06	-8.14	-25.56	43.92	0.00	12.37	7.62	0.25	0.07	0.76	77.82	0.03	-166.20	-21.79
26	19-Aug-14	24.05	8.28	-8.14	-25.53	46.00	0.00	12.94	7.21	0.26	0.07	0.90	77.08	0.13	-164.11	-21.29
27	31-Aug-14	26.14	8.9	-9.10	-27.53	39.68	0.48	11.74	7.53	0.18	0.11	0.71	77.77	0.04	-166.92	-21.19
28	7-Sep-14	30.36	6.1	-8.29	-27.93	52.12	0.61	14.87	9.67	0.23	0.07	3.29	100.66	0.00	-168.07	-21.28
29	11-Sep-14	30.96	5.7	-6.83	-28.15	51.34	0.61	15.72	12.36	0.23	0.06	1.36	107.81	0.01	-168.21	-21.52
30	20-Sep-14	32.38	4.3	-7.95	-28.12	60.86	0.66	16.33	9.53	0.26	0.08	1.91	122.49	0.00	-168.50	-21.62
31	21-Apr-15	53.71	0.75	-7.81	-26.62	67.19	0.90	21.67	11.24	0.24	0.06	10.23	91.02	0.46	-172.96	-22.24
32	24-Apr-15	56.5	5.4	-7.60	-26.69	67.41	0.93	23.03	11.22	0.25	0.08	9.99	90.42	0.46	-173.82	-22.39
33	29-Apr-15	44.87	2.12	-7.03	-27.58	59.33	1.07	22.28	11.18	0.21	0.05	8.72	85.70	0.20	-177.85	-22.84
34	1-May-15	52.1	4.9	-8.20	-27.20	64.54	0.82	21.24	11.86	0.23	0.07	7.81	89.35	0.20	-175.26	-22.67
35	4-May-15	44.68	2.06	-7.76	-27.08	57.56	0.90	20.30	10.56	0.21	0.07	7.17	85.33	0.15	-176.12	-22.54
36	10-May-15	17.83	10.30	-8.40	-26.69	28.41	0.95	8.69	5.96	0.12	0.02	1.20	47.68	0.00	-184.18	-23.64
37	10-May-15	18.64	9.95	-9.13	-25.82	29.13	1.01	9.06	6.13	0.12	0.04	1.20	47.69	0.00	-184.76	-23.59
38	12-May-15	12.80	12.05	-8.49	-27.44	22.24	0.98	6.04	4.04	0.10	0.03	0.68	38.93	0.00	-186.39	-23.78
39	14-May-15	9.86	14.28	-8.61	-27.99	18.03	1.14	5.32	7.87	0.09	0.05	0.64	42.33	0.00	-189.79	-24.20
40	23-May-15	14.48	5.67	-10.40	-27.73	21.37	0.46	5.91	4.57	0.10	0.41	0.57	37.92	0.01	-180.8	-23.56
41	28-May-15	19.83	6.15	-9.33	-27.58	29.17	0.66	8.42	7.91	0.14	0.09	0.81	61.93	0.09	-175.3	-23.04

PCA Input (cont'd):

		DIC	DOC	D13C (DIC)	D13C (DOC)	Ca	K	Mg	Na	Sr	F	Cl	SO4	NO3	D2H	D18O
42	4-Jun-15	27.51	4.86	-8.07	-27.32	42.12	0.73	12.86	12.26	0.20	0.06	1.73	97.26	0.01	-173.4	-22.45
43	18-Jun-15	31.84	4.25	-7.51	-27.54	50.37	0.43	15.45	14.94	0.24	0.10	2.30	120.22	0.00	-170.1	-22.14
44	03-Jul-15	28.14	5.55	-8.87	-27.55	42.25	0.45	12.82	8.35	0.18	0.06	1.47	84.81	0.08	-168.6	-21.66
45	27-Jul-15	34.15	4.22	-8.20	-27.16	55.36	0.49	16.95	15.97	0.26	0.06	2.18	134.06	0.15	-166.6	-21.51
46	22-Aug-15	34.10	8.83	-8.91	-27.38	44.39	0.94	12.43	10.74	0.21	0.07	1.09	103.91	0.00	-161.8	-21.58
47	28-Aug-15	31.34	10.1	-8.54	-27.42	41.33	0.82	11.16	8.98	0.19	0.07	0.85	89.97	0.01	-163.8	-21.28
48	31-Aug-15	25.82	12	-8.16	-27.52	37.70	0.86	10.50	7.75	0.18	0.06	0.77	79.62	0.00	-162.5	-21.63
49	31-Aug-15	24.98	12.23	-8.18	-27.54	37.87	1.23	10.53	7.77	0.18	0.06	0.74	82.29	0.00	-163.7	-21.53
50	01-Sep-15	29.18	13.03	-8.31	-27.42	39.05	0.89	10.81	7.71	0.18	0.07	0.82	84.05	0.01	-163.4	-21.61

PCA Output:

Importance of components

	PC1	PC2	PC3	PC4	PC5	PC6	PC7	PC8	PC9	PC10	PC11	PC12	PC13	PC14	PC15
Standard deviation	2.677	1.656	1.197	1.109	0.9962	0.7334	0.5889	0.4814	0.37298	0.26059	0.21612	0.16956	0.1534	0.1055	0.05713
Proportion of Variance	0.478	0.183	0.0955	0.082	0.0662	0.0358	0.0231	0.0154	0.00927	0.00453	0.00311	0.00192	0.00157	0.00074	0.00022
Cumulative Proportion	0.478	0.661	0.7561	0.838	0.9042	0.9401	0.9632	0.9786	0.98791	0.99244	0.99556	0.99747	0.99904	0.99978	1

Rotation:

	PC1	PC2	PC3	PC4	PC5	PC6	PC7	PC8	PC9	PC10	PC11	PC12	PC13	PC14	PC15
DIC	**-0.32924**	0.19367	-0.18503	0.053	-0.1838	0.00268	-0.1104	0.02709	-0.17823	0.44221	-0.325	0.2878	-0.3023	0.4909	-0.14904
DOC	**0.30565**	-0.10044	0.10062	0.313	-0.2475	0.07256	0.1507	-0.33251	-0.69505	-0.01367	-0.2195	0.049	0.2234	-0.06981	-0.00397
D13C..DIC.	-0.21747	0.00539	0.2784	0.257	0.37	-0.76673	-0.1047	-0.21072	-0.1231	-0.00807	0.0919	0.0259	-0.057	0.03614	0.00986
D13C..DOC.	-0.08664	0.10699	**0.72304**	-0.0413	-0.2057	-0.00546	0.5312	0.29745	0.10585	0.14117	-0.0775	0.0321	0.0325	0.0655	0.00554
Ca	**-0.36136**	0.05872	-0.06556	0.0434	-0.13	-0.01951	-0.0932	0.2398	-0.13559	-0.26621	-0.2214	0.1907	0.0239	-0.20361	0.74811
K	0.0981	**0.34368**	**-0.38418**	0.37	-0.3372	-0.24512	0.4474	0.0116	0.1571	-0.28763	0.2299	0.0529	-0.2171	0.00636	-0.05839
Mg	**-0.35158**	0.17125	-0.0727	0.0317	-0.0593	-0.01478	-0.0696	0.19503	-0.11298	0.10841	0.02	0.2302	0.236	-0.64713	-0.4917
Na	-0.27087	-0.08671	-0.2156	0.0175	0.4595	0.25074	0.5687	-0.31917	-0.00836	0.28975	0.1399	0.1462	0.0482	-0.08199	0.19745
Sr	**-0.33046**	-0.18736	0.12962	-0.0856	0.0687	0.2507	0.0545	0.08304	-0.41607	-0.43631	0.2705	-0.1252	-0.5014	0.06266	-0.21559
F	0.00217	-0.05771	-0.1726	-0.7972	-0.2269	-0.40103	0.2265	-0.16316	-0.18211	-0.04664	-0.0146	0.0539	0.0487	-0.01475	-0.00587
Cl	-0.23238	**0.45428**	-0.0315	-0.0358	-0.1024	0.0543	-0.0872	0.00717	-0.24289	0.1885	0.3776	-0.5676	0.3314	0.16864	0.13668
SO4	**-0.32244**	-0.22529	-0.18723	0.106	0.0741	-0.06132	0.207	0.06657	0.12665	-0.32178	-0.4948	-0.3556	0.3726	0.2348	-0.2402
NO3	-0.18914	**0.41788**	0.25639	-0.1018	-0.0893	0.21443	-0.1263	-0.66559	0.25712	-0.29858	-0.1829	0.0754	-0.031	-0.04867	-0.05335
D2H	-0.21497	**-0.39617**	0.00329	0.1274	-0.4259	-0.07599	-0.024	-0.24853	0.18784	0.32847	-0.0428	-0.4221	-0.3092	-0.32313	0.08867
D18O	-0.23882	**-0.39418**	0.05749	0.0971	-0.3448	0.03353	-0.1166	-0.12452	0.14202	-0.07943	0.4624	0.3853	0.3869	0.29505	-0.01464

Plot

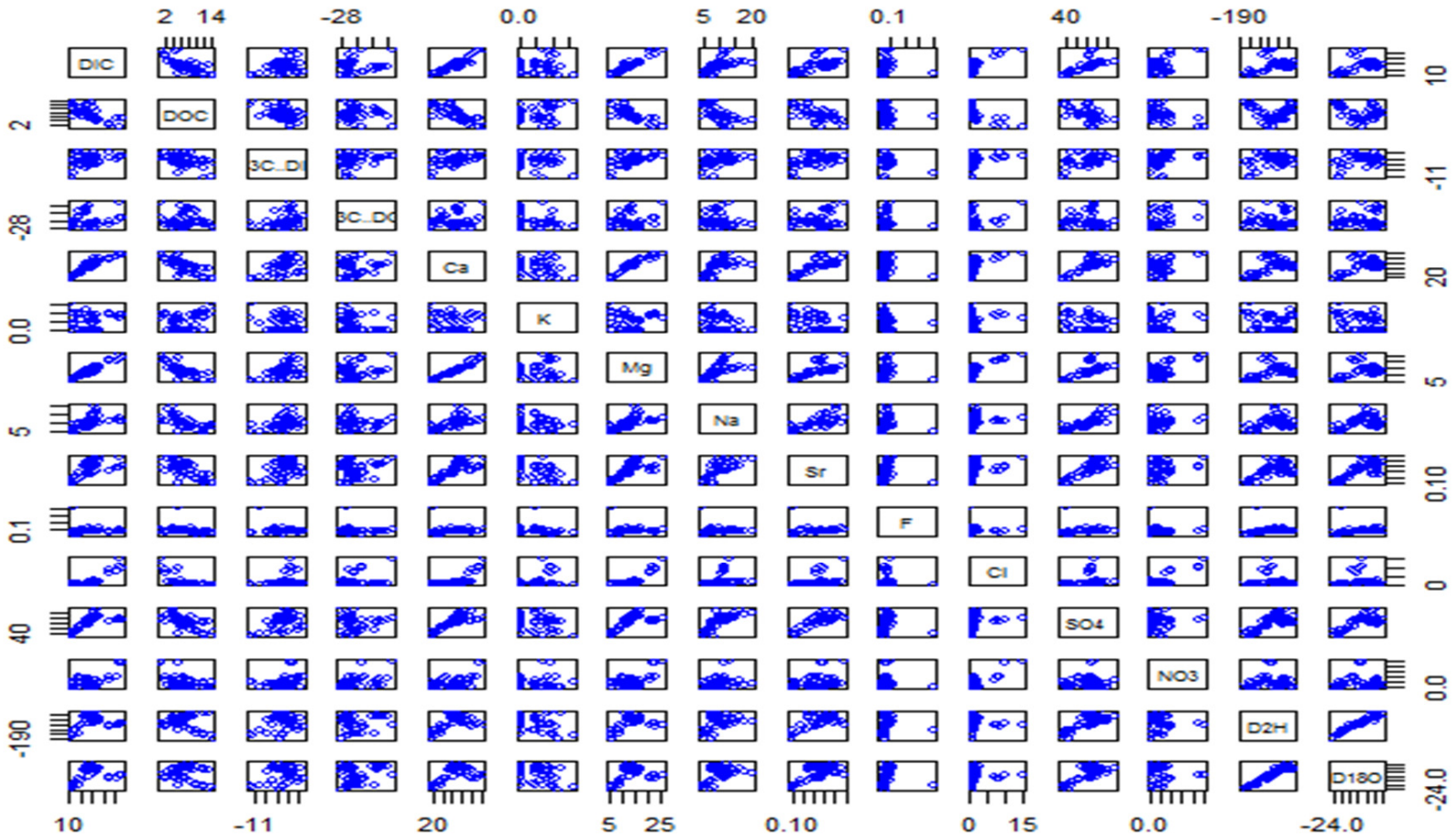
DIC
DOC
δC_DI
δC_DO
Ca
K
Mg
Na
Sr
F
Cl
SO4
NO3
D2H
D18O
2 14
-28
0.0
5 20
0.1
40
-190
10
-11
20
5 25
0.10
0 15
0.0
-24.0